INVESTIGATION OF NEW PRINCIPLES FOR HUMAN DECOMPRESSION SCHEDULES USING DOPPLER ULTRASONIC BLOOD BUBBLE DETECTION

INSTITUTE OF ENVIRONMENTAL MEDICINE AND PHYSIOLOGY

PREPARED FOR

OFFICE OF NAVAL RESEARCH

23 JULY 1974

UNCLASSIFIED

SECURITY CLASSIFICATION OF THIS PAGE (When Data Entered)

REPORT DOCUMENTATION PAGE	READ INSTRUCTIONS BEFORE COMPLETING FORM
1 REPORT NUMBER: 3	2 GOVT ACCESSION NO.
	3 RECIPIENT'S CATALOG NUMBER: AD-784476
4 TITLE (and Subtitle): INVESTIGATION OF NEW PRINCIPLES FOR HUMAN DECOMPRESSION SCHEDULES USING DOPPLER ULTRASONIC BLOOD BUBBLE DETECTION	5 TYPE OF REPORT & PERIOD COVERED: TECHNICAL 1967 - 1974
	6 PERFORMING ORG. REPORT NUMBER
7 AUTHOR(s): MERRILL P. SPENCER DAVID C. JOHANSON	8 CONTRACT OR GRANT NUMBER(s): N00014-73-C-0094
9 PERFORMING ORGANIZATION NAME AND ADDRESS: INSTITUTE OF ENVIRONMENTAL MEDICINE & PHYSIOLOGY 556 18th Ave. Seattle, WA 98122	10 PROGRAM ELEMENT, PROJECT, TASK AREA & WORK UNIT NUMBERS
11 CONTROLLING OFFICE NAME AND ADDRESS: CAPT. R.C. BORNMAN, M.D., USN SUBMARINE DIVING MEDICINE/RESEARCH DIVISION DEPT. OF THE NAVY WASH. D.C. 20390	12 REPORT DATE: 23 JULY 74 13 NUMBER OF PAGES: 12
14 MONITORING AGENCY NAME & ADDRESS (if different from Controlling Office): DEFENSE CONTRACT ADMINISTRATION SERVICES DISTRICT BUILDING 5-D NAVAL SUPPORT ACTIVITY SAND POINT, SEATTLE, WA 98115	15 SECURITY CLASS (of this report): UNCLASSIFIED 15a DECLASSIFICATION/DOWNGRADING SCHEDULE

16 DISTRIBUTION STATEMENT (of this Report)

DISTRIBUTION OF THIS DOCUMENT IS UNLIMITED

17 DISTRIBUTION STATEMENT (of the abstract entered in Block 20, if different from Report)

DISTRIBUTION OF THIS ABSTRACT IS UNLIMITED

18 SUPPLEMENTARY NOTES

19 KEY WORDS (Continue on reverse side if necessary and identify by block number)

precordial
vge
direct decompression
doppler ultrasound blood bubble detection

20 ABSTRACT (Continue on reverse side if necessary and identify by block number)

The development of doppler instrumentation for non-invasive detection of gas emboli moving through the arteries and veins is traced from it's beginning in 1967 through 1974. The design and construction of the IEM&P precordial blood bubble detector is described in detail. The use of the doppler technique in the study and solution of decompression problems in divers is described.

DD FORM 1 JAN 73 1473 EDITION OF 1 NOV 65 IS OBSOLETE S/N 0102-014-6601

UNCLASSIFIED

SECURITY CLASSIFICATION OF THIS PAGE (When Data Entered)

TECHNICAL REPORT

INVESTIGATION OF NEW PRINCIPLES FOR HUMAN DECOMPRESSION SCHEDULES USING THE DOPPLER ULTRASONIC BLOOD BUBBLE DETECTOR

BY
MERRILL P. SPENCER
DAVID C. JOHANSON

SUBMITTED TO:
THE OFFICE OF NAVAL RESEARCH
DEPARTMENT OF THE NAVY

23 JULY 1974

THIS RESEARCH WAS SPONSORED BY THE OFFICE OF NAVAL RESEARCH, ONR CONTRACT NUMBER N00014-73-C-0094

TABLE OF CONTENTS

LIST OF ILLUSTRATIONS AND TABLES

FIGURE NUMBER | PAGE

FIGURE NUMBER | PAGE

SUMMARY

The development of doppler instrumentation for non-invasive detection of gas emboli moving through the arteries and veins is traced from it's beginning in 1967 through 1974. The design and construction of the IEM6P precordial blood bubble detector is described in detail. A comprehensive range of doppler transducer types is presented including many new designs for flow, velocity and bubble detection.

The use of the doppler technique in the study and solution of decompression problems of divers is described. Results from the use of doppler blood bubble detection include the following advances in diving safety, pathophysiological knowledge, and improved instrumentation for further advances.

General Principles and Susceptibility to Decompression Gas Emboli

1. Intravascular gas emboli are produced by excess inert gas in the blood and tissues resulting from decompression after breathing high pressure atmospheres. They are clearly detected with the Doppler Ultrasonic Blood Flowmeter, appearing as chirps, whistles, and snaps on the audio output.
2. Decompression gas emboli form early in the veins and appear in the systemic arteries only after severe violation of accepted decompression schedules.
3. Vge forming in the periphery, develop first in specified localized areas without general distribution, collect in the small peripheral veins or capillaries, and are extruded into the venous return by local blood flow or compression of the tissues.

4. The Precordial ultrasonic blood bubble detector senses venous gas emboli (vge) which arrive from any peripheral vein. It has the advantage over any peripheral bubble detector, whether detecting moving or static bubbles, in serving as a whole body monitor of decompression vge, regardless of their regional source.

5. The direct decompression limits for man breathing hyperbaric air has been experimentally established in objective terms of venous gas emboli. These limits will be useful in testing the adequacy of any decompression model and serve as a guide for the development of safer and more efficient decompression tables.

6. Vge are frequently produced in hyperbaric chamber exposures of the U.S. Navy tables of exceptional exposure over 150 feet of sea water pressure.

7. The "long pull" first step in decompression from 200 ft/30 minutes exposures does not produce more venous gas emboli than a shorter step utilized in the older Navy tables.

8. There is a reproducible susceptibility of certain individuals to develop decompression vge, while others tend to be "bubble resistant". Among those susceptible individuals, there is a unique regional source which frequently produces the first detectable bubbles.

9. It appears probable that diving trainees may be selected, at least in part, on the basis of their susceptibility to vge after hyperbaric exposures.

10. Theoretical and experimental evidence indicates that excess nitrogen bubbles are not induced by 5 megahertz ultrasound applied at 10 milliwatts per square centimeter to the surface of the body.

Relationship of Venous Gas Emboli to Bends

1. Decompression vge are detected ultrasonically before symptoms of decompression illness develop. Decompression illness has never been observed in our laboratory before detectable vge are found in the pulmonary artery or in peripheral veins.
2. The most frequent regional sources of vge are in the upper and lower extremities. They develop in the venous return, downstream to tissue regions where bends pain develops. They have not been found to accompany skin bends peculiar to dry chamber exposures.
3. Those subjects prone to develop vge in chamber exposures are the same subjects whom are more likely to develop bends following open water exposures.
4. The human brain and other body tissues can tolerate hundreds of doppler detectable arterial gas emboli without producing clinical signs or symptoms.

Treatment of VGE and Bends

1. Vge signals are dissipated by recompression with or without oxygen breathing, and may be used as a guide for adequate decompression or oxygen therapy.
2. Oxygen therapy at 30 feet of sea-water pressure is highly effective in dissipating decompression vge and bends caused by much deeper exposures.

Open Water Findings

1. It was established that precordial doppler blood bubble detection provides practical information to prevent bends in open-ocean diving operations. Of special value is the advice to the diver to avoid repet dives should any particular dive produce vge.

2. A technique was found among Oahu seafood divers allowing them to shorten surface intervals considerably on repetitive dives, which involves their consistent use of the shallow water dive as the final dive of the day.

3. In Maui black coral divers, we demonstrated that vigorous exercise at depth reduces the regional propensity for vge in the exercised arm.

4. Vge are detectable in asymptomatic breath-hold divers following repeated and frequent excursions to 15 meters of water depth.

Special Animal Findings

1. Sheep have been established as a useful animal model for man in studying blood bubble formation following hyperbaric exposures.

2. Vge, in sheep, may persist for 72 hours without signs of decompression illness.

3. Sheep studies indicate that nigrogen vge do pass the pulmonary vasculature if intravenous nitrogen is injected at a rate exceeding 0.015 milliliter per kilogram per minute, and if the pulmonary systolic pressure rises above 35 mm Hg.

4. Air injected for 10 minutes at rates which do not produce arterial gas emboli in sheep will be passed across the pulmonary vasculature upon compression to 100 feet sea-water pressure.

Instrumentation

1. The doppler ultrasonic flowmeter and a variety of detectors has been specially adapted to the detection of blood bubbles using transcutaneous, catheter tip, and surgically implanted cuffs.

2. Several schemes for counting doppler blood bubble signals have

been investigated, including the phase lock loop, the IEM&P-Reid Doppler Flowmeter, as well as various band passed zero crossing techniques.

3. Unique instrumentation in hyperbaric facilities has been developed over the course of these studies, including a method of calibrating and evaluating decompression meters in the field.

4. A dual-lead low capacitance radio frequency isolated through-hull has been developed which is isolated from the chamber shell.

5. We have devised and put into operation a rate-of-change indicator to assure more constant and controlled rates of "descent" and "ascent" during hyperbaric chamber experiments.

6. A method of lighting hyperbaric chambers from external port-focused lamps has been developed.

I.

DOPPLER ULTRASONIC DETECTION OF VASCULAR GAS EMBOLI

A. HISTORY

Respiration in hyperbaric atmospheres requires protection from oxygen toxicity. This is conveniently provided by dilution of the oxygen with mixtures of "inert" gases. These inert gases, such as nitrogen and helium, are not consumed by the body, but dissolve from the lungs into the blood and tissues without harm if partial pressures do not exceed narcotic levels. During decompression, when the pressure grsdients of the gases are reversed, the inert gases are prone to evolve from solution forming gas bubbles. It is generally agreed, since first proposed by Bert and Haldane, that expansion of these bubbles and the interruption of local circulation is the primary etiology of bends and decompression sickness.

Diagnostic devices are greatly needed which will detect the presence, size, and number of both static and moving decompression bubbles. The doppler ultrasonic blood flowmeter represents a sensitive device to detect the presence of moving intravascular gas emboli. Its usefulness rests primarily on its objectivity, simplicity of operation, its adaptability for transcutaneous and noninvasive detection and its reliability in detecting venous gas emboli (vge) before development of decompression illness. As a research tool, the ultrasonic blood flowmeter can be used to elucidate the events related to bubble nucleation, circulation and dissipation. Special modifications that make it a useful tool for developing safe, efficient decompression proceuures, include the diagnosis and treatment of bends and aeroembolism. It also possesses a potential, through wise usage, in the prevention of bends and bone necrosis in divers and caisson workers.

The use of doppler ultrasound for bubble detection is an application of the doppler ultrasonic blood flowmeter first proposed and demonstrated to be useful for the cardio-vascular system by the Japanese worker, Satomura, (1957). In the United States, this technique was introduced by Franklin, Schlegal and Rushmer, (1961). In brief, it involves irradiating the body with high frequency sound, nominally between 5 and 10 Megahertz, and receiving the reflected signals scattered from moving acoustical interfaces. When compared with the transmitted frequency, the backscattered frequencies provide the different frequencies which are in the audible range. As a blood flowmeter, the interfaces are primarily blood cells and the received doppler shifted frequency spectrum is interpretable as the velocity distribution of flow streams under the ultrasonic beam. In the case of motions of the heart and vascular walls, the interfaces are represented by the walls of the heart chambers and blood vessels.

During the course of early attempts to calibrate doppler flowmeters in vitro, inclusion of micro bubbles in the blood, milk or other particulate fluid produced annoying artifacts as they passed the transducer. The best calibrations of doppler flowmeters are now produced by comparison with simultaneous electromagnetic blood flow recordings.

All surgical doppler flowmeters serve somewhat as blood bubble detectors, but transcutaneous instruments possess several drawbacks. Among these is the tendency of bubble signals to overload the electronic circuits. A wide dynamic range incorporated in the IEM&P circuits circumvents this problem. Also, most previously available doppler flowmeters used very small crystal elements in their transducers because larger crystals possessed low impedances which were difficult to operate with simple electronic schemes. The IEM&P electronic circiuts have solved this impedance matching problem for large sized crystals and gain the advantage of monitoring large blood vessels as well as small.

The ability to operate larger crystals with improved signal-to-noise ratios

has materially improved the blood flow measuring abilities of doppler ultrasonics. Other doppler blood flowmeter advances in this institute have, by their association with the blood bubble detection problem, taken place more rapidly. These include single crystal operation; solution of the problem of variation of transducer frequency by use of plug-in crystal oscillators which also provide a more stable frequency; the use of integrated circuits; a better understanding of transducer dynamics; and improved flow calibration testing by expert use of the square wave electromagnetic blood flowmeter.

The first use of the doppler ultrasonic flowmeter for objective detection of circulating decompression gas emboli moving in the flow streams of the larger arteries and veins was that of Spencer and Campbell, (1968). Gillis, Peterson, and Kargianes, (1968,) following our lead, reported similar findings in swine. Circulating gas emboli were also found at the time of open-heart surgery in the cardio-pulmonary by-pass circuit and in the heart and carotid arteries after closure; Spencer, Lawrence, et al, (1969). The first decompression investigations performed on sheep disclosed that decompression gas emboli were obliterated by hyperbaric recompression, but arterial bubbles without adequate treatment caused death following convulsions and unconsciousness. Venous gas emboli (vge) signals are shown in Figure 1.

Early attempts to demonstrate venous gas emboli in human subjects, (Fig. 2) on exposures and tables producing positive results in animals, were dissapointing, Spencer, Campbell, Sealey, et al, (1969). None were unequivocally detected in the peripheral veins in the extremities and neck using transcutaneous detectors, even though signs and symptoms of decompression occurred. The first recognized human decompression vge are now known to have been heard in 1968 on diving instructor Spencer Campbell following decompression on the U.S. Navy tables of exceptional exposures after 200 feet for 30 minutes. They were not clear-cut chirps and whistles, and therefore were questioned at the time. Later results

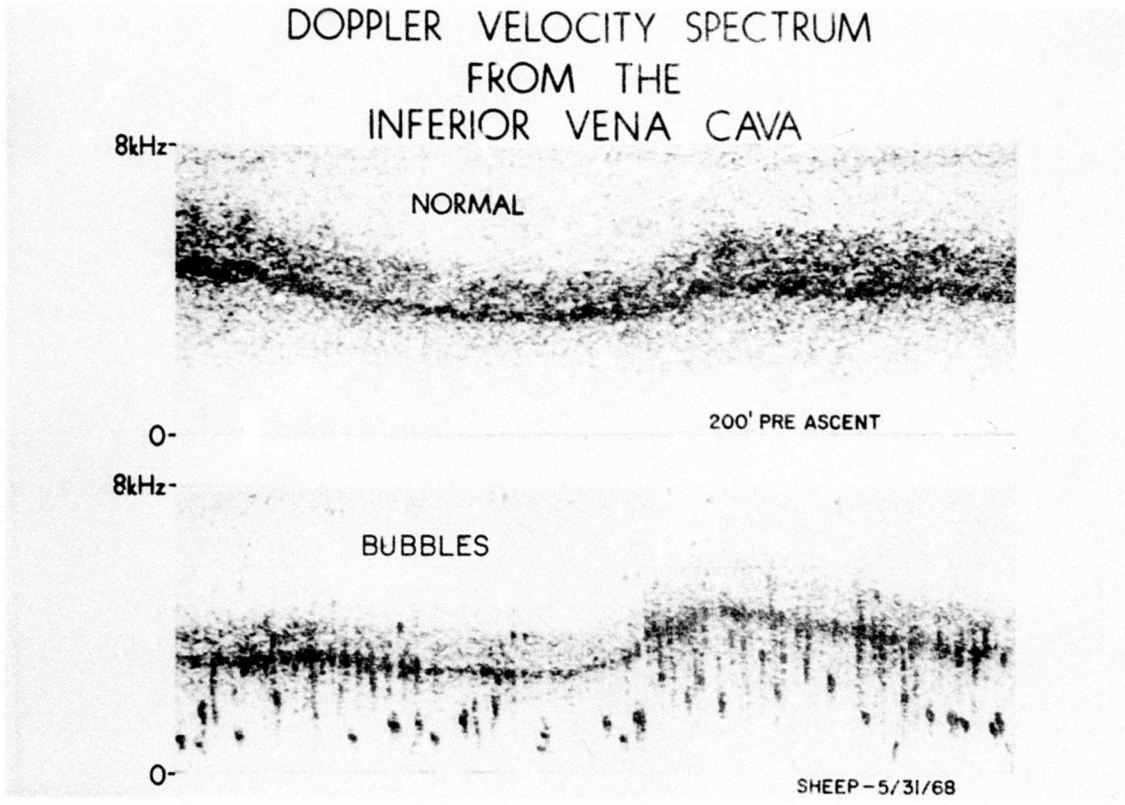

Fig. 1. Two and one-half second interval strips showing normal flow and bubble signals in the vena cava of a sheep.

Fig. 2. Lindbergh and Campbell in 1968 listening over peripheral veins for bubble signals using 10MHz doppler unit.

have shown that the quality of loud clicks, such as heard when listening on Campbell, are produced either by large bubbles or by non-optimal positioning of the transducer. A 60 degree angle with the blood vessel, rather than a more acute angle, allows the development of more easily recognized whistles and chirps. The second instance of human blood bubble signals occurred in the subject's right brachial vein, downstream to the upper-arm site. The signals were produced after redness and pain were produced by a 15 minute excursion to 300 feet and following decompression, according to the U.S. Navy Manual. After the subject developed a mild muscle pain and redness of the skin of the right upper arm, the brachial vein was found to provide many gas embolic signals, while the left arm was asymtomatic and yielded no embolic signals. After recompression to 60 fsw, the embolic signals entirely disappeared along with the pain and redness.

At this time, we fully realized the necessity of developing a precordial detection scheme by which we could monitor all of the venous return within the right ventricle or pulmonary artery. This would allow us to detect the earliest developing gas bubbles immediately after their release into the larger veins. A suitable detector was designed by M.P. Spencer, and the large crystals in it were developed by Howard F. Clarke. Many other peripheral detectors and surgically implantable detectors have been developed in this laboratory as a part of this and other Institute engineering programs.

B. THE PRECORDIAL GAS EMBOLUS DETECTOR

The Transducer

The original Spencer Precordial Transducer, (Fig. 3) in use since 1970, consists of two ½ inch square piezoelectric crystals separated 1.3 cm and tilted at a 13 degree angle so that the ultrasonic transmitter and receiver beams, (Fig. 4) cross in a region 3 to 7 centimeters distant.

The essential advantage of this transducer is that it covers a large tissue volume at its focus, so that positioning is less critical and there is more assurance that the vge, if present in the pulmonary blood, will be detected. Since the directional properties of a piezoelectric crystal are the same when it is receiving sound as when it is transmitting it, this geometry defines a sensitive region shaped as a rhomboid having a rectangular cross section. As the sensitive area for this transducer lies well below the surface, it eliminates many large clutter signals from the motion of the outer wall of the heart and enhances the blood flow and bubble signals in the right ventricle and pulmonary artery.

The Electronics

The original electronics used with this transducer, which, in subsequent work, became known as the "model A", presented a number of drawbacks and difficulties. The device was sensitive to lead length and had such serious tendencies toward instability that it could not be depended upon to remain tuned. Moreover, the signal-to-noise ratio seemed to vary in a random manner. Under United States Navy contract number N00014-72-C-0095, these difficulties were remedied. The first modified version of the original "model A", incorporated a redesigned transmitter, designated "model AB". A completely redesigned unit called "model B" incorporated redesign of both transmitter and receiver.

Redesign of the transmitter in "model AB" consisted of replacing a single

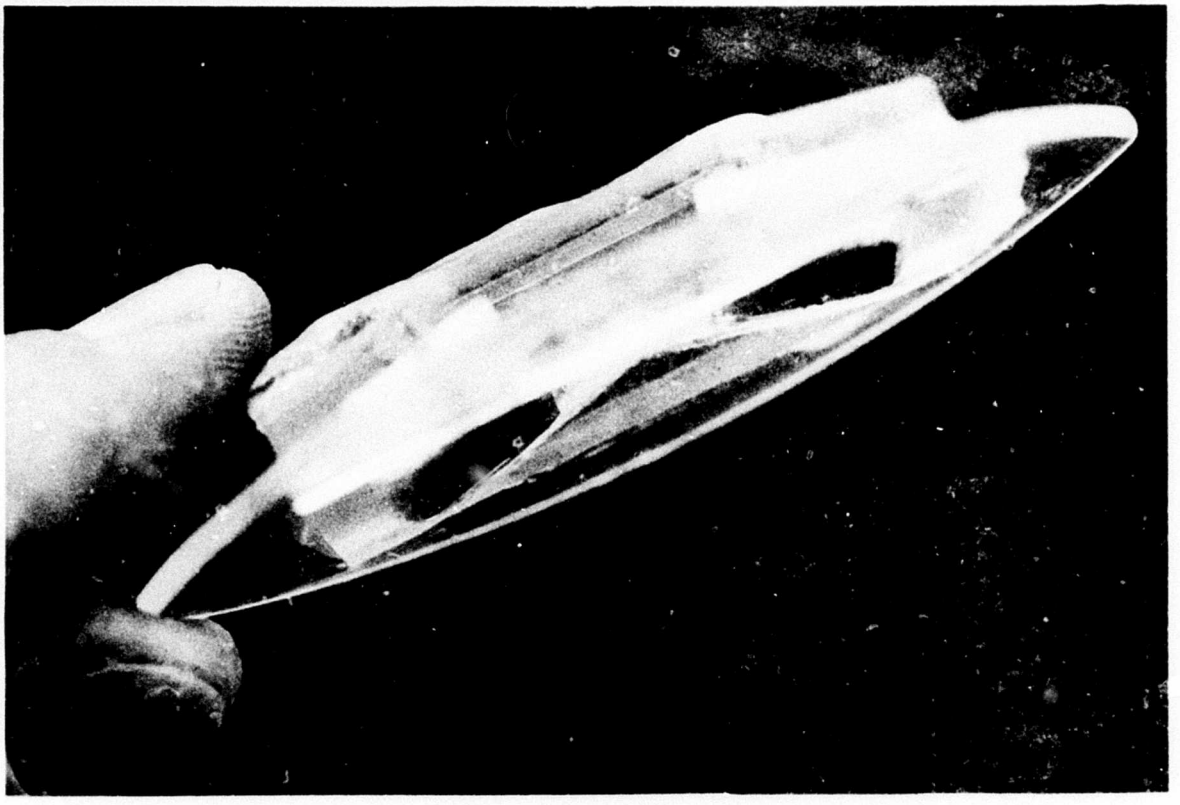

Fig. 3. Precordial doppler probe. Side view showing overall configuration and angle of crystal mounting to achieve 5cm focus.

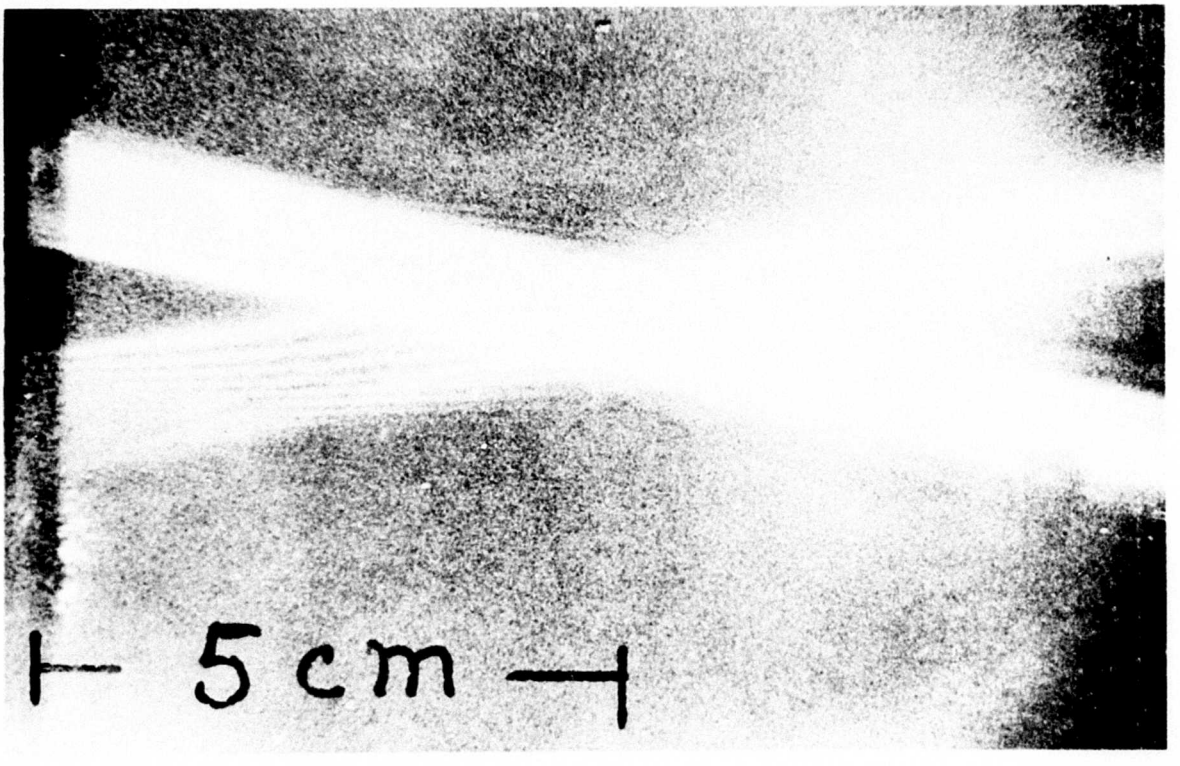

Fig. 4. Schlieren picture of radiation pattern of deep 5 cm focus of crystals.

transistor in the "model A" with a field effect transistor oscillator which was more stable in frequency than the single transistor of the "model A". The buffer amplifier following the oscillator presented a constant load to the oscillator, and accommodated great variations in the lead length of the transducer. Changes in electrical characteristics caused by mechanical loading changes do not affect the redesigned transmitter which can, in addition, be tuned easily and smoothly across the frequency range of a variety of transducers.

Redesign of the receiver produced "model B" (Figs. 5 & 6), and was aimed at eliminating sensitivity to lead length and tuning instability. It was concluded that instability of the "model A" lay in the use of handmade coils and use of a regenerative receiver. Commercially available, individually shielded coils were substituted for tuning in both transmitter and receiver. They are built to confine the magnetic field of the coils to their ferrite cores and are well shielded. The use of the coils has eliminated the regeneration and stabilized the receiver.

An additional feature of the redesign is the matching of the transducer, the transmitter and the receiver to a value of 50 ohms, purely resistive. Since the characteristic impedance of the majority of radio frequency transmission lines now on the market is 50 ohms, modern test equipment is more applicable in construction, maintenance and repair. Also, since standard coaxial leads have a 50 ohms characteristic impedance, lead length is not a critical factor in practical use. Matching of impedances also improves the signal-to-noise ratio of the receiver and increases the efficiency of the oscillator.

Matching the Ultrasonic Crystal Impedance

To accomplish the 50 ohm impedance advantages, we incorporated a bipolar transistor in the grounded base configuration at the input of the receiver. This transistor has an input impedance inversely proportional to the collector current. An additional advantage in using the bipolar transistor in this grounded base configuration is that it provides the system with better high frequency char-

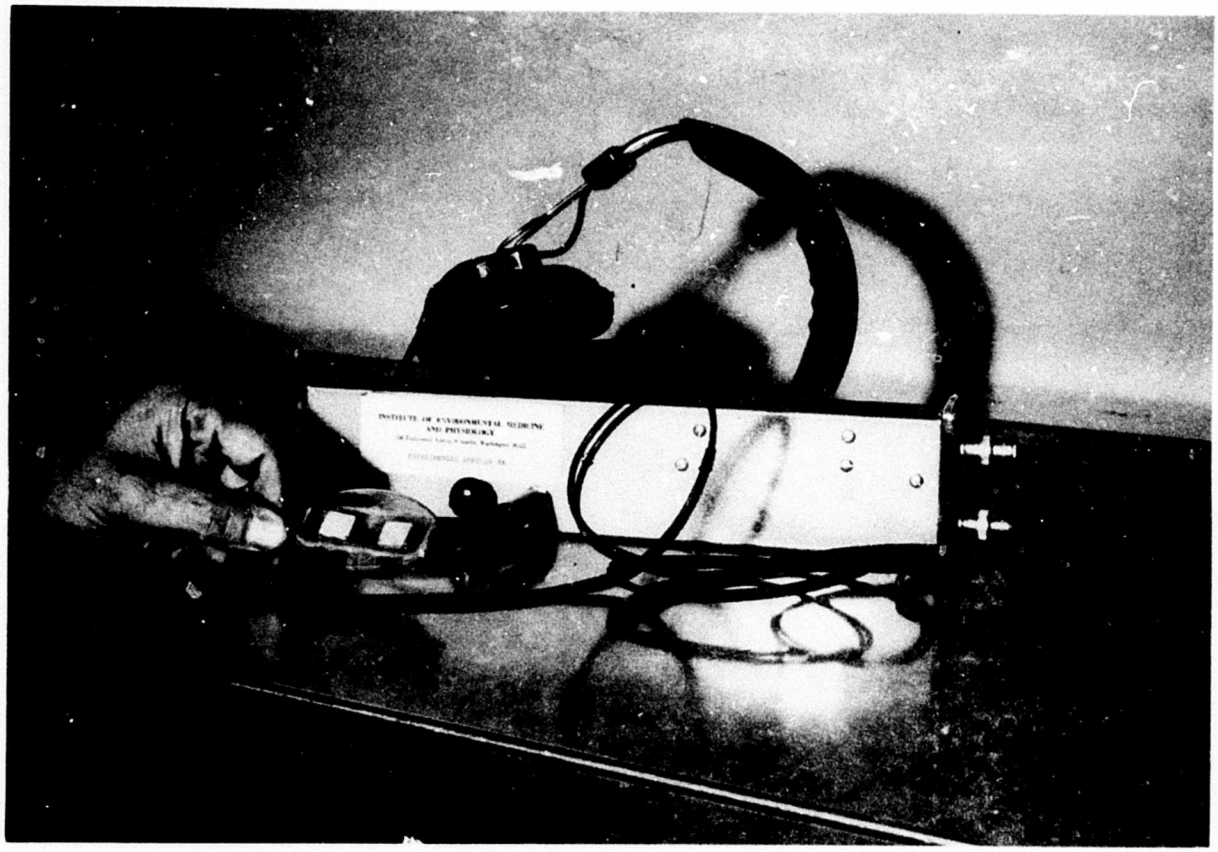

Fig. 5. The completely assembled I.E.M.&P. Doppler ultrasonic blood bubble detector ready for use.

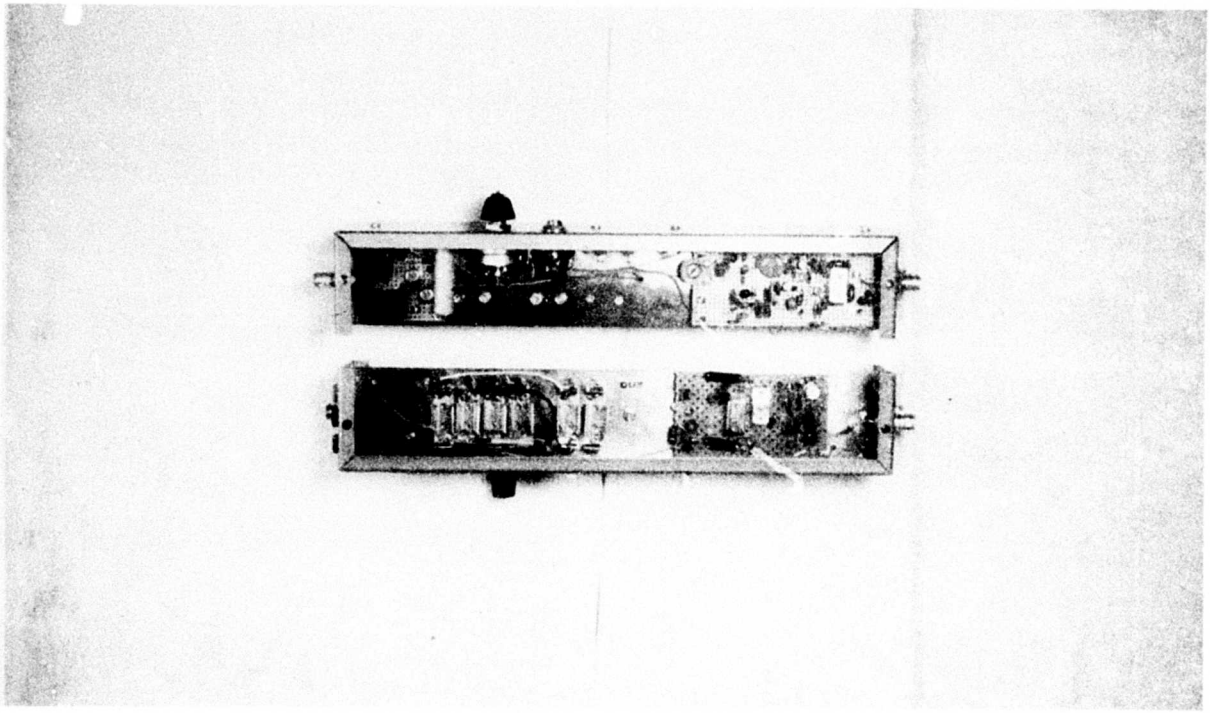

Fig. 6. Interior of the Model "B" Doppler showing the electronics divided by a copper ground plane. For purposes of shielding, the transmitter and receiver are on opposite sides of the ground plane.

acteristics than normally achieved in the usual grounded emitter circuits.

The second stage is a conventional resistance coupled amplifier, followed by one stage of cascade which, in turn, is followed by an emitter follower buffer. The receiver of the "model B", as a whole, has less gain than the "model A" receiver, but gives better overall performance. Figure 7 represents the circuit of the "model B" electronics. Figure 8 represents an electrical model of a piezoelectric crystal.

To match the transducer to 50 ohms, we made use of a mathematical cut-and-try procedure. After the probe is constructed, the crystal's active frequency is determined by the dimple test procedure described further on in the text. The active values of impedance around the mechanically active point are measured on a vector impedance meter and plotted in polar form, (Fig. 9). This gives the impedance in polar form:

$$\overline{Z} = Z\underline{/\theta}$$

which is converted to the usual complex form:

$$\overline{Z} = R + j\omega x$$

We then empirically choose a small reactive element in series with the transducer and another in parallel with this series combination, and calculate the resulting impedance, (Fig. 10).

The reactances are added one at a time. For example, if the transducer impedance above measures 13 ohms with a phase angle of minus 10 degrees, this is 12.8 - j2.26. Since it is desired to transform this to 50 ohms, this means a step-up circuit configuration is necessary, (Fig. 10). The inductance is added first, its value being selected by experience. For example, let .5 microhenry be added; this has an inductive reactance at 5 Megahertz of 15.7 ohms, so that when added to the transducer crystal, the total series impedance is 12.8 + j13.4y. If the admittance of this be taken, it is 6 = .037 -j.039. Since the -j.039 can be cancelled with a shunt capacitor, the resulting series impedance will be 27 ohms. Since this is the right direction, this confirms the correctness of this kind of network,

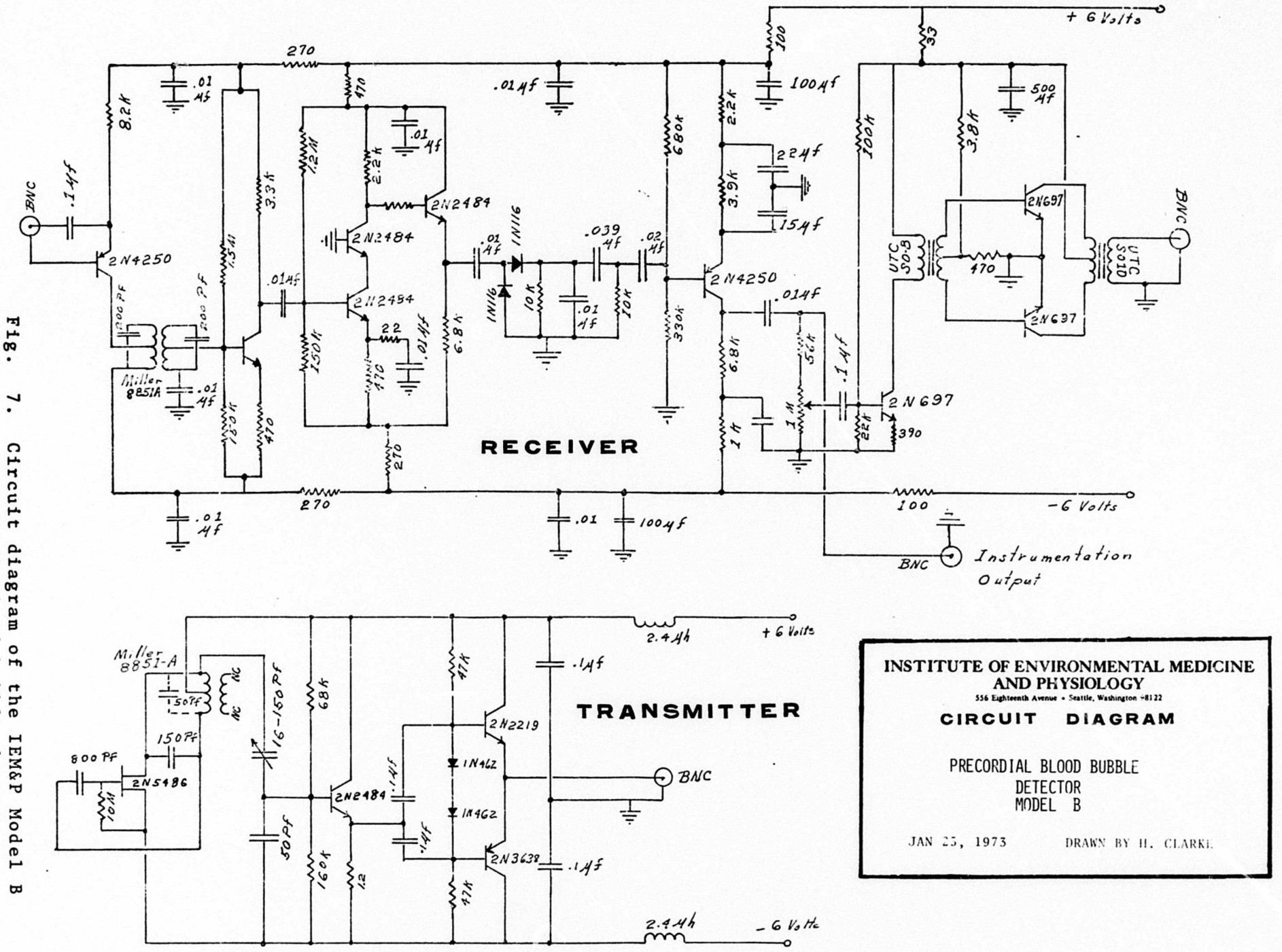

Fig. 7. Circuit diagram of the IEM&P Model B precordial blood bubble detector.

INSTITUTE OF ENVIRONMENTAL MEDICINE AND PHYSIOLOGY
556 Eighteenth Avenue • Seattle, Washington 98122

CIRCUIT DIAGRAM

PRECORDIAL BLOOD BUBBLE DETECTOR
MODEL B

JAN 25, 1973 DRAWN BY H. CLARKE

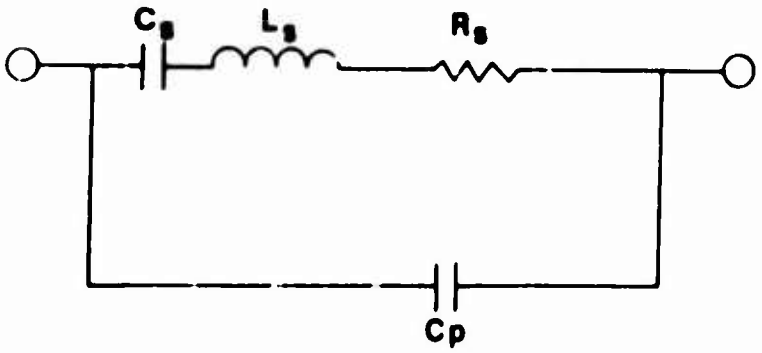

Fig. 8. Schematic diagram of equivalent electrical circuit representing a piezoelectric crystal.

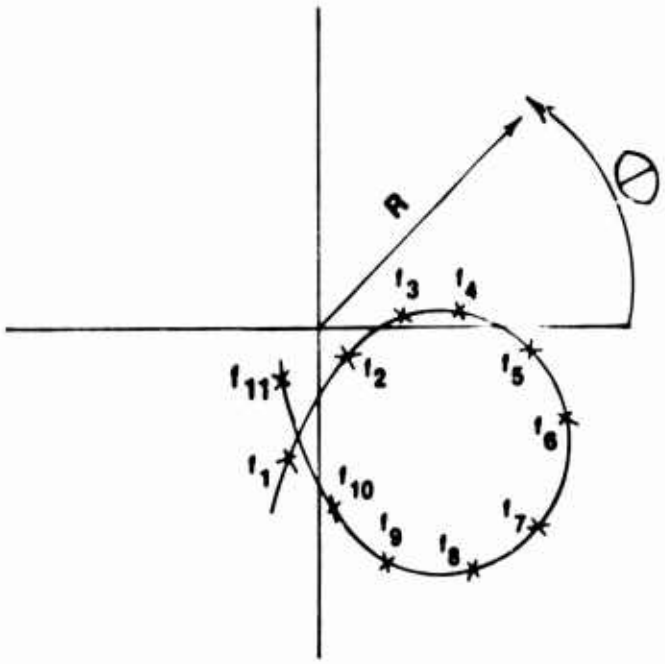

Fig. 9. Polar impedance plot of a piezoelectric crystal. R = radius, θ = the angle as measured from the axis, f1-11 = frequencies at selected measurement points.

but says a larger one should be used. Instead of the .5 microhenry inductor, let a .75 microhenry inductor be placed in series with the crystal. This gives a series impedance of 12.8 + j21.3, or a shunt admittance of .0207 - j.0344. Since the reciprocal of .0207 is 48.3, this will be a sufficiently close match. There remains only to apply a shunt capacitor to cancel the admittance of j.0344, which at five megahertz is .001 microfarads, leaving a transducer with a matching network having at five megacycles an input impedance of 48.3 ohms of pure resistance.

If the real value of the transducer impedance is too large, the procedure is exactly the reverse: a capacitor is added in shunt with the transducer and then a series inductor is used to follow it, (Fig. 11).

Although this method seems preponderous, it is, in practice, relatively fast, and has the advantage of being able to accomodate almost any kind of impedance transformation. Figure 12 illustrates a detector whose 50 ohms matching network is incorporated on its backside.

The "Dimple" Test for Resonant Frequency

The measurement of the mechanically active frequency of the transducer was tried by several different methods. Originally, a method called the dimple test was used, with the transducer in a dish of water. A simple version of the dimple test was found difficult to use at the energy levels desired and there was some uncertainty as to how trustworthy it was, (Fig. 13).

An improvement in the dimple test makes use of the fact that an ultrasonic wave, striking an interface of different sonic characteristic impedances, exerts a pressure on the interface. If the difference in the impedances is such as to give total reflection, the pressure upward from the bottom of a dish of water towards the surface produces a slight elevation in the surface of the water. The elevation, although very slight, is readily detected by looking at the reflection of a bright object in the surface. The reflection will be distorted

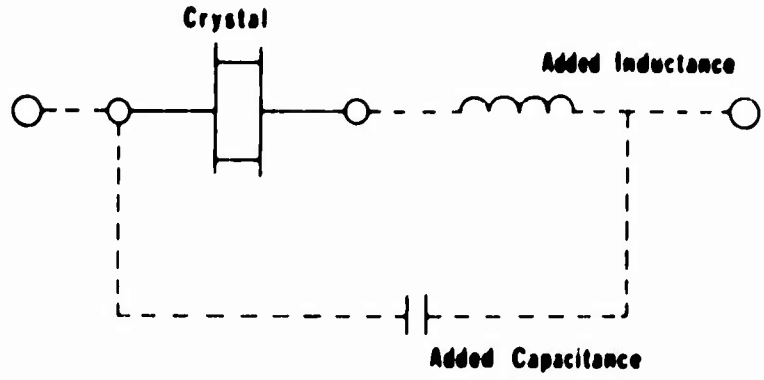

Fig. 10. Schematic diagram of a parallel resonant circuit for impedance transformation.

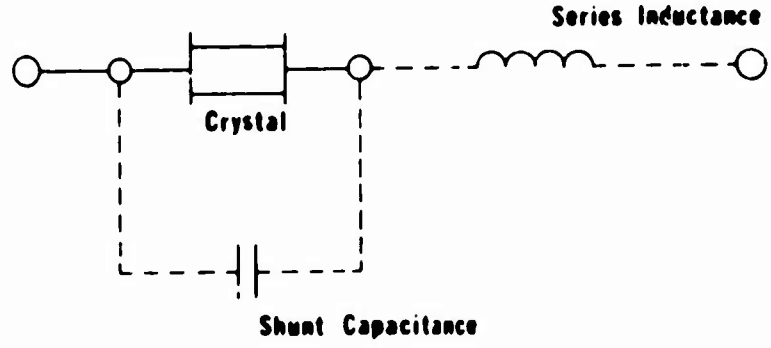

Fig. 11. Schematic diagram of a series resonant circuit for impedance transformation.

at the point where the ultrasonic beam strikes the surface, (Fig. 13).

In practice, the method was refined by the following procedure: the dish of water was replaced by a small aquarium with parallel plate glass sides. A sheet of ruled (graph) paper, to make a grating, was illiminated from behind with a lamp, and the image of the paper was observed as it was reflected from the water surface, (Fig. 14). This procedure is improved considerably by deeply coloring the water so that the only image seen when looking at the surface is the grating reflection. The image of the ruled paper will display a distortion similar to the "pin cushion distortion" of a simple lens, (Fig. 15).

The visibility of the distorted pattern can be further enhanced by amplitude modulating the power fed to the transducer by a frequency of about ten cycles; this produces waves which are easily detected at some distance from the tank. (The pattern seen in Fig. 15 is viewed at a distance of three feet.)

Quality Control

In working with the doppler units, the need often arises to evaluate the overall performance of one unit, as compared to another. The transmitter and receiver can be evaluated by use of oscilloscopes, voltmeters and signal generators, but this fails to take into account the interaction of the transducer with the electronics. It is desirable to have some method of comparing the overall performance of the combined electronics and transducer, as compared to another combination of electronics and transducer.

For this purpose, a method was first tried using the dropping of water onto the surface of a container, filled with water, in which was placed the transducer with its crystals pointing toward the surface, (Fig. 16).

With the transducer in the above position and the electronics turned on, one hears, as might be expected, an extremely loud sound at each drop of water. Layers of wet cloth are then successively laid over the transducer. It is found that the cloth acts as an attenuator on both the transmitted and received signals,

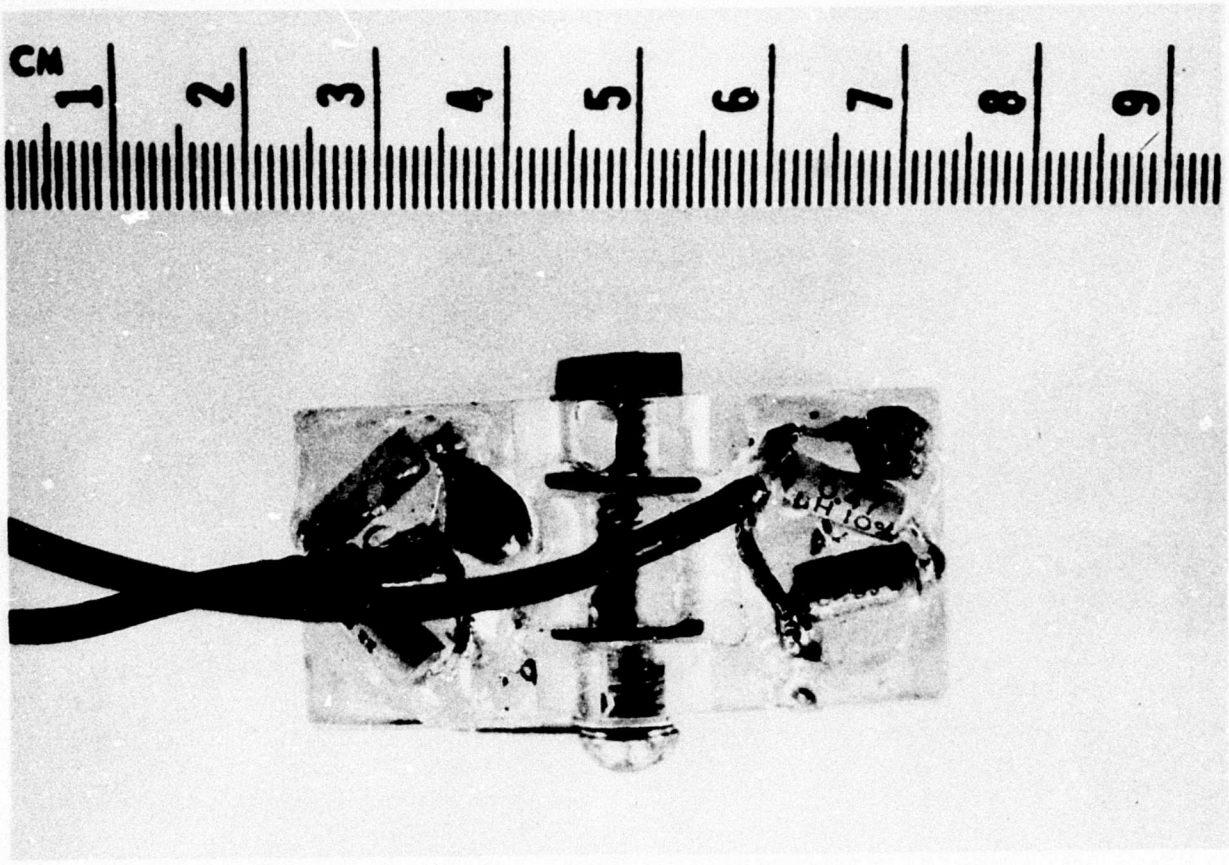

Fig. 12. Variable focus doppler ultrasonic transducer matched to 50 ohms. Matching network is visible on the backside of the transducer.

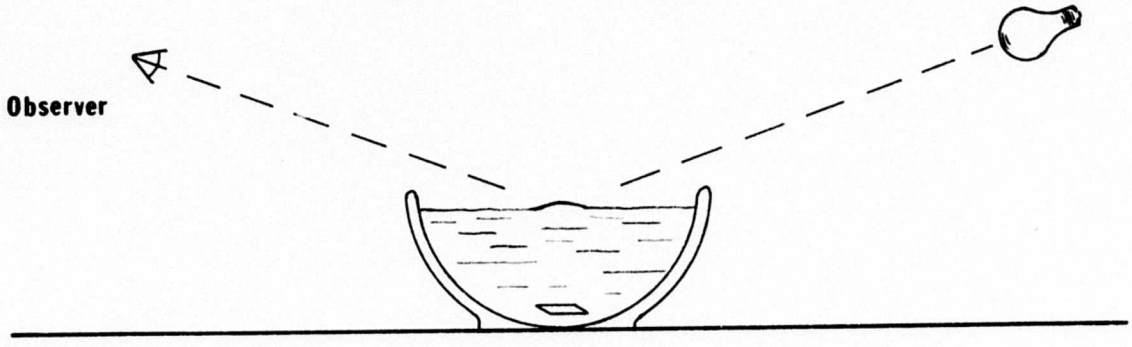

Fig. 13. Original version of resonant frequency test incorporating energized probe in a small dish of water with observation of water surface (at an angle to the reflected light) for maximum disturbance.

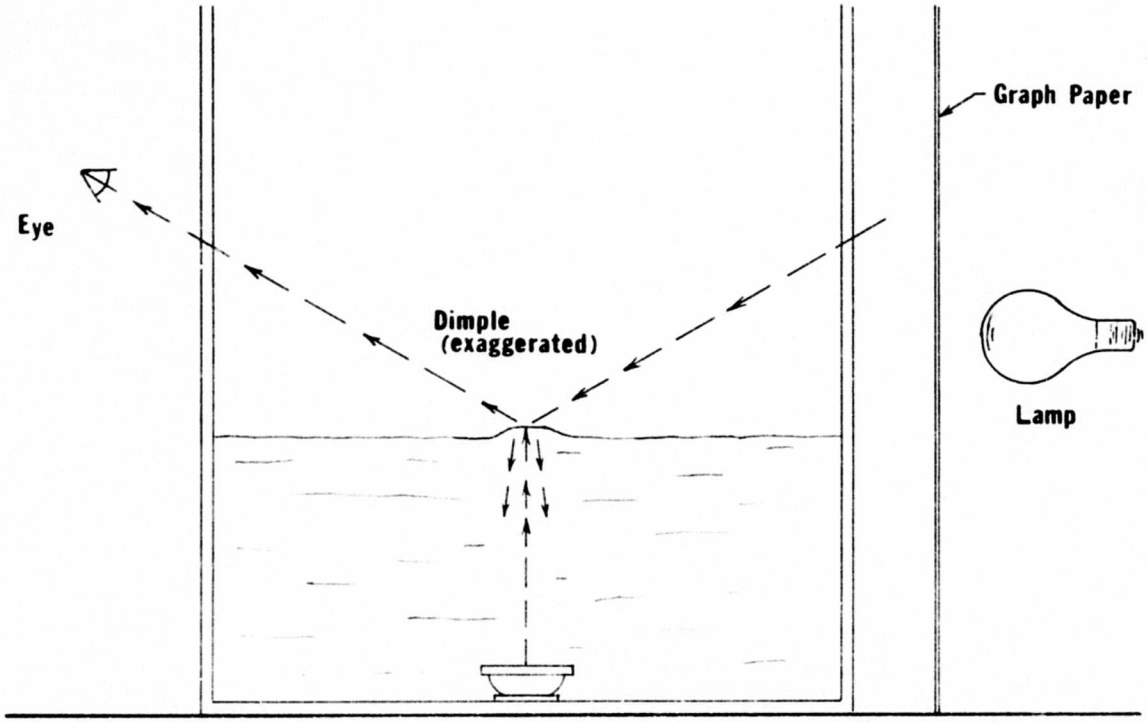

Fig. 14. Improved dimple test using graph paper rulings projected on the surface of the water.

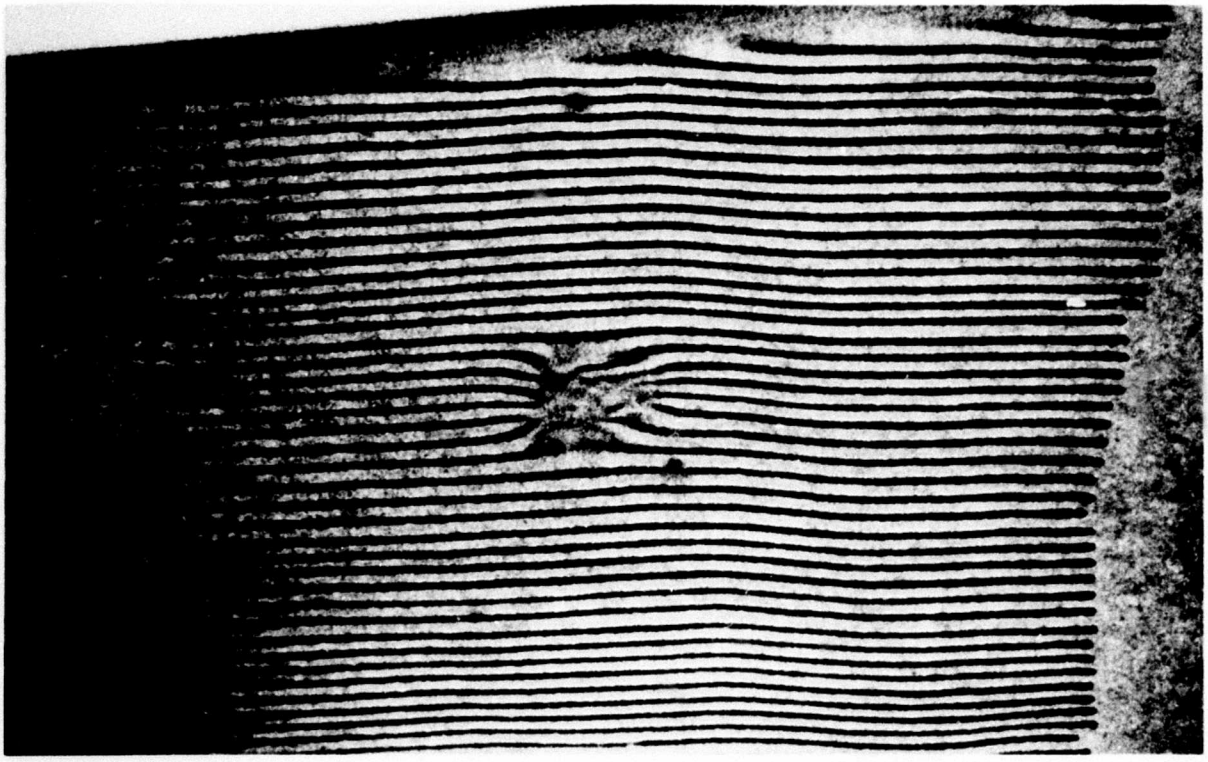

Fig. 15. Resultant dimple image using improved test. Maximum disturbance of reflected parallel lines represents area of resonant frequency.

and as successive layers of cloth are added, a thickness of cloth layers will be achieved where the signal fades out completely. The best doppler unit is the one requiring the greatest number of layers of cloth to bring the signal just to the point where it is lost in the receiver noise. Difficulties are encountered with decay of the cloth, but over a short period of several days, one may compare several units with this method.

A rather simple device, which eliminates the decay problem, may be made by attaching a small speaker of the kind used in intercom units to the bottom of a soft plastic jar. The jar is now filled with water, and the transducer is inserted facing downward toward the bottom of the jar, (Fig. 17).

If the speaker is set in motion, the driving frequency will be heard in the receiver output of the doppler unit. Because of standing waves of the five megacycle frequency, the transducer may be moved only slightly, to maximize the signal. Standing waves of the audio frequency driving the speaker are avoided by driving the speaker with a swept frequency, so that standing waves at any one frequency do not build up. With the doppler unit operating at full gain, the voltage of the swept frequency driver is diminished until the swept frequency is barely audible in the receiver noise. The device seems to give repeatable results, provided that the position of the transducer is maximized for the five megacycle standing waves as explained above.

Since the characteristics of the speaker will remain constant, this type of test apparatus does not give varying results with time as does the cloth method which is confronted with decay problems in the fabric. Further, since one nominally selects a speaker driving frequency which best activates the speaker in use, and since this will not change, a repeatable standard is available for testing the doppler units. The measurement itself is made by decreasing the voltage to the speaker until the transducer is no longer able to respond to it and all that remains is receiver noise.

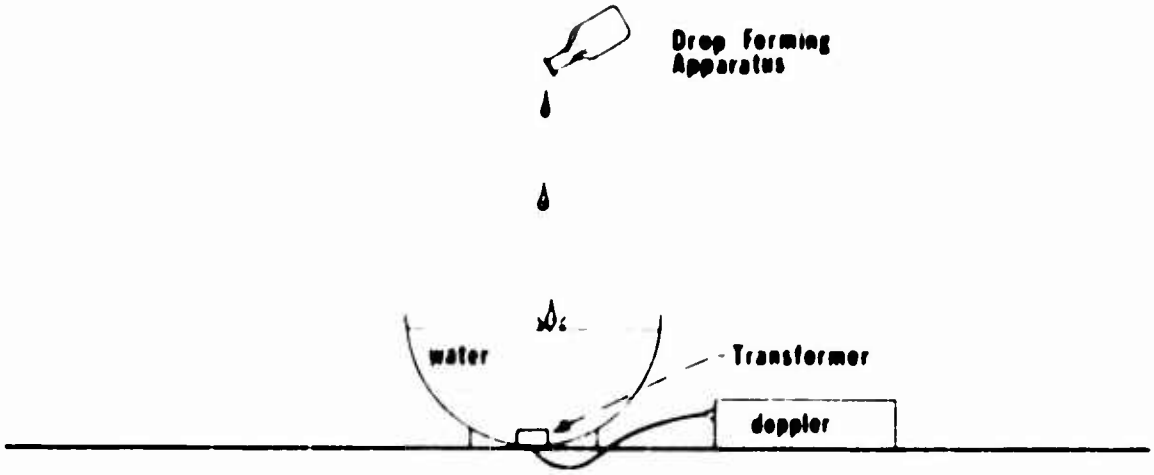

Fig. 16. Original method of measuring electronics/transducer sensitivity. Uniformness of driving signal (impact of falling water droplet) was not constant or repeatable.

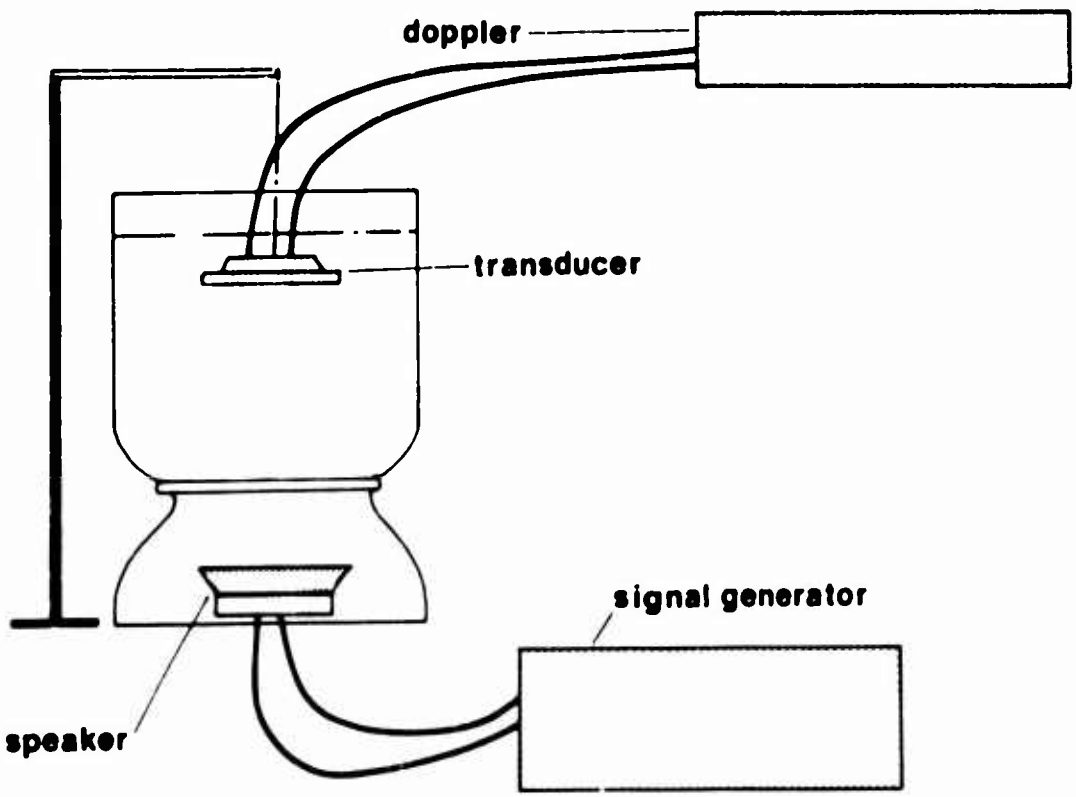

Fig. 17. Improved method of measuring doppler sensitivity. Signal generator produces constant, repeatable, and easily measured exciting signal.

Usage Technique for the Precordial Detector

Utilizing an acoustical coupling medium, the precordial sensor is applied along the left midsternal border, (Figs. 18, 19 & 20). To locate this position, a finger is run along either collar bone moving toward the center of the chest until the finger rests in a notch at the midline. This is the suprasternal notch of the sternum; at the lower (abdominal) end of the sternum is a wide and long (somewhat pliable) cartilaginous bone, the xiphoid process. By placing the finger of one hand on the xiphoid process and a finger of the other hand in the suprasternal notch, the mid-point between the two fingers can be estimated and the probe placed 1-2 inches to the left of this mid-point. The pulmonary artery and right ventricle lie just behind this left midsternal area. Through this part of the heart, all of the circulating blood flows on its way to the lungs. Any venous gas emboli in the venous blood from any part of the body will eventually pass through the right ventricle to the pulmonary artery, and therefore, must pass through the focal field of the transducer. The optimum probe position may vary for each individual, but due to the large crystals and their large focal volume, the positioning is not critical within 2 inches of the left midsternum point described.

The major normal sounds heard at the left midsternum, vary from 4-5 in number for each heart cycle, but are repetitious and regular, (Fig. 21). For an optimum position, move the probe around until a squeaking sound is heard as a regular part of the normal sounds. This sound represents the closure of the pulmonary valve. By exhaling and leaning forward in the upright position, the sounds become louder. A superimposed swishing or "breezy" sound represents blood flowing under the transducer.

A bubble or gas embolus sound may "chirp" with a singular quality very much like the valve closure signal, but the valve sound is regular in its

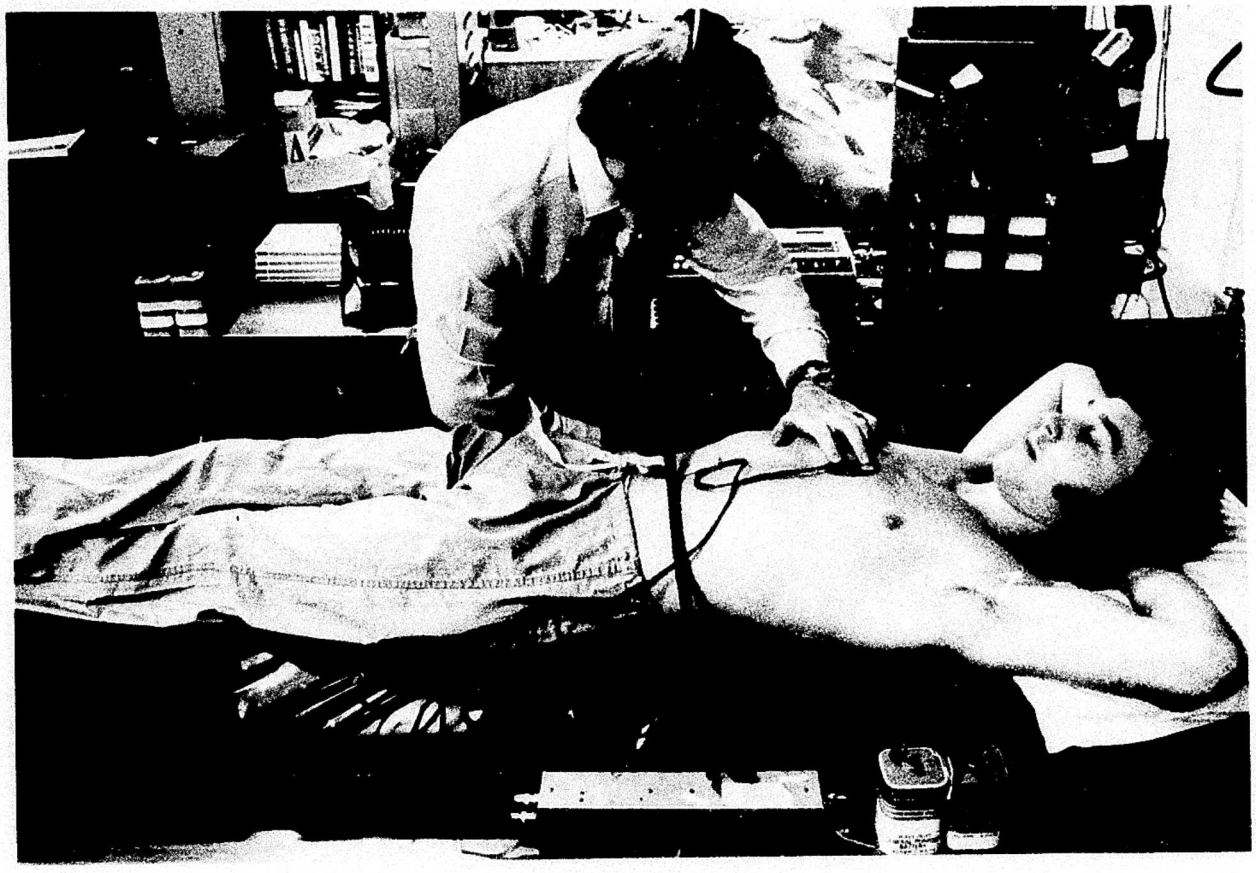

Fig. 18. Laboratory measurement of diver using precordial doppler following chamber exposure on experimental profile.

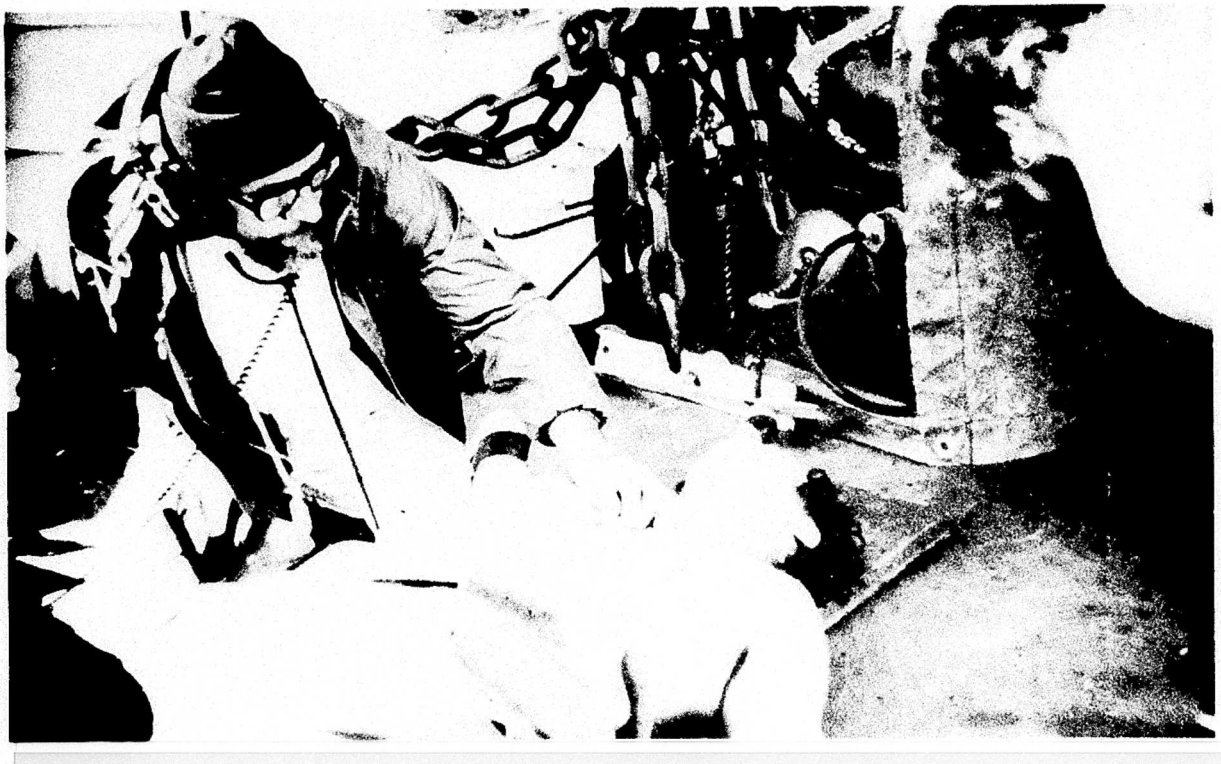

Fig. 19. Field use of precordial doppler. Bubble detection in surfaced diver confirms advisability of deck decompression treatment.

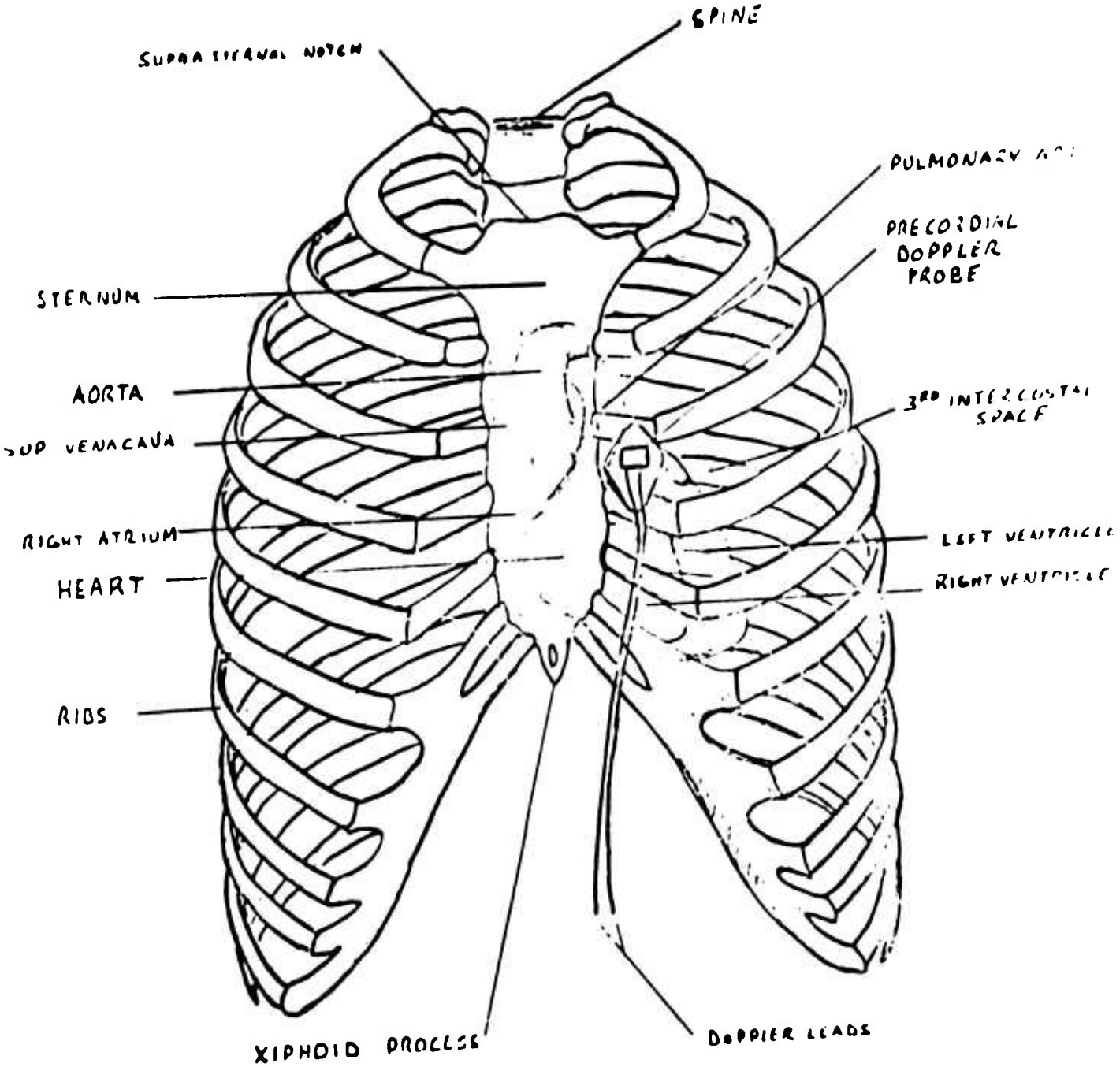

Fig. 20. Correct position of probe over the right heart outflow track immediately behind the left mid-sternal border.

occurrence, and it's regularity will help to differentiate the two signals. Sporadic bubble emboli, when there are few passing the sensor, are irregular in timing and may occur at any point in the heart cycle. (See "Interpretation of Signals" for further details.) Users of the doppler are advised to listen to many different normal individuals to both familizarize and satisfy themselves that they recognize the range of normal heart sounds. Such users will then be better qualified to recognize the earliest and smallest gas emboli signals.

After recognition of clear precordial gas embolism signals, the user may wish to substitute various peripheral probes and listen to the peripheral vessels to identify the region of bubble emission. With the peripheral probes, one can monitor the jugular, brachial and femoral blood vessels, as well as over the precordium.

Interpretation of the Precordial Signals

The Normal Precordial Signals. The left midsternal border is the preferred location of the precordial transducer, because the middle third of the border is contacted dorsally by the wal. of the right ventricle, pulmonary conus and main pulmonary artery, as well as the appendage of the right atrium. Figure 21 illustrates typical "dopplergram" precordial signals from this site. Correlations with the ECG wave form suggest these signals represent (P) contraction of the right atrium, (S) closure of the tricuspid valve, (S') systolic blood ejection, (V) closure of the pulmonary valve, and (D) peak diastolic inflow through the tricuspid valve.

Bubble Signals. In order to demonstrate the sounds of venous gas emboli, normal subjects may be administered 4 cc. of carbon dioxide by means of a sterile syringe and small needle inserted into a peripheral arm or leg vein. Medical supervision is advised, but no harm will result from embolization of small quantities of gas to the lungs. Figure 22 illustrates a control "dopplergram", as

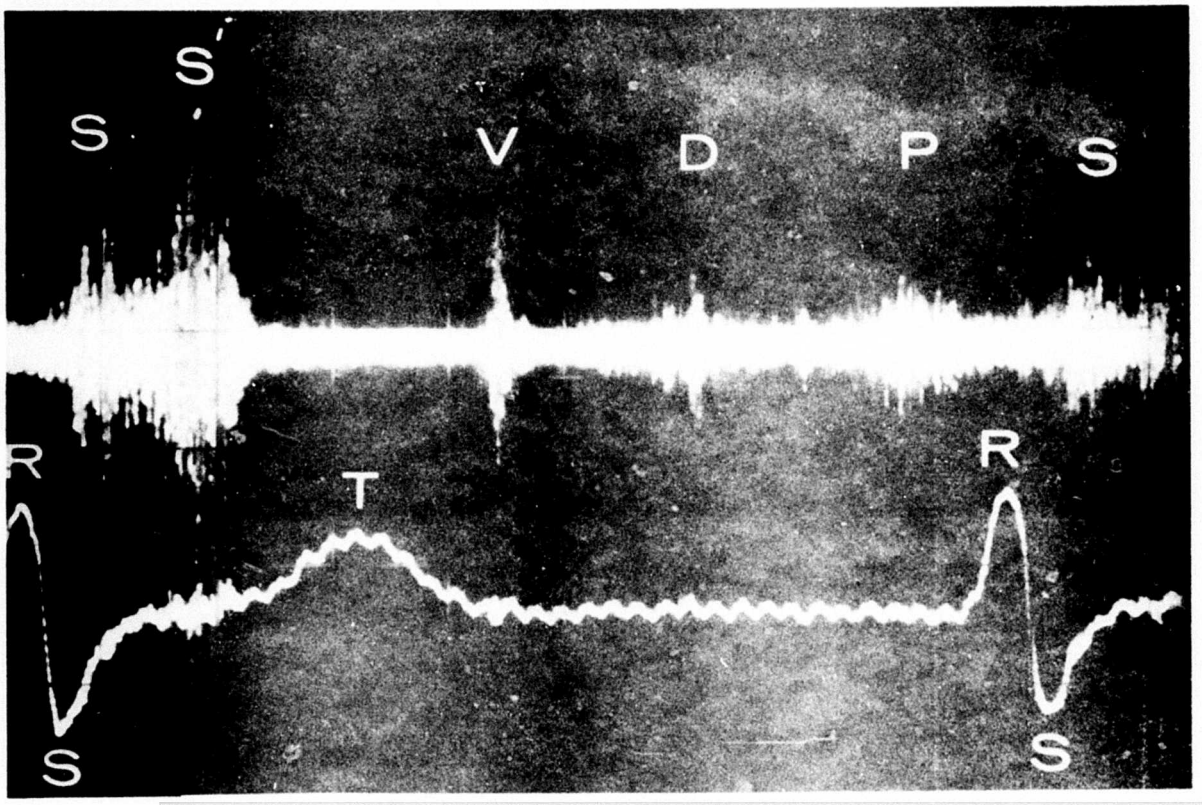

Fig. 21. Precordial ultrasonic "dopplergram". Comparison of the ECG tracing and the audio signal representing the cardiac cycle.

CONTROL

IV - CO_2

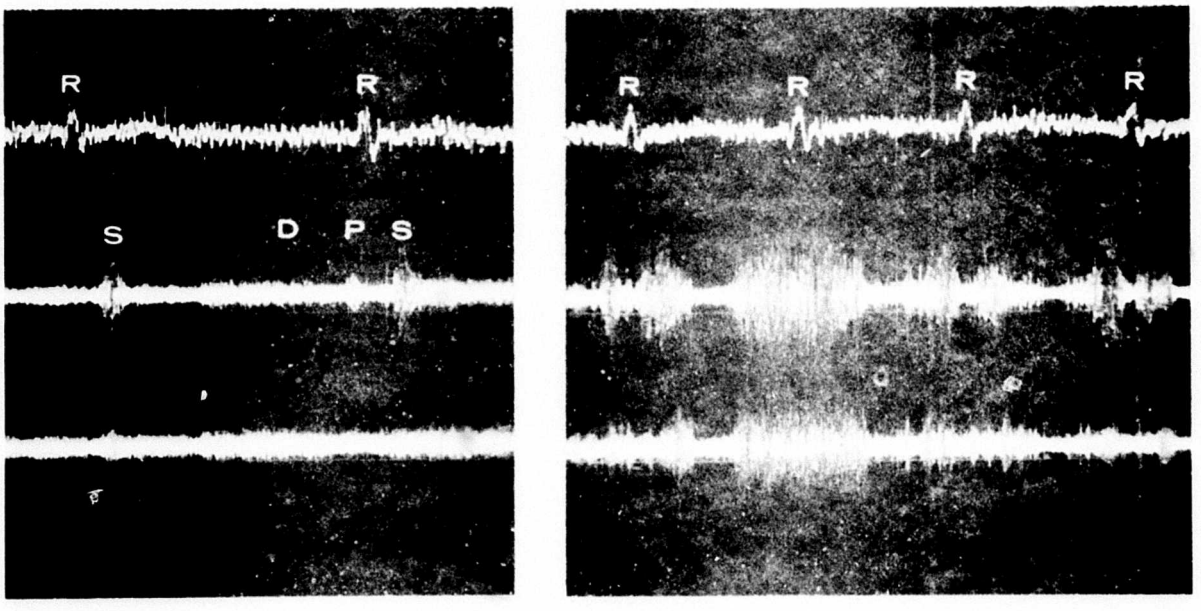

Fig. 22. Intravascular carbon dioxide signals on human precordial "dopplergram". Tachycardia at time of passage of gas was apparently due to apprehension of subjects. Upper tracing is electrocardiogram; middle and bottom tracings are "dopplergram" -- bandpass at 0.6KHz and 2-3KHz respectively.

well as the blood flow signals produced by the carbon dioxide as it passes beneath the precordial detector. The range of bubble sounds heard include discrete squeaks, chirps, clicks and more prolonged coarse sounds with large quantities of gas. The quality of the single bubble sound is dependent on the angle its pathway makes with the ultrasonic beam. If the bubble passes perpendicular to the beam, a click is produced; if it passes along the axis of the sound beam, it produces a chirping or whistling quality. The higher the velocity of the bubble, the higher the frequency or pitch of the chirp. Since the flow profile within a given blood vessel is made up of many different velocities, varying in time with the heart cycle or body motions, a shower of bubble signals will appear as a range of frequencies. If hundreds or thousands of bubble signals are superimposed, the signal will sound like a loud roar, regardless of the angle of the sensor beam.

For precordial signals, a zero to four scale for estimating bubble quantities is recommended. The subject should be breathing quietly and otherwise motionless in a sitting or supine position.

Zero - Is taken to indicate a complete lack of bubble signals.

Grade 1 - Indicates an occasional bubble signal discernable with the cardiac motion signal with the great majority of cardiac periods free of bubbles.

Grade 2 - Is designated when many, but less than half, of the cardiac periods contain bubble signals, singularly or in groups.

Grade 3 - Is designated when all of the cardiac periods contain showers or single bubble signals, but not dominating or overriding the cardiac motion signals.

Grade 4 - Is the maximum detectable bubble signal sounding continuously throughout systole and diastole of every cardiac period, and overriding the amplitude of the normal cardiac signals.

Further details on interpretation and use of gas emboli signals during decompression and in open heart surgery can be found in Section II--"A New Model

for Body Tolerance to Excess Inert Gas Methods", as well as in the references cited in the bibliography, section X.

C. PERIPHERAL DETECTORS

The first occurence of venous gas emboli is most reliably monitored with the precordial sensor because all venous return passes the right ventricle and pulmonary artery. A bubble signal is, however, usually more clearly separated from the background blood flow signal in the peripheral blood vessels because the cardiac motion signals often present a confusion factor. Peripheral detection of gas emboli is possible with special probes available for transcutaneous, catheter tip or perivascular implantation. Figure 24 illustrates a variable focus transducer whose depth of sensitivity can be varied by means of a hinge to listen to both deep or superficial blood vessels; also useful for very deep, as well as superficial vessels, is the single crystal detector shown in Figure 23. It is operated at 2.5 MHz for greater penetration, as well as to drive its one inch square crystal, which provides an exceptionally broad beam. A balanced bridge completion coupler is placed between the transducer and the electronics, similar to that used with the catheter tip detector described later.

Shallow focus 10 MHz transcutaneous detectors are illustrated in Figures 25 and 36. The depth to which one wishes to probe may determine the ultrasonic frequency and power required for driving the transmitter crystal.

Figures 27 and 28 illustrate the geometric and ultrasonic features of a dual crystal 5 MHz probe focused to 1.5 mm diameter at a depth of 2-4 cm by means of an epoxy lens. This design works very well to monitor a small volume of blood at the focus depth. For more general use over peripheral arteries and veins, a broader beam is more likely to intercept blood gas emboli. Such a detector is illustrated in Figure 29. It presents a geometry with 3/8" diameter crystals that represent a useful compromise between beam diameter and overall shape. It can be effectively used for precordial monitoring (Fig. 31), as well as for peripheral arteries and veins, (Fig. 32). The center focus is 2.5 cm.

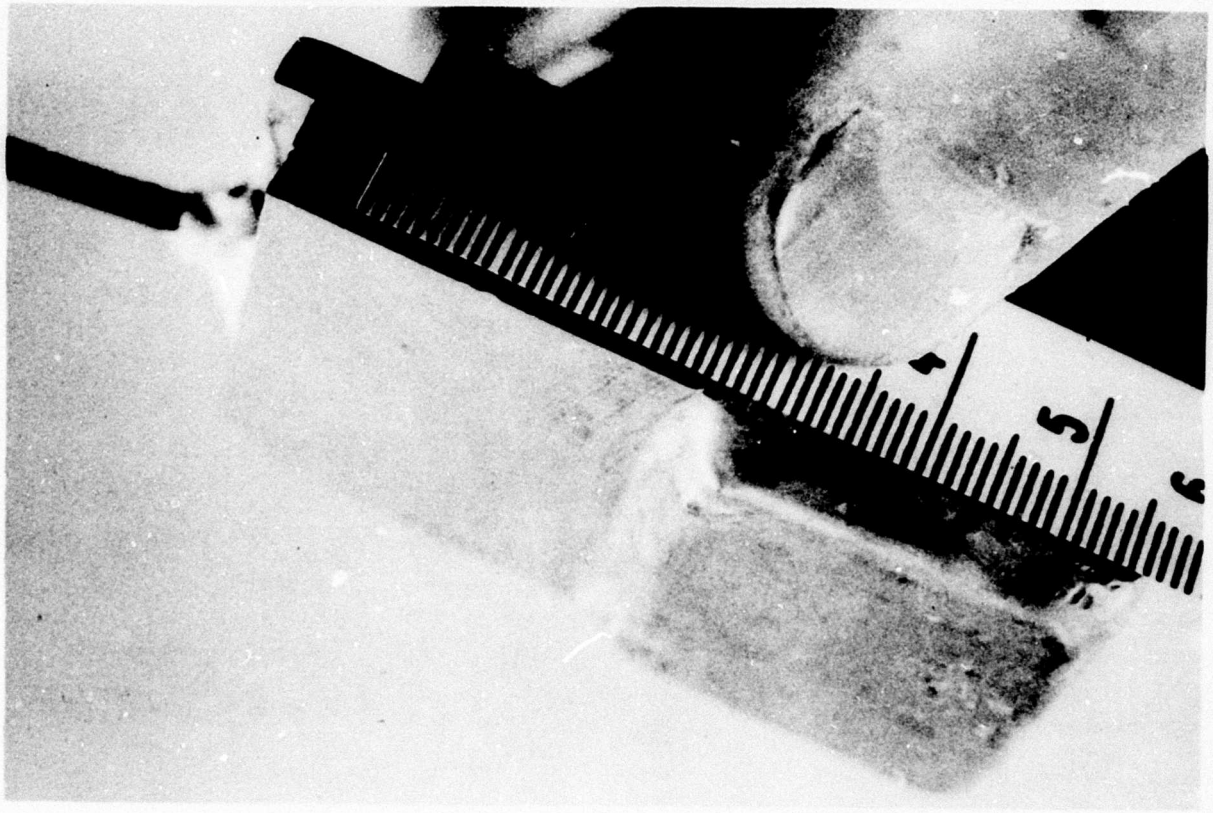

Fig. 23. Extremely large single 1 inch square crystal doppler flow sensor allowing detection of the deep vessels, vena cava and aorta.

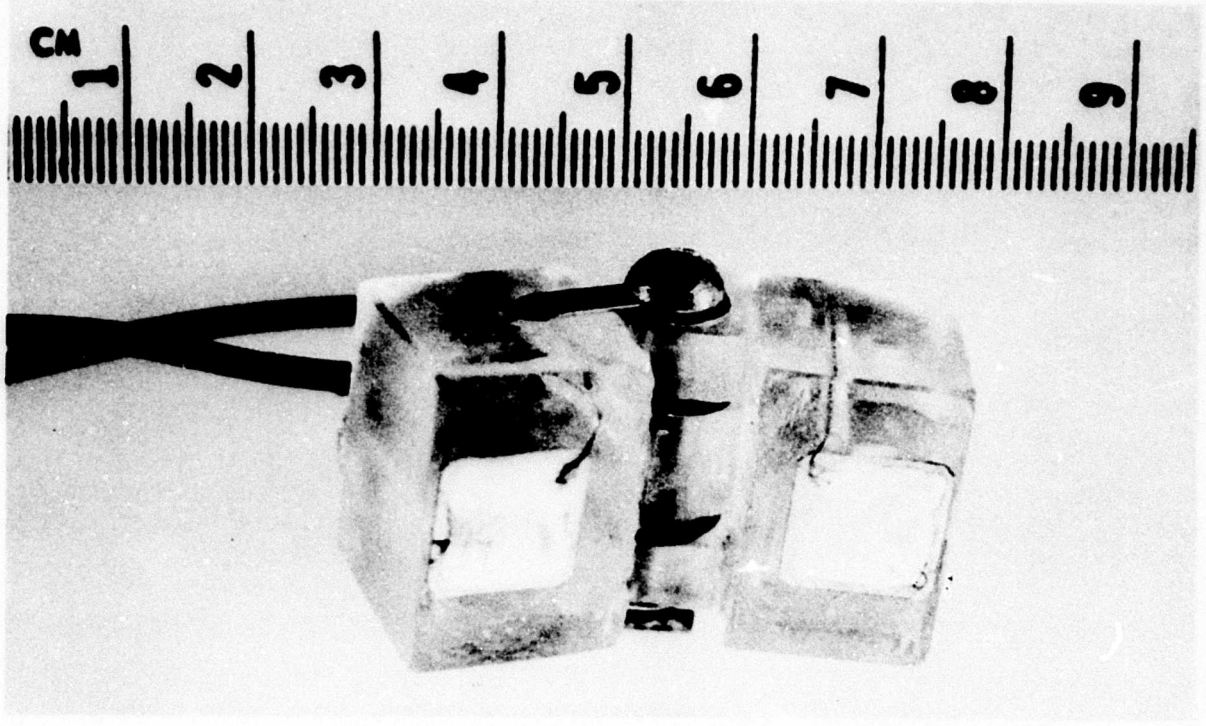

Fig. 24. Dual crystal hinged doppler flow sensor offers a wide range of focusing angles for varied depth of detection.

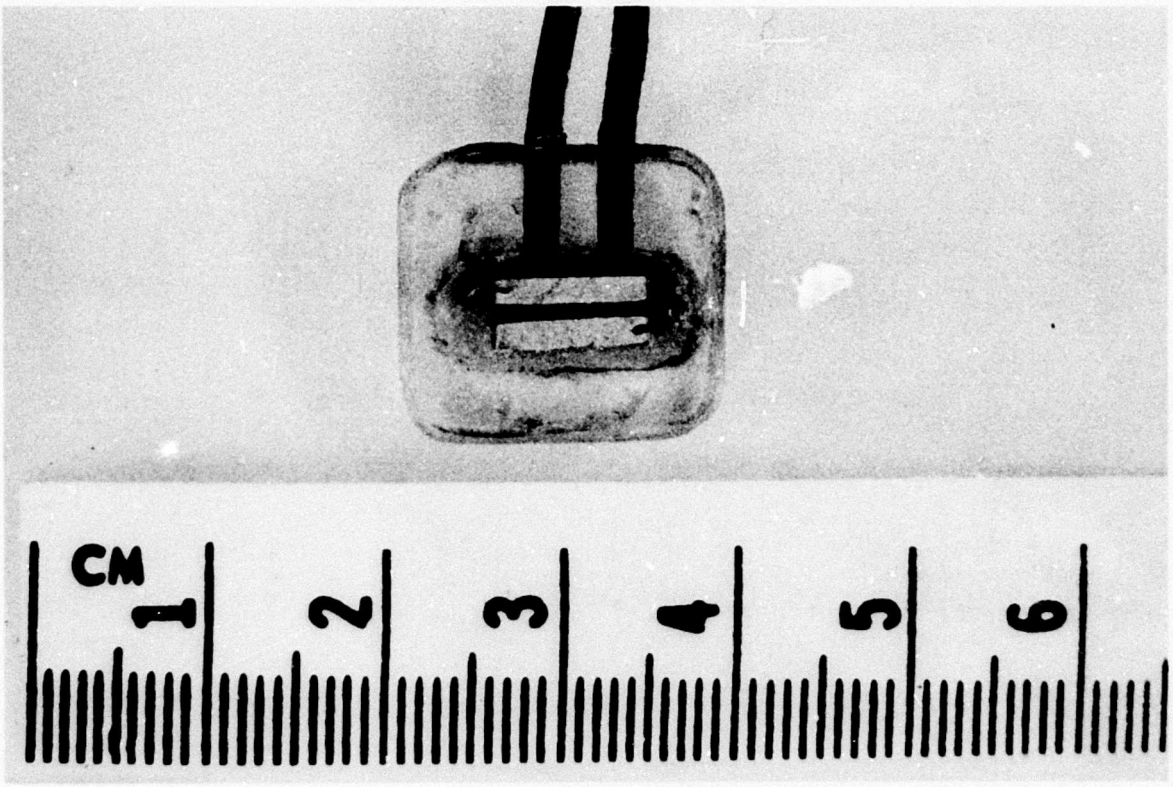

Fig. 25. Flat shallow-focus, dual crystal sensor for transcutaneous detection of blood velocity and gas emboli.

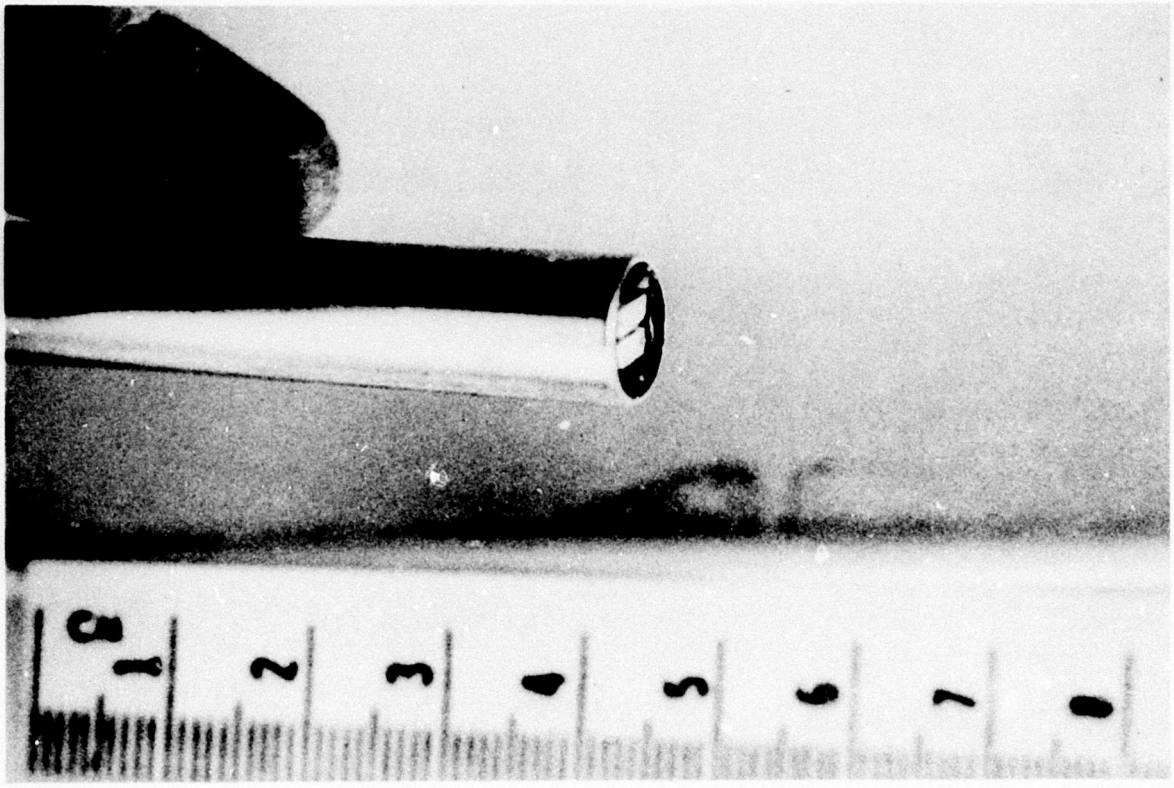

Fig. 26. Pencil shaped shallow-focus sensor for transcutaneous use, 10MHz crystals. (Parks Electronics)

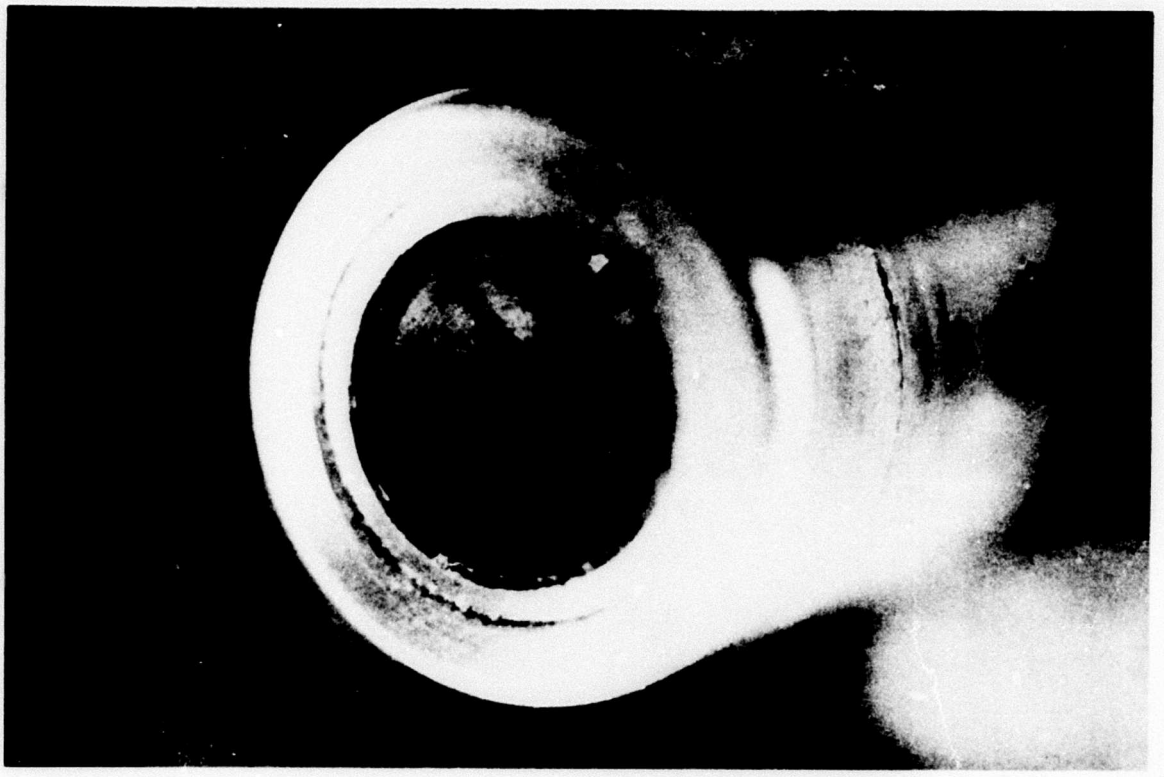

Fig. 27. Peripheral doppler probe dual-crystal lens focussing, end view.

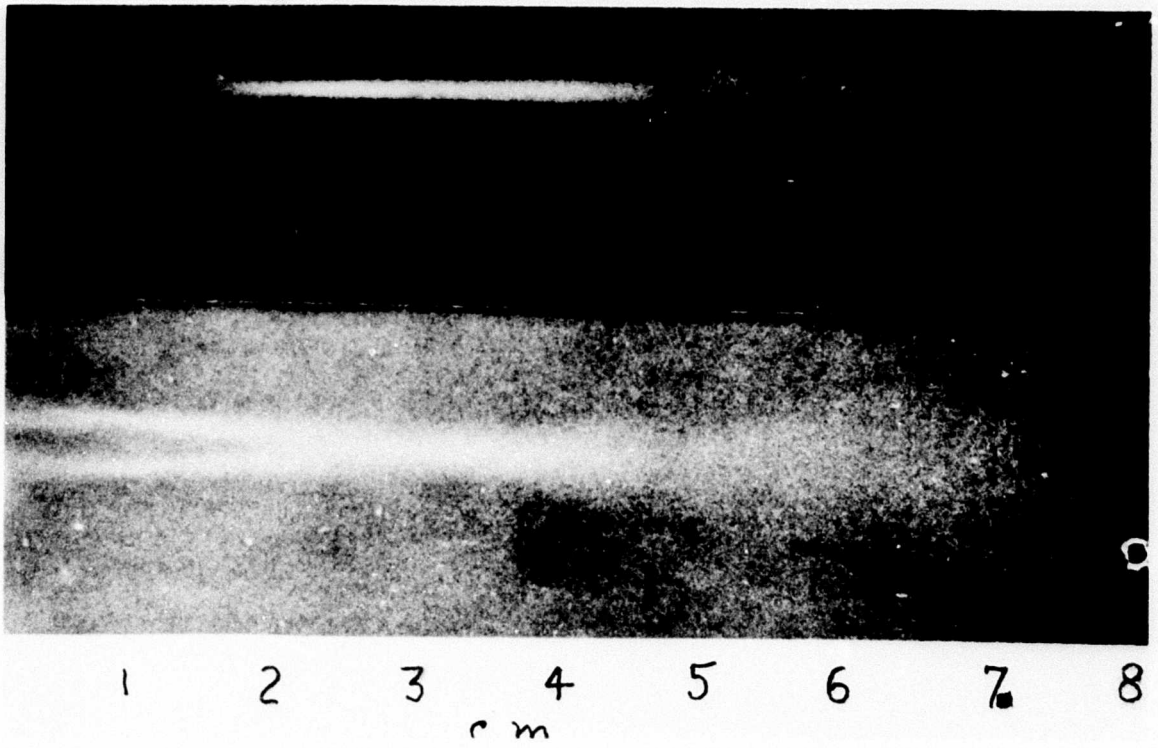

Fig. 28. Schlieren photo of focussing characteristics of epoxy lens probe. Upper and lower sections are produced by turning the probe on its axis 90°.

The shape of the transducer, insofar as whether it is flat or pencil-like, is governed by special application features, such as whether it is to be used under a wet suit or hand held.

The peripheral monitoring sites most useful for regional localization of embolic signals are illustrated in Figure 30. When listening over the peripheral veins, the sensor should be tilted to approximately 45 degrees with the skin surface in order to achieve the more recognizable chirping quality of the bubble signals, (Fig. 32). The peripheral vein sounds may be separated from the arterial, highly pulsatile signal by first locating the artery and then slightly sliding the sensor to the medial side of the artery where the quieter, more continuous and breezy sound of the venous blood flow can be heard.

Experience to date indicates that the most frequent sources of decompression bubbles are the upper and lower extremities. One optimal sequence of listening sites is precordial, innominate-jugular, subclavian, brachial and femoral. Several maneuvers are useful to confirm both the presence and regional source of decompression emboli. With the subject relatively immobile in a standing, sitting, or reclining position, and while listening to the precordial or peripheral signals, ask the subject to clench one fist slowly. If the bubbles are arising from the same hand, or arm, a shower of bubbles will be heard at the brachial, innominate or left sternal border sites, (Figs. 31-32). If the entire arm is raised above shoulder height, or if the straightened leg is passively raised, a similar response will confirm the raised extremity as a source of gas emboli. Passive compression by the observer is an additional method of regional localization of gas nucleation and can narrow the source down to tissues of the upper or lower leg, foot, upper or lower arm, hand, or to the abdominal organs.

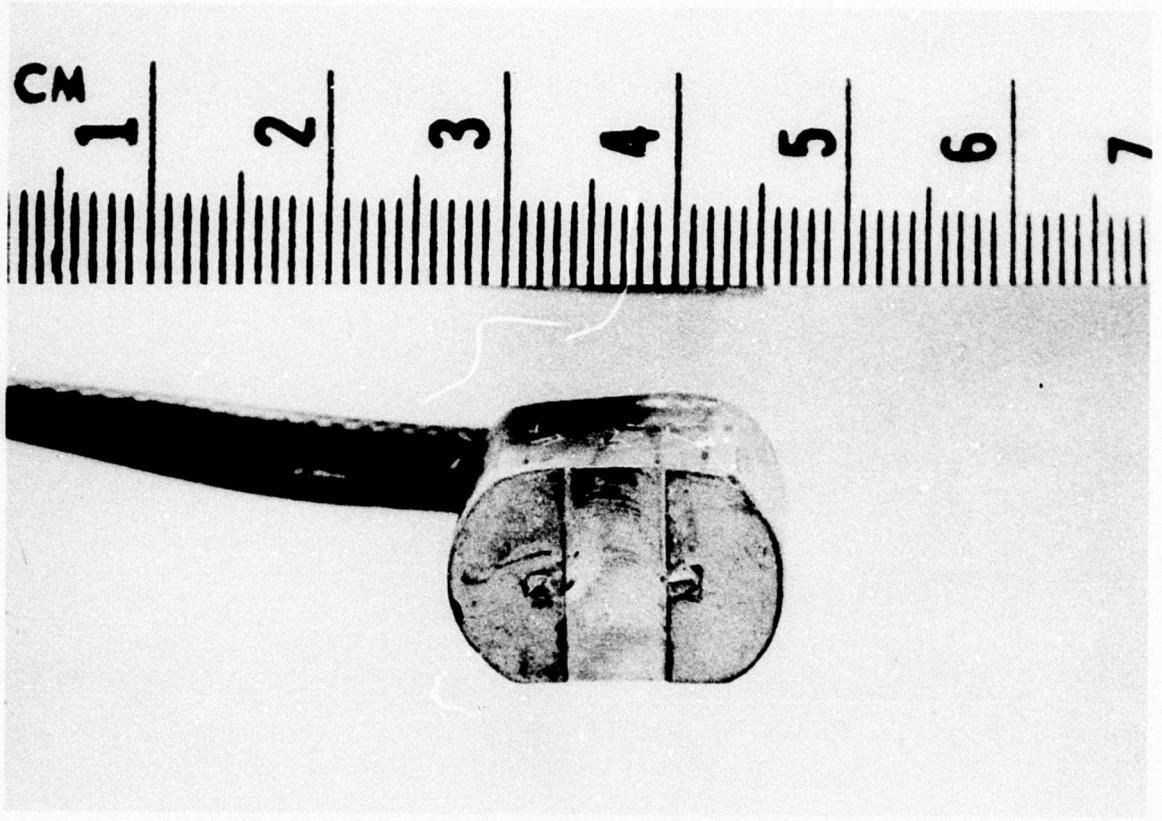

Fig. 29. Three-eights inch diameter beam dual-crystal focussing probe for combined monitoring of peripheral and precordial sites.

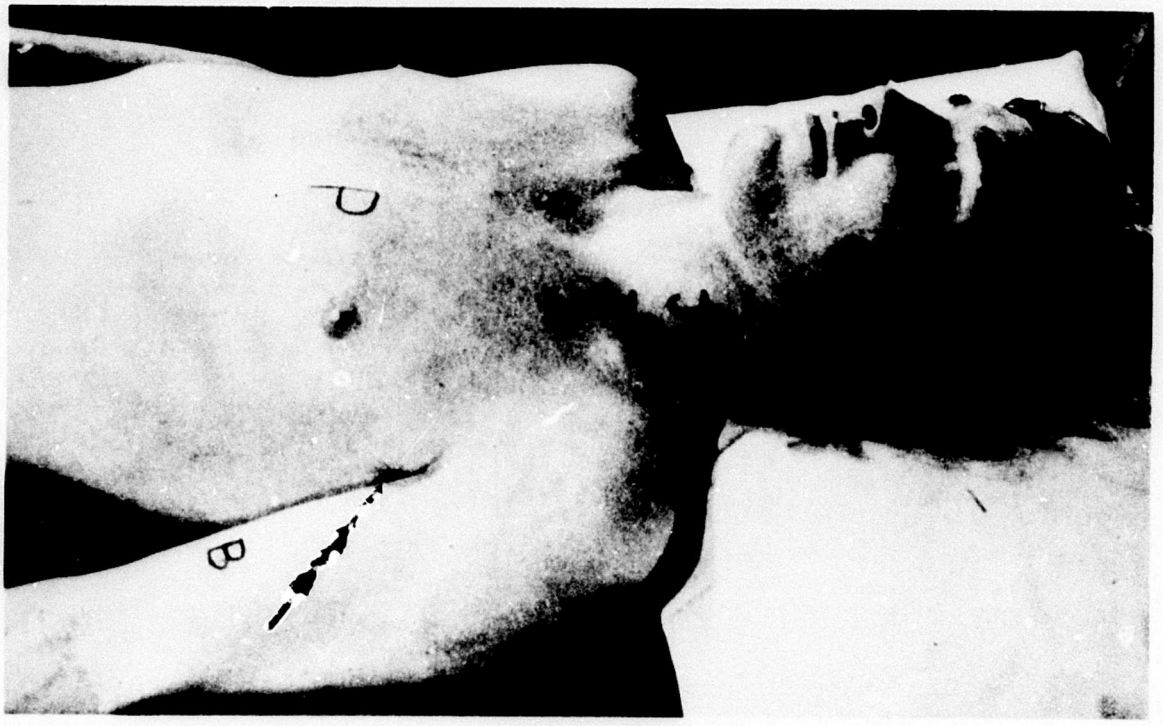

Fig. 30. Preferred monitoring sites for regional localization of venous gas emboli. J = Jugular vein, I = Junction of Jugular and Subclavian veins, B = Brachial vein, P = Precordial monitoring site.

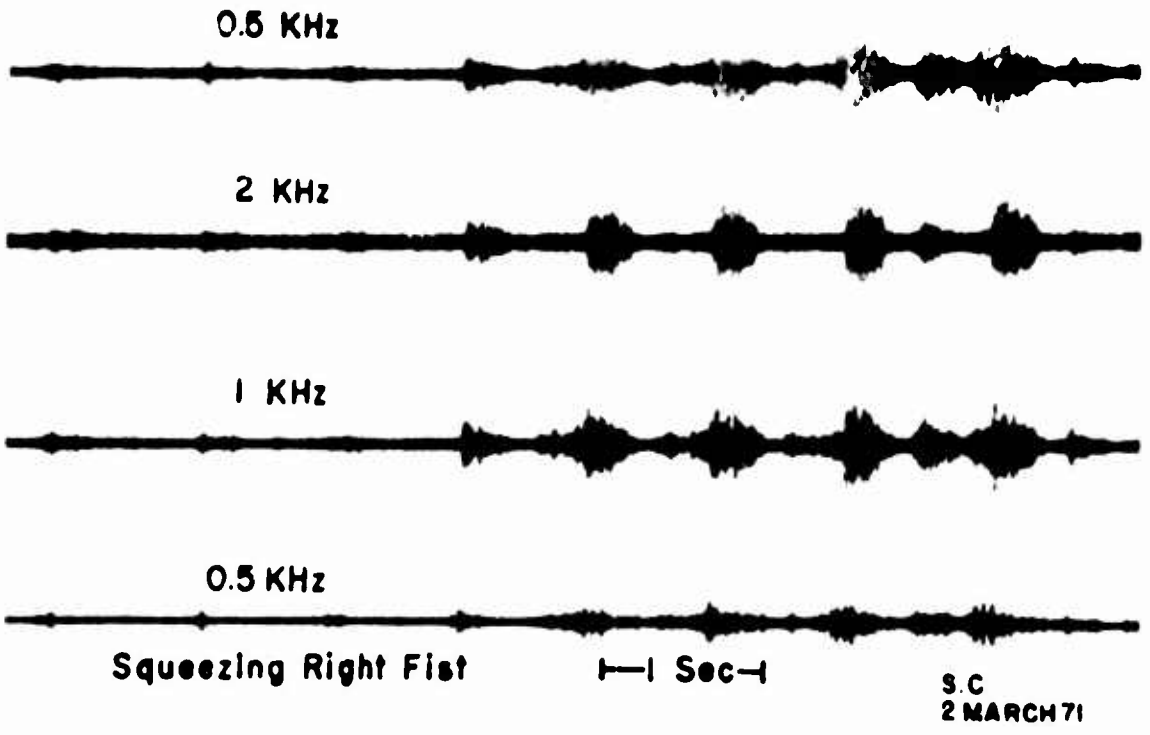

Fig. 11. Decompression bubble signals detected with the precordial doppler probe following muscular contraction of right fist.

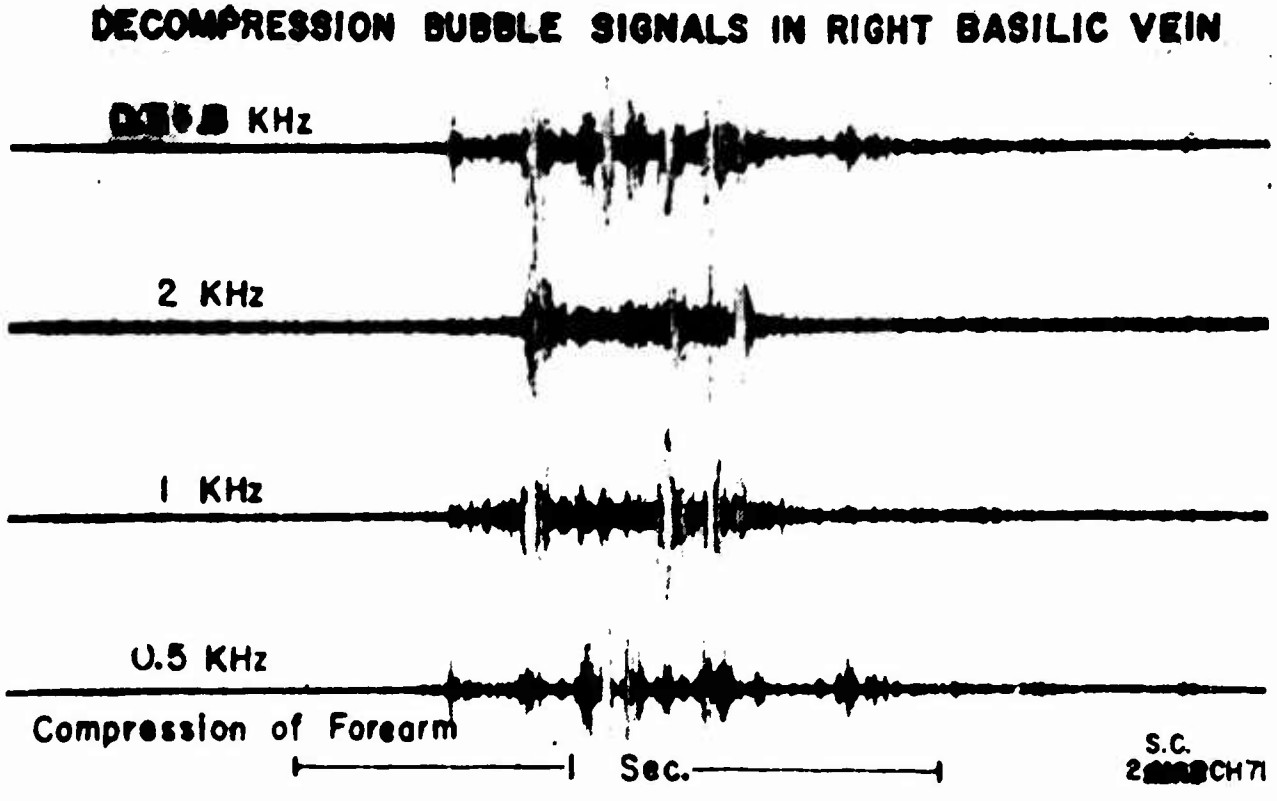

Fig. 12. Decompression bubble signals detected in the right [illegible] vein following [illegible] compression of right forearm.

D. SURGICAL DETECTORS

Surgical implantation of ultrasonic doppler flowmeter cuffs allow the investigator to measure not only the blood flow in a vein or artery, but to detect the earliest possible occurrence and/or number of gas emboli which may be passing through the flow stream under study. Both animal and human applications require a variety of perivascular cuffs which meet various anatomical requirements. The original type of perivascular cuff, illustrated in Figure 33, is commercially available. It consists of two styrofoam hemicylinders hinged on one side, and is provided with an umbilical tape to tie it in position around the vessel. In its final placement, the crystals are oriented at 60 degree angles with the flow stream, each facing the same volume of blood enclosed by the cuff. For the most accurate results, it is desirable that the crystal be of sufficient width so that the entire blood flow stream across a section of the blood vessel be flooded by the ultrasonic beam.

A variation developed by this investigation team is illustrated in Figure 34, and consists of placement of the two crystals side by side, oriented in a styrofoam cup, such that they both view the same volume of blood across the vessel over a longer cross sectional slice of the vessel. The cups are applied to only one side of the vessel and an umbilical tape passing from the cup around the opposite side of the vessel holds it in place. This particular design is especially useful for easy application where minimal dissection on the back side of the blood vessel is necessary.

For extracorporeal blood circuits, we have utilized a stainless steel connector with dual crystals mounted on a flat outside surface. The presence of bubbles is detected by a change in signals usually consisting of sharp clicks that occur as they pass.

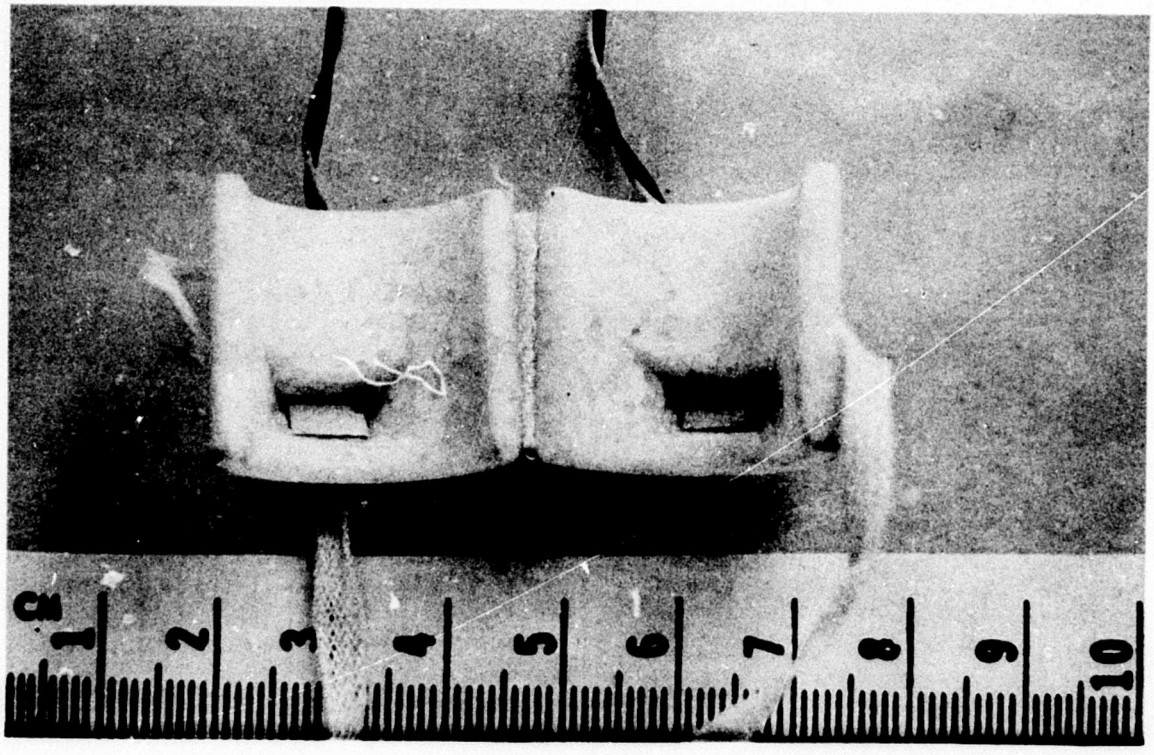

Fig. 33. Standard surgically implantable perivascular cuff to fit a 2 centimeter o.d. blood vessel. The crystal diameter is insufficient to flood the entire cross section. (Parks Electronics)

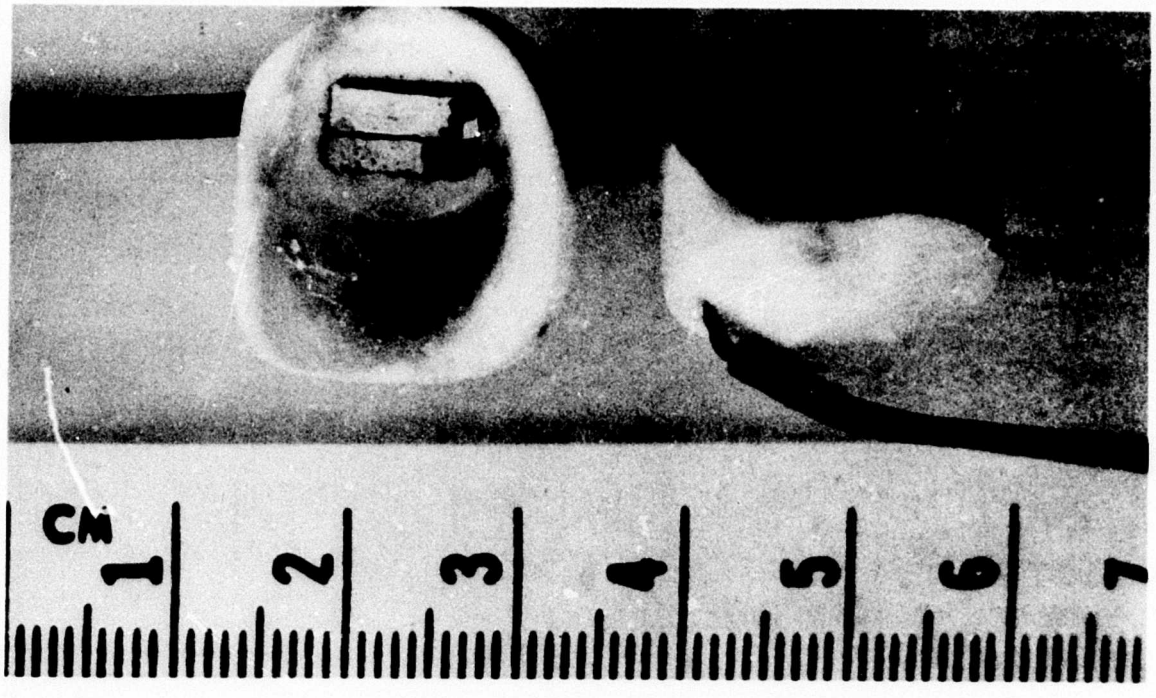

Fig. 34. The Spencer hemicup allows easy placement by passing the stay suture around the cuff and vessel. Long rectangular crystals provide greater flooding of the entire flow stream diameter.

Catheter-tip detectors designed for blood velocity flow measurements are convenient to detect blood bubbles. When inserted into large arteries or veins, some bubbles may pass undetected past the same transducer. It is for this reason that they become local velocity detectors when they do not monitor the entire flow cross section. Significant numbers of bubbles will not, however, pass undetected because the sensitivity of doppler detection for blood bubbles extends beyond its blood velocity range. A single blood bubble normally produces a doppler signal 16 db above the background blood flow signal. The fall-off of sensitivity with distance is on the order of 5db/cm; therefore, blood bubbles may be heard 3 cm further distant than the same blood flow signal produced by the red cells. Figure 35 illustrates a single crystal catheter-tip device with it's bridge completion circuit card.

To operate any or all of the transducers described in this report as blood bubble or blood flow detectors, Reid and Davis, et al, (1974) have, at this institute, developed a CW directional doppler flowmeter. It is a very compact unit (Fig. 35), and operates any single or dual crystal transducer from 2-10 MHz by use of plug-in control crystals and bridge completion cards.

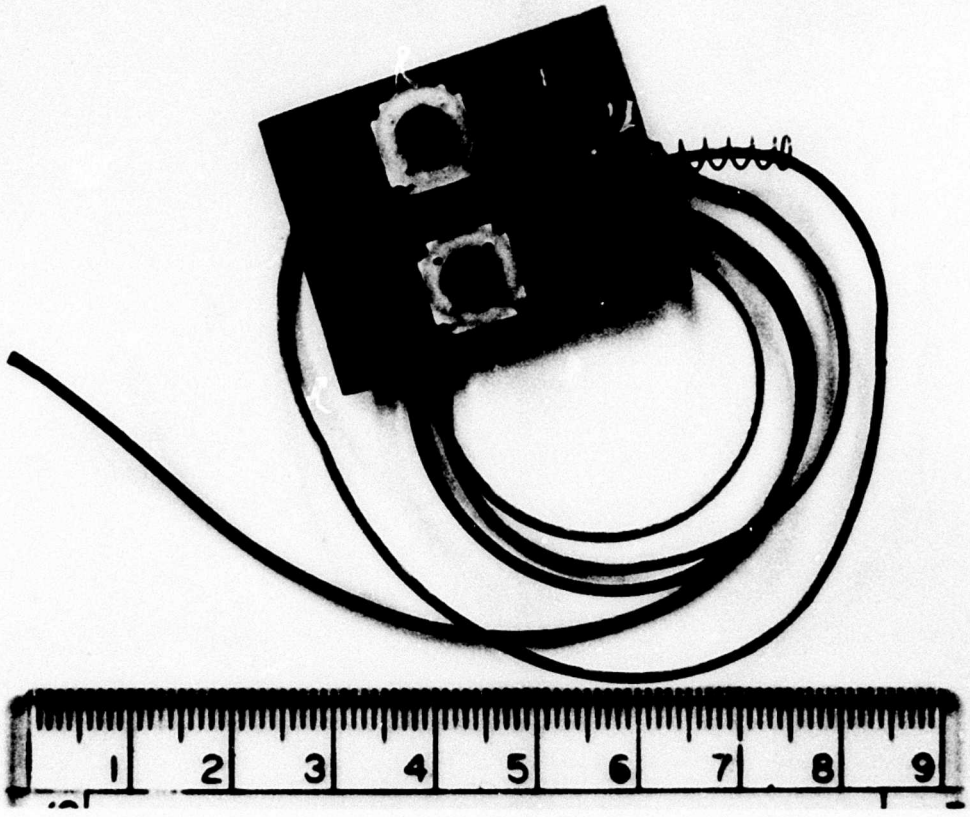

Fig. 35. Single crystal catheter-tip doppler flow sensor with its matched bridge completion circuit card.

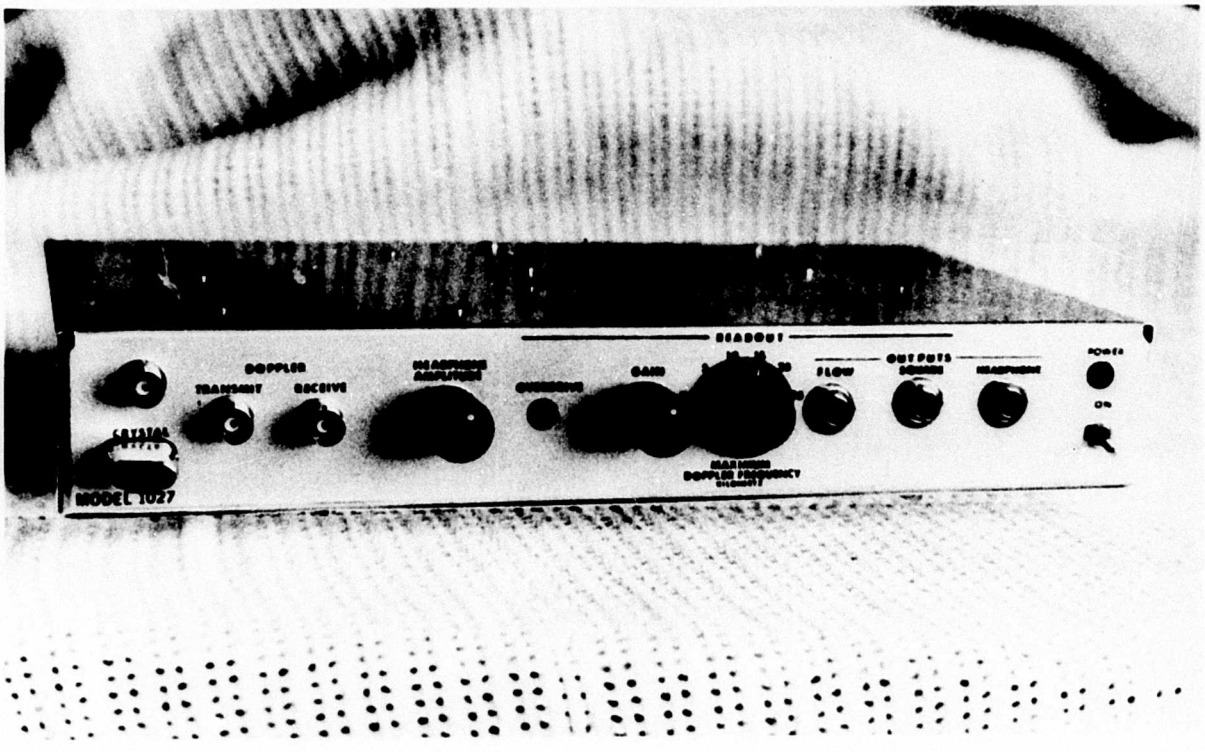

Fig. 36. The Reid-IEM&P C W directional doppler flowmeter capable of operating any single or dual crystal transducer from 2-10 MHz. Multiple units can be slaved together.

II.

A NEW MODEL FOR BODY TOLERANCE TO EXCESS INERT GAS

Presently used models for decompression tables were developed on an elaboration of principles laid down by Haldane. A series of theoretical tissue compartments defined by ½ times to saturation are each considered to have their allowable supersaturation tolerance, the so-called M values. These M values are tested by exposing a subject to hyperbaric respiration and a decompression schedule which is calculated to not exceed estimated safe limits and adjusted in a more conservative direction if bends develop. Based on experience, difficulty arises in improving the model because the investigator must guess which theoretical compartment is to blame when he makes his adjustment.

A. METHODS

The model developed by this project is based on a time-pressure approach to the whole body's reaction to excess nitrogen in the tissues using the objective "prebends" endpoint of venous gas emboli (vge) ultrasonic signals. The model describes the maximum pressure allowable for all practical exposure durations from which the subject is decompressed. "Allowable" is defined as the time-pressure limit which produces nonsymptomatic vge detectable with the IEM&P precordial blood bubble detector. "Directly" decompressed is defined as return to 1 ata at the rate of 60 feet per minute without staged decompression steps. The term Direct-Decompression (D-D) is used here to be a more appropriate term for what the Navy calls No-Decompression (No-D). Our decompression model can be experimentally developed by the "black box" concept of presenting the body with a square-wave input signal (a pulse input of known pressure for a known period of time) and observing the output (the occurrence of detectable precordial gas emboli signals). Once various output responses are determined for a range of simple input exposures,

they are plotted on graph paper, and a family of iso-incidence curves are drawn through points representing the same percentage incidence of vge.

The experimental input exposures were chosen on the basis of finding and delineating the gradient between no vge and no bends, and 100% vge and 100% bends. The presently recommended USN No-D table and theoretical predictions, based on the N_2 elimination work of Behnke, were used as predictors of the locus of that gradient. Behnke measured the cumulative nitrogen elimination of normal subjects breathing oxygen at one atmosphere, (Fig. 37). If it is assumed that saturation of the body follows the same time constants under increased PN_2, one can predict the contour of the excess N_2 D-D limits and decompression table. After beginning a given hyperbaric exposure at t_0, being y% saturated at time t_y is equivalent to being 100% saturated at y% of the hyperbaric pressure. For example, (Fig. 37) if a 2:1 overall excess N_2 ratio is considered allowable, a diver can immediately decompress after 29 minutes exposure to 4 ata because being 50% saturated, he can tolerate a 50% (2:1) reduction in ambient pressure. Likewise, he is safe to decompress after 8 minutes at 8 ata because his equivalent saturation is 100% at 2 ata. For other allowable excess N_2 ratios, Figure 37 provides a simple graphic method of finding the D-D limits. The effect of using alternate excess N_2 ratios is to shift the limits on the pressure axis, but the general contour remains determined by the contour of the N_2 elimination curve.

Other predictors of the shape and position of the D-D exposure model include the USN recommendations for no-decompression, (Fig. 38). The experimental data of Hawkins, et al (1935), Behnke (1955), and Albano (1960) is shown in Figure 39; and experimental animal data of Gillis (1971), Smith (1970), and Hempleman (1963), is shown in Figure 40. Though all of this data was based on the development of bends as an endpoint, it indicates severe limits which must not be used if a zero bends incidence is to be required. The most extensive data of Hempleman's goats indicates the D-D limits follow a countour parallel to the N_2

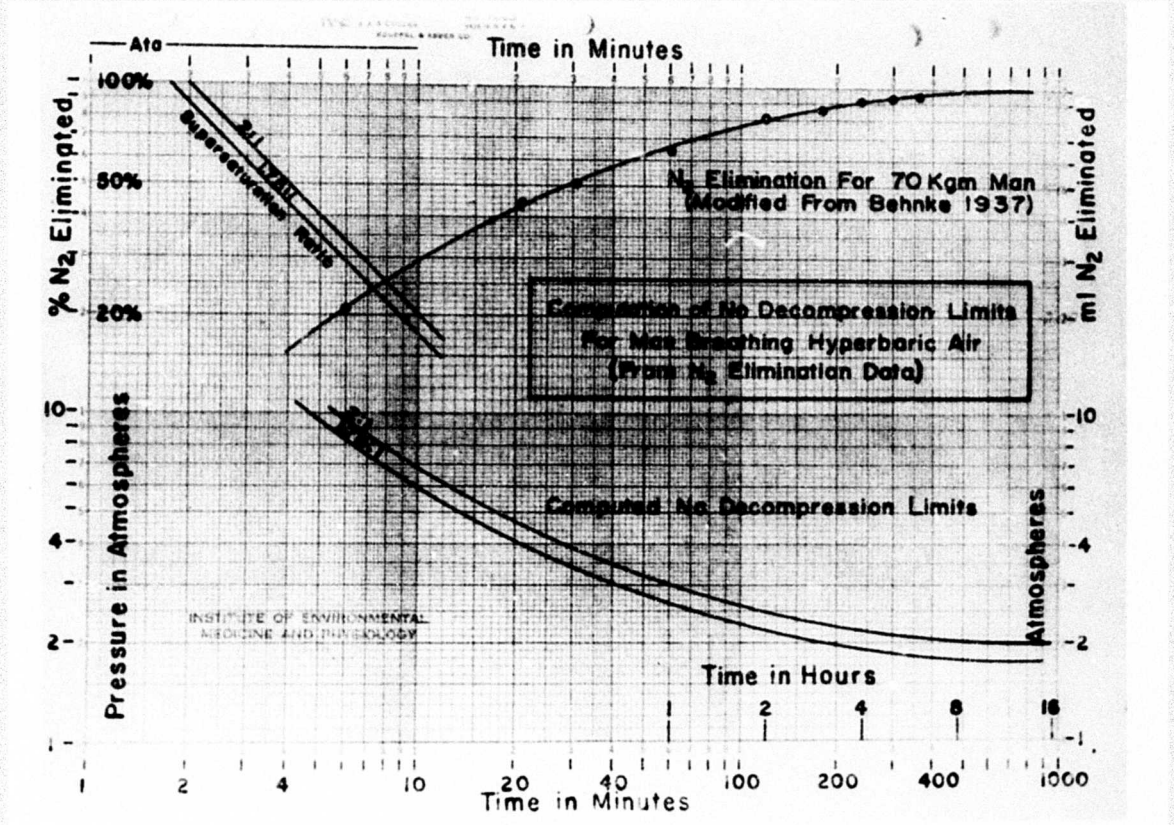

Fig. 37. N_2 elimination method of computing the No (direct @ 1 ft./sec.) decompression limits for men after breathing in hyperbaric air.

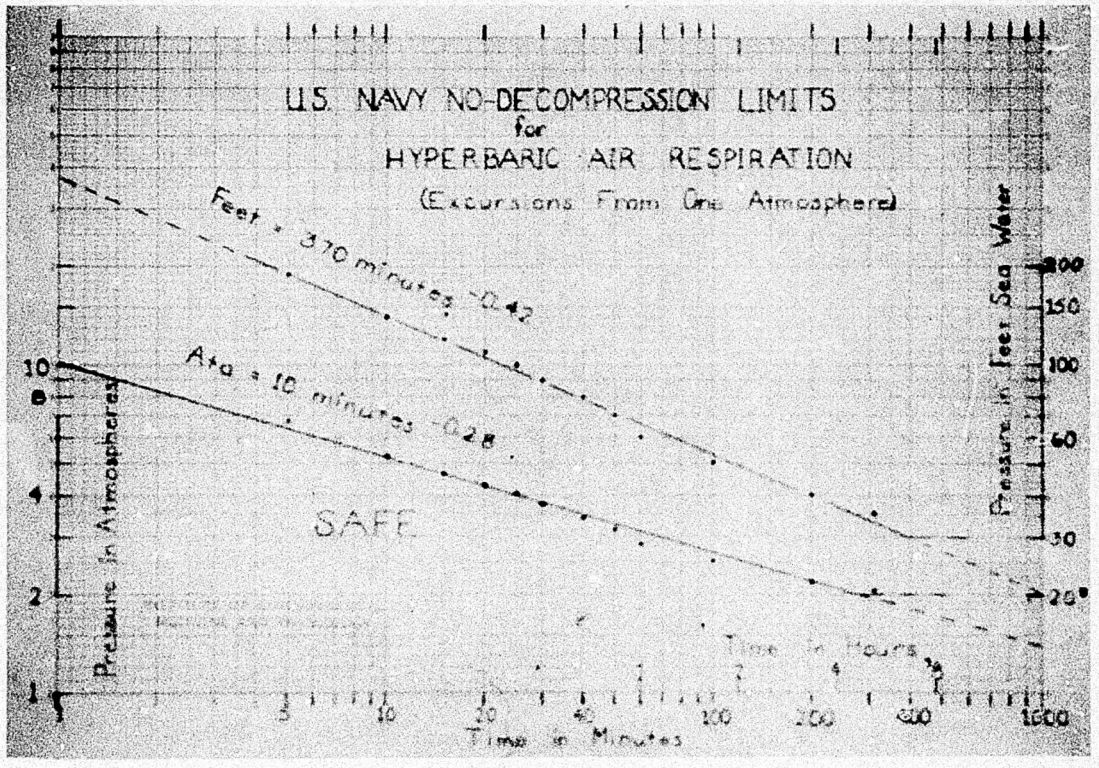

Fig. 38. Currently employed U.S. Navy no decompression limits for hyperbaric air respiration.

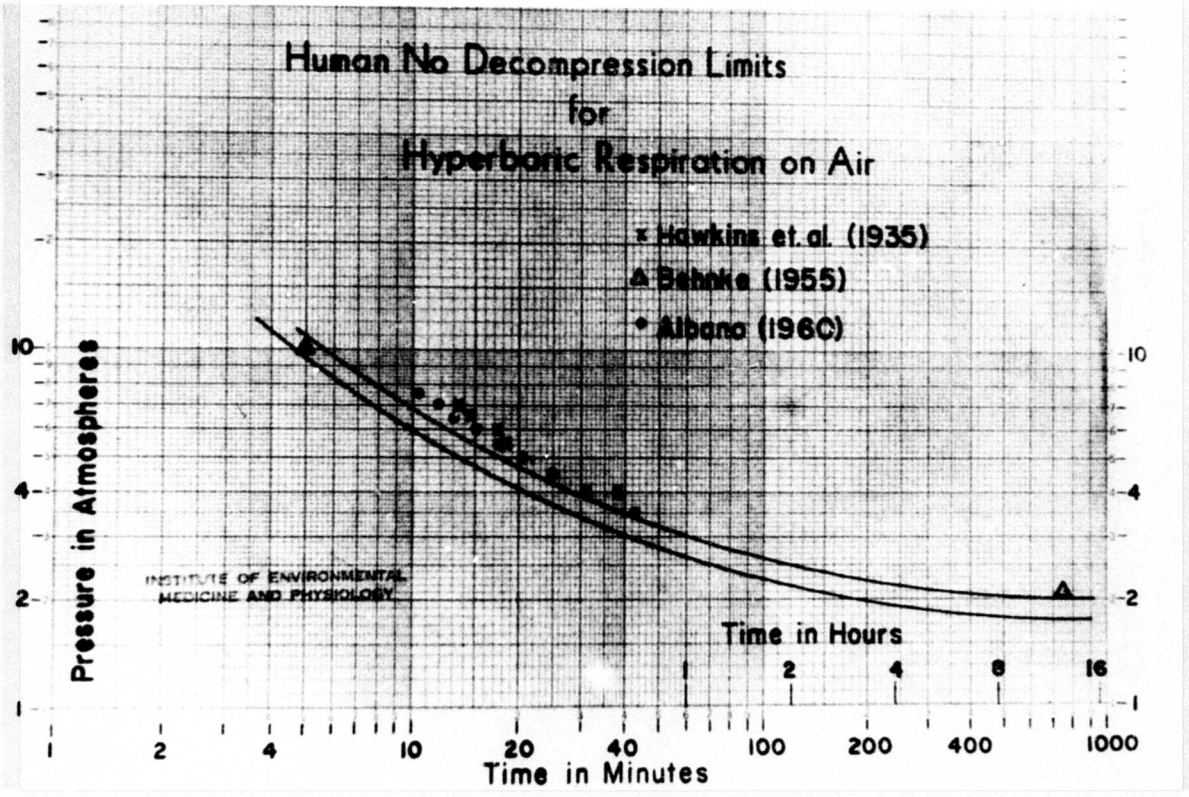

Fig. 39. Human no decompression limits as determined by Hawkins, 1935, Behnke, 1955, and Albano, 1960 compared to the predicted curve determined from N_2 elimination data.

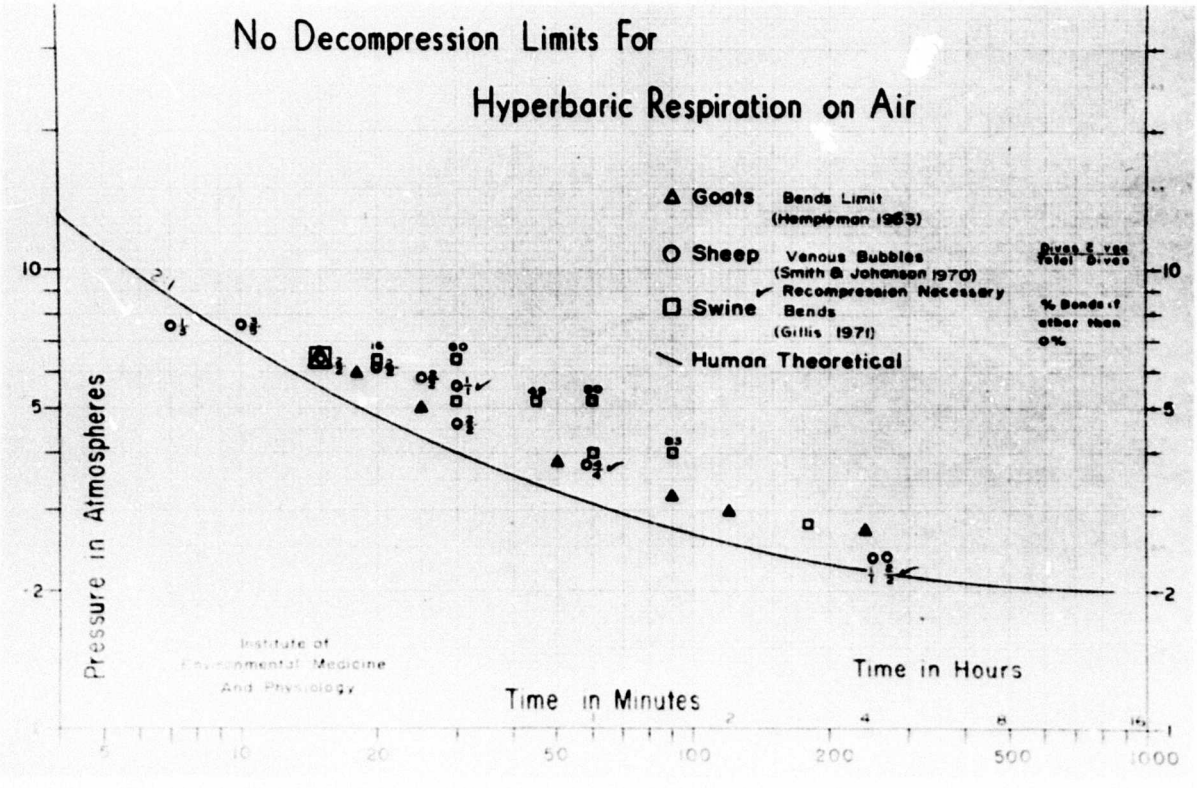

Fig. 40. Animal No-D data from goats, sheep, and swine bends, and sheep vge compared to the predicted no decompression limits for man on hyperbaric air respiration.

elimination predicted limits.

We developed our decompression model by defining the D-D limits using venous gas emboli (vge) signals as an objective endpoint, concentrating on three widely spaced sets of data. Only three sets of data appeared to be required because the theoretical limits predicted from N_2 elimination were well described by a circle contour when plotted on log-log coordinates.

Experimental determination of our decompression model by the input-output vge method was carried out by testing human subjects in the three widely spaced exposures around 30 ft/720 minutes, 70 ft/50 minutes, and 233 ft/7 minutes.

Eighteen expert scuba divers, residing in the Seattle area, ranging in age from 21 to 37 years (Table 1) volunteered for the study. These experimental divers, including three full time instructors, frequently perform scuba dives in the waters of the Puget Sound area. Progressive results, as they were obtained, modified and directed our choice of subsequent exposures. In each of the exposures the subjects were resting quietly in a sitting or semi-recumbant position throughout the exposure.

Immediately before, and for 1 to 5 hours after decompression, the divers were monitored with the precordial blood bubble detector for the presence of vge. The pre-dive recordings gave a baseline with which to compare the post-dive recordings and also made certain that all the divers were bubble-free prior to compression. None of the subjects had been diving within 24 hours of the experiments. Post-exposure precordial recordings were made at 5, 10, 15, 20, 30, 40, and 60 minute intervals during the first hour and at 30 minute intervals during a subsequent 60-300 minute period. This sequence was followed for 60 minutes if doppler ultrasonic signals of vge were not detected over the precordium. Longer monitor periods were used when vge developed.

The precordial transducer was positioned, as illustrated in Figures 18, 19 and 20, along the midsternal border. Its focus includes the right atrial appendage, the right ventricular outflow tract, the pulmonary valve, and the pulmonary artery. Optimum positioning is confirmed by locating the closure sound of the pulmonary valve which has a chirping quality similar to some vge signals, but does, of course, occur regularly at the end of systole. All vge signals were recorded on magnetic tape along with voice notations. The tapes were later replayed for confirmation and documentation of vge signals. If, during the monitoring, precordial vge were detected, the divers were then asked to flex the limbs--one at a time--while monitoring continued. Bursts of vge signals from bubbles, thus dislodged, gave a more specific idea as to the regional source of the vge. A 5 MHz shallow-focusing doppler probe was then substituted for the precordial probe and a search was made over left and right femoral, brachial, and jugular veins. Later refinement of the technique resulted in addition of the innominate veins (Fig. 30) as a key peripheral listening site using a new 3.5 cm focal length 5 MHz flooding probe, (Fig. 29). When monitoring the peripheral veins, manual compression of the upstream tissues of the limb or neck identified the regional source of vge. The arteries were also monitored for possible arterial bubble signals. No arterial vge signals were detected in any of these subjects.

We recorded the time of first occurrence of the bubble signals following decompression and an estimate of their duration, as well as a graded indication of their quantity along with the absence or presence and severity of any symptoms of decompression sickness. The grading system for the venous return bubbling rate heard over the right heart consisted of a five point scale: Zero--is taken to indicate a complete lack of bubble signals; Grade one--indicates an occasional bubble discernable within the cardiac motion signal and with the majority of the cardiac periods free of signals; Grade two--is designated when many, but less

than half, of the cardiac cycles contain bubble signals; Grade three--is designated when most of the cardiac periods contain bubble signals, but not overriding the cardiac motion signals; Grade four--is the maximum detectable bubble signal, heard continuously throughout systole and diastole of every cardiac period and overriding the amplitude of the cardiac motion signals.

Subjects were recompressed for therapy if bubbles occurred in more than grade three quantitites, or if bends pain developed. Recompression treatment in the 30 foot dives was to 60 feet on the U.S. Navy treatment. For the remaining dives, recompression treatment was for 1 hour at 30 fsw with the subject breathing 100% O_2. In most cases, where bubbles were heard in grade one or early grade two quantities, the subject breathed 100% oxygen at 1 atmosphere until the bubble signals diminished or disappeared.

B. RESULTS

Chamber Exposures

Our laboratory results are plotted in Figure 41; the attendant percentage of vge occurrence as well as the percentage of bends occurrence among the experimental divers is given beside each of the exposures. In addition, a percentage-weighted profile average for each of those exposure groupings is given beside each of the exposures. (Table I gives further details.) At the 150/15 exposure (5.6 ata) a 50% bubbles rate and 25% bends rate corresponds roughly to the predicted 2:1 limit. The results at the 30 foot (1.9 ata) exposure, however, indicates that selection of a lower supersaturation ratio would be necessary to produce 50% bubbles. This finding is at variance with the presently accepted concept that 30 feet (13.3 psig, 1.9 ata) is a safe No-D exposure for any period of time since we found a coincident 25% bends rate after 12 hours.* Three data points, from the three ata groupings (averaging the 3.12, 5.54, and 7.96 ata profiles), indicate that the D-D lines of iso-embolic occurrence follow a log-log curvature slightly less convex than that indicated by the nitrogen elimination data limits.

Results of this black-box method of determining the direct decompression limits for hyperbaric exposure on air from one atmosphere surface saturation has shown that, indeed, the limits are described by a curve when plotted on log-log paper rather than a straight line suggested by the USN No-D limits. The incidence of bends also followed the same curvilinear contour, but at higher pressure-time products.

*At press time we are currently exploring a 25 ft/12 hrs. exposure. Initial results on nine exposures has resulted in a 44% bubbles rate and 11% bends rate.

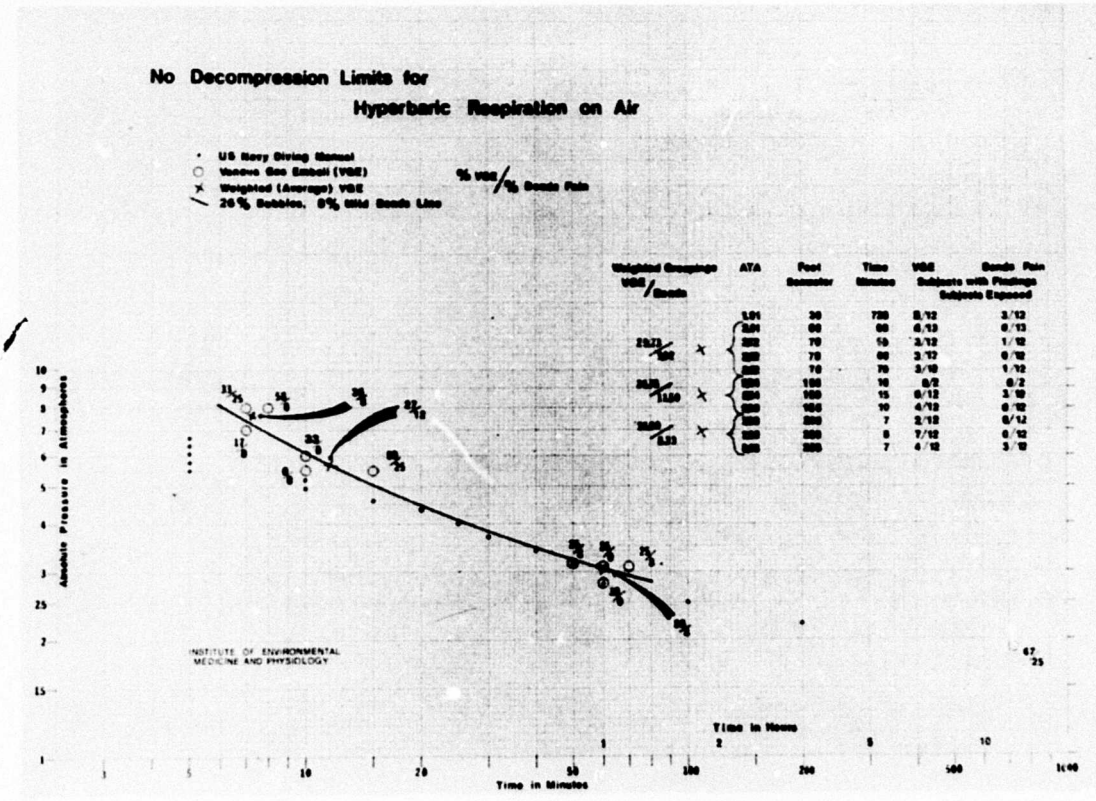

Fig. 41. Human no decompression limits for hyperbaric respiration on air using precordial venous gas embolism detection as compared to bends and U.S. Navy Diving Manual recommendations.

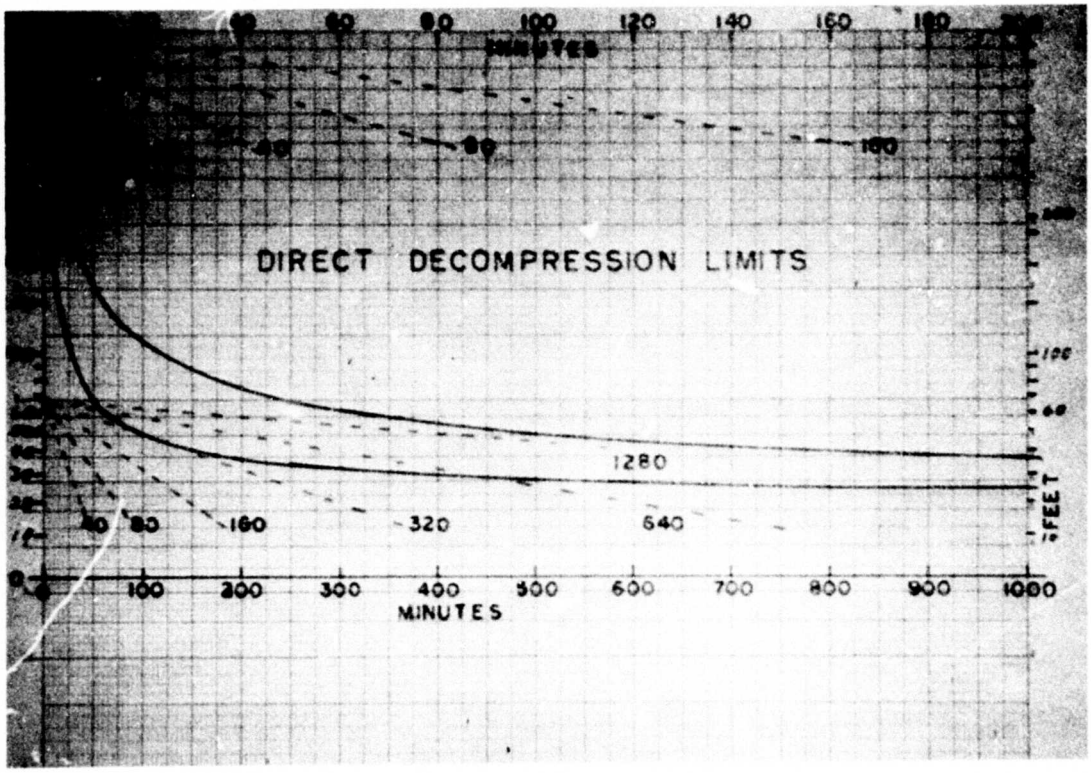

Fig. 42. Human direct decompression zero bends incidence limits for air respiration, semi-log plot.

Open Water Trials

Fifty-two open-water scuba dives were performed in the 50 degree waters of Puget Sound. These were training dives on beginners, and ranged from 110 feet to 30 feet with 15 to 70 minute bottom times. All dives were less than those prescribed by the U.S. Navy No-D limits except for three dives, two of which were at 70 feet for 50 minutes, and the other at 80 feet for 40 minutes. In none of the divers were venous gas emboli detected immediately upon surfacing. However, in some repetitive dives following an initial conservative dive, venous gas emboli were detected. One especially interesting exposure, on expert diver Spencer Campbell, was 80 ft/40 minutes which produced no vge, but if performed in the dry chambers would surely have produced some vge in this subject. Additional open water conditions, not present in the chamber, including involved psychological conditioning of open-water submergence, cold and exercise, were of course, present. The uptake and elimination of N_2 is undoubtedly altered by these conditions. (Additional open-water experience with vge detection is described in other sections of this report.)

The Long Pull

The present USN 200 ft. Exceptional Exposure tables call for the first decompression stop at a depth of 40 fsw (for a 30 minute bottom time) while the 1935 tables require this first stop at 70 fsw. The older tables also brought the diver to the surface six minutes sooner than does the present Navy tables.

Initial decompression to 70 fsw represents a change of 55% of the total pressure at depth; decompression to fsw represents a 69% total pressure change. Though the percentage difference does not appear to be substantial, it must be remembered that the increase of volume, per unit decrease in pressure, results in an exponentially increasing spherical or cylindrical diameter. Compounding this effect is the constantly increasing volume of free gas available as the surface (1 ata) pressure is approximated.

Many have suggested that the newer tables, while admittedly bringing the diver closer to the surface and therefore in a safer position, are producing bubbles by the initial "long pull" which are then in effect "treated" by the extended decompression. (The older tables removed the diver 10% sooner than the new tables.)

Our findings do not agree with this suggestion. Rather than producing bubbles, we found the newer tables produced far fewer bubbles. We compared the two Navy profiles of 200/30 on two individuals on a four dive series. The new tables produced grade 1 and 3 bubbles in one diver (M.P.) and grades 1 and 2 bubbles in the other diver (M.R.) on two subsequent exposures. On the same two subjects, the older tables produced, in one diver (M.P.), grade 3 precordial bubbles on one exposure requiring 180 minutes surface 100% O_2 respiration to dissipate and grade 3 bubbles on the other exposure, traceable to the left external jugular vein and treated by 60 minutes 100% O_2 respiration at 60 fsw. The other diver (M.R.) exhibited grade 3 and grade 2 bubbles respectively on the same dives.

Bubble Proneness

Table I, which gives the results of the chamber experimental dive, is arranged according to decreasing order of proneness of the individual divers to form vge. It is clear from this data that two of the experimental divers consistently formed venous gas emboli on nearly every experimental "dive", while other members of the group tended to be both bends and bubbles resistant. On those divers, who frequently and most consistently bubble, there was a clear tendency towards bubbles being elicited from a general body area. Owing to improved methods in isolating the specific peripheral vessels in which bubbles are detected, it can be shown that the most commonly occurring bubble locations are the tissue beds drained by the femoral and subclavian veins. We were not suprised to find a difference in occurrence of bubbles between divers on the same dive, but we were

TABLE I

HYPERBARIC CHAMBER EXPOSURES

Diver			NO-D	GRADE	Peripheral Bubbles						Time	Duration		Symptoms	Duration	Location of
Age in Years	Weight in kg	Height in cm	profile depth/ time	of Pre-Cordial Bubbles	J_r	I_r	F_r	J_l	I_l	F_l	of 1st Bubbles	(time) of Bubbles		R_x	of pain or other Symptoms	pain or other Symptoms
37	81	175	30/720	2	Ø	+	Ø	Ø	Ø	Ø	6	84	B,C		75	R Arm
			60/60	3	Ø	+	Ø	Ø	Ø	Ø	7	> 120	B			
			70/50	2	Ø	+	Ø	Ø	+	Ø	10	110	A,B		120	L Arm
			70/60	3	Ø	x		Ø	x		10	30	B	O_2		
			70/70	3	Ø	+	Ø	Ø	Ø	Ø			B			
	S. C.		150/10	Ø									B			
			150/15	1	Ø	+	Ø	Ø	Ø	Ø	2	33	B,C		30	R Shoulder
			165/10	2	Ø	+	Ø	Ø	Ø	Ø			B			
			200/7	Ø	Ø	+	Ø	Ø	Ø	Ø	12	50				
			230/8	2	Ø	+	Ø	Ø	+	Ø	3	> 60	B			
			233/7	4	Ø	x		Ø			3	< 40	D	O_2P		R Shoulder&Neck
22	76	179	30/720	1	Ø	Ø	Ø	Ø	Ø	Ø	< 500	> 530	B			
			60/60	1	Ø	Ø	Ø	Ø	Ø	Ø	60	> 60	B			
			70/50	3	Ø	Ø	+	Ø	Ø	Ø	10	95	B,C	O_2	20	R Knee
			70/60	Ø									B			
			70/70	1	Ø	Ø	Ø	Ø	Ø	Ø			B			
	M. P.		150/15	3	Ø	Ø	Ø	Ø	Ø	+	< 15	95	B,C	O_2	130	R Shoulder
			165/10	Ø									B			
			200/7	1	Ø	Ø	+	Ø	Ø	Ø	< 20	61	B			
			230/8	3	Ø	+	Ø	Ø	+	Ø	15	> 63	B			
			233/7	4							5	23	B,C	O_2P		R Leg
22	71	174	30/720	4	Ø	Ø	+	Ø	Ø	Ø	30	> 740	B	O_2P		
			60/60	3	Ø	Ø	+	Ø	Ø	Ø	30	> 360	B			
			70/50	Ø	Ø	Ø	Ø	Ø	Ø	Ø						
			70/60	Ø									B			
			70/70	Ø												
	M. R.		150/15	2	Ø	Ø	Ø	Ø	Ø	+	5	80	B	O_2		
			165/10	Ø									B			
			200/7	Ø									B			
			230/8	1	Ø	+	Ø	Ø	Ø	Ø	70	80	B			
			233/7	2							3	20	B	O_2P		

21	74	[illegible]	30/720	3	Ø	Ø	+	Ø	Ø	+	30	150	A	O_2P	20	R Knee
			60/60	Ø									B			
			70/50	1	Ø	Ø	+	Ø	Ø	+	30	25	B			
			70/60	Ø									B			
			70/70	Ø									B			
	A. G.		150/15	3	Ø	Ø	+	Ø	Ø	Ø	13	55	B	O_2P		
			165/10	1	Ø	Ø	+	Ø	Ø	Ø	15	40	B			
			200/7	Ø												
			230/8	2	Ø	Ø	+	Ø	Ø	Ø	8	> 60	B			
			233/7	Ø									B			
25	84	173	30/720	3	Ø	Ø	Ø	Ø	Ø	+	> 90	115	D	O_2P	145	L Thigh
			60/60	Ø									B			
			70/50	Ø	Ø	Ø	Ø	Ø	Ø	Ø			B			
			70/60	Ø									B			
			70/70	3	Ø	Ø	+	Ø	Ø	+	2	> 250	B,C		300–1080	R Leg
	P. M.		150/15	2	Ø	Ø	Ø	Ø	Ø	Ø	< 15	170	B	O_2		
			165/10	1	Ø	Ø	Ø	Ø	Ø	Ø	3	15	B			
			200/7	Ø									B			
			230/8	2	Ø	Ø	Ø	+	+	Ø	12	< 100	B			
			233/7	Ø									B			
26	76	178	30/720	1	Ø	Ø	Ø	Ø	Ø	Ø	15	< 45				
			60/60	Ø									B			
			70/50	1	Ø	+	Ø	Ø	Ø	Ø	30	30	B			
			70/60	1							40	42				
			70/70	Ø									B			
	A. F.		150/15	Ø	Ø	Ø	Ø	Ø	Ø	Ø			B			
			165/10	1	0	0	+	0	0	0	12	40	B			
			200/7	Ø									B			
			230/8	1	Ø	Ø	+	Ø	Ø	Ø			B			
			233/7	Ø									B			
29	77	179	30/720	Ø									B			
			30/720	3	Ø	Ø	Ø	Ø	Ø	+	30	200	B,C		250	R Knee, L Arm
			60/60	3	Ø	+	Ø	Ø	+	Ø	12	> 300	C			L,R Shoulder, R Side Head
			70/50	Ø	Ø	Ø	Ø	Ø	Ø	Ø						
			70/50	Ø	Ø	Ø	Ø	Ø	Ø	Ø						
	D. J.		70/60	Ø												
			70/70	Ø	Ø	Ø	Ø	Ø	Ø	Ø						
			150/10	Ø									B			
			150/15	Ø	Ø	Ø	Ø	Ø	Ø	Ø			B			

			150/15	Ø	Ø	Ø	Ø	Ø	Ø	Ø			B		
			165/10	Ø											
		D. J. cont.	200/7	1	Ø	Ø	Ø	Ø	Ø	Ø	6	50	B		
			230/8	Ø									B		
			233/7	2	Ø	Ø	Ø	Ø	Ø	Ø	13	60	C		
21	96	188	30/720	2	Ø	Ø	Ø	Ø	Ø	+	<15	200	B	O_2P	L Knee
			60/60	Ø									B		
			70/50	Ø	Ø	Ø	Ø	Ø	Ø	Ø					
			70/60	0									F		
			70/70	Ø									B		
		B. A.	150/15	2	Ø	Ø	Ø	Ø	Ø	+	<15	80	B,C	O_2	L Knee
			165/10	Ø									B		
			200/7	Ø											
			230/8	Ø									B		
			233/7	Ø									B		
23	89	188	30/720	Ø	Ø	Ø	Ø	Ø	Ø	Ø					
			60/60	Ø											
			70/50	Ø	Ø	Ø	Ø	Ø	Ø	Ø					
			70/60	Ø											
			70/70	Ø											
		G. A.	150/15	Ø	Ø	Ø	Ø	Ø	Ø	Ø			B		
			165/10	Ø											
			200/7	Ø											
			230/8	1	Ø	Ø	Ø	Ø	Ø	Ø	<10	25	B		
			233/7	Ø									B		
23	82	178	30/720	Ø	Ø	Ø	Ø	Ø	Ø	Ø			A,C		L Knee
			60/60	Ø											
			70/50	Ø	Ø	Ø	Ø	Ø	Ø	Ø			B		
			70/60	Ø											
			70/70	Ø									B		
		J. E.	150/15	Ø	Ø	Ø	Ø	Ø	Ø	Ø					
			165/10	Ø									B		
			200/7	Ø											
			230/8	Ø									B		
			233/7	Ø									B		

22	80	180	60/60	Ø									B	
			70/60	Ø									B	
			70/70	Ø									B	
			165/10	Ø									B	
			200/7	Ø									B	Extreme Skin Itching
	K. P.		230/8	Ø									B	
			233/7	Ø									B	
29	102	183	60/60	Ø										
			70/60	Ø									B	
	V. R.		233/7	Ø									B	
30	81	185	70/60	1	Ø	Ø	Ø	Ø	Ø	Ø	35	65	B	
			165/10	2	Ø	Ø	Ø	Ø	Ø	+	4	> 80	B	
	C. P.													
26	75	170	70/70	Ø									B	
			200/7	Ø									B	
	B. B.													
21	81	185	60/60	Ø									B	
			230/8	Ø									B	
	P. McK													
29	79	178	30/720	Ø	Ø	Ø	Ø	Ø	Ø	Ø				
													B	
	G. G.													
31	67	173	150/15	Ø	Ø	Ø	Ø	Ø	Ø	Ø				
	L. B.													
31	84	188	70/50	Ø	Ø	Ø	Ø	Ø	Ø	Ø				
	M. S.													

Encircled = Area Not Monitored
Ø = Bubbles Detectable with Passive Listening
+ = Bubbles Detectable when Area Manipulated
Ø = No Detectable Bubbles
1 = Occasional Bubble
2 = Many Cardial Cycles with Several Bubbles
3 = Most Cardial Cycles having Overriding Bubble Signals
4 = Bubble Signals Continuous Throughout Both Systole and Diastoll of Every Cardiac Cycle

A = Vague, Uneasy Feeling
B = Skin Itching
C = Mild Pain
D = Moderate Pain
E = Severe Pain

O_2 = Means Treated by 100% Oxygen

O_2P = Means treated by 100% Oxygen at 33 fsw

J_l = Left Jugular Vein
J_r = Right Jugular Vein
I_l = Left Innominate Vein
I_r = Right Innominate Vein
F_l = Left Femoral Vein
F_r = Right Femoral Vein

All Times in Minutes, Depths in Feet

All Subjects are Normal, Healthy Experienced Male Divers

suprised to note the consistency with which each diver tended to form bubbles on any border line exposure located on the limits gradient. As seen from Table I*, all vge that were regionally localized came from the extremities with the exception of two divers, one in whom they were thought to come from somewhere within the chest or abdomen, and the other in whom they were localized coming from the left external jugular. On a few occasions, we have been unable to detect peripheral bubbles even though precordial bubbles were much in evidence. In no instance have we detected arterial emboli.

Arterial Passage of Air Emboli

In the course of working with decompression related problems, the question has often been raised as to whether or not recompression of a bent (i.e, bubbling) diver might possibly worsen the pathological condition already present by pushing the venous gas emboli across the pulmonary circuit and into the arterial system.

In an attempt to address this question, we catheterized six sheep (Desert E-Z CATH 16 gauge, 18 inches) and injected 50 cc. of air (5 cc./minute for 10 minutes) into the right heart. Confirmation of the air passage through the right heart was achieved via transcutaneous doppler ultrasound precordial monitoring. Subsequent to the 50 cc. air injection, the animals were compressed at 60 ft/minute to a depth of 165 fsw for 9 minutes bottom time, and then decompressed, again at 60 ft/minute, to the surface with decompression stops for 2 minutes at 20 fsw and 8 minutes at 10 fsw. Decompression was decided upon to definitely eliminate the possibility of decompression vge occurring.

Continuous monitoring of all animals was made utilizing perivascular cuffs (Fig. 33), surgically placed around an artery and its conjugate vein, with percutaneous leads connected to the IEM&P through-hull. The electronics

*The 150 foot for 10 minutes and the 200 foot for 7 minutes dives were preliminary experimental tests for conservatism before testing the 150 ft/15 minute exposure because it exceeded the presently accepted No-D limits.

(Fig. 36), were maintained outside the chamber throughout the procedure.

The paired vessels monitored for this experiment were either the carotid artery and jugular vein or the renal artery and renal vein. In the experiments with renal observation, the paired vessels were encapsulated within a single cuff.

Controls were run on all animals prior to and throughout the entire air injection period. Although precordial bubbles were detectable in great quantities (grade 3 & 4) during the air injection procedure, no arterial bubbles were ever detected during this same period. During the compression mode of the experiment, the arterial transducers were monitored continuously with an oscilloscope, on a paper recording strip chart, and with simultaneous recording on magnetic tape, providing instantaneous playback over audio speakers. No arterial bubbles were ever heard or recorded during the compression phase at depths shallower than 100 fsw. Arterial bubbles, however, were heard in every experiment (often at grade 3 levels) once the 100 fsw depth had been reached. The earliest detectable arterial bubbles occurred at depths as shallow as 105 fsw. On no occasion during the entire bottom time while we were detecting arterial bubbles did we detect any venous bubbles. In almost every instance, arterial bubble detection ceased within eight minutes bottom time.

Upon decompression from depth, arterial bubbles were again detected on occasion, suggesting that very small bubbles tend to hang up in the vasculature, only to be freed when reduced pressure--allowing for increase in size--provides the momentum necessary for their continued passage.

Throughout these entire procedures, the animals exhibited no untoward signs or symptoms, even when carotid arterial embolism was occurring at grade 3 levels.

Pneumatic Decompression Meters

Another decompression model is represented by the most widely used pneumatic

decompression meter on the world market today. We have calibrated seven "DeSanctis" decompression meters including one new model, and six which have been used in the field by the Black Coral divers. Table II illustrates the time constants which we found to be followed by these meters. Over their operational ranges, they followed a single exponent description. For short-water dives, the meters tended to agree more closely with the vge D-D limits. The U.S. Navy No-D limits appeared more conservative in the short deep end of the curve, and insufficiently conservative in the long shallow range. This again is a reflection of a linear versus a curvilinear log-log limit.

Figure 42 illustrates a plot of the No-bends D-D limits for air, graphed on semi-log paper. Also appearing there are representations of half-times of single exponent functions. It will be seen that the shorter the div the shorter the half-time involved in a model describing the function of the body for the short dive. At the same time, for long exposures, longer time constants govern the decompression function of the body. The DeSanctis decompression meter, for example, with a half-time of 25 minutes, would appear to adequately describe the body decompression dosage response function to dive durations of 10 to 15 minutes. The choice of a single exponent to describe the functions for a dive lasting 60 minutes requires the use of an 80 to 100 minute half-time.

Hyperbaric Oxygen Treatment for Bends

In our experimental subjects, bends has been successfully treated in all cases by recompressing the subject to 30 feet of sea water pressure and causing him to respire 100% oxygen for one hour. The decision for recompression and high pressure oxygen treatment has been made in all cases where bends pain develops. All bends pain has been minor and never progressed to what would be considered a serious level. Pain was judged to be present if developed to the point where it was considered by both the physician and the subject to be of a

TABLE II

CALIBRATION OF SOS DECOMPRESSION METERS

OWNER	METER #	½ TIME MINUTES	REMARKS
TL		24	STUCK AT 23 FT MARK
RS	9742	26	STUCK AT 32 FT MARK
DN	11472	28	STUCK AT 29 FT MARK
JT	A-0186	31	DID NOT STICK
TS	7491	33	DID NOT STICK
BO	6195	37	STUCK AT 30 FT MARK
IEMP	14890	25	DID NOT STICK

sufficient level to require at least 2 aspirins for relief. Other subjects have been recompressed before bends pain if grade 3 and grade 4 bubbles signals persisted. Both subjects, who have previously gone on to bends following development of grade 3 and grade 4 bubbles, have been treated before pain developed by means of hyperbaric recompression and oxygen respiration. This procedure has no doubt reduced the overall incidence of bends in our experiments, but was felt to be necessary for safety of the volunteer subjects.

From more than 125 exposures performed to date on our experimental divers, we have treated 11 subjects with recompression oxygen treatment. In 10 cases, arterial flow signals were monitored transcutaneously during the recompression treatment and no arterial bubbles were detected even though precordial gas emboli were present in grade 2 to grade 4 quantities.

In many instances, surface oxygen has been used to stave off the development of bends and to test it's effect on bubble frequency. Although it is difficult to quantitate the effect of this procedure, it is our distinct clinical impression that hyperbaric respiration on oxygen for 30 minutes will frequently eliminate grade 1 and grade 2 bubbles without recompression being necessary. In all cases of surface oxygen treatment bends was not present. In no case where surface oxygen was used had the subject gone on to bends development. In two subjects, grade 3 bubbles persisted for more than one hour on hyperbaric oxygen without bends pain, and the subjects were released to their homes without development of symptoms.

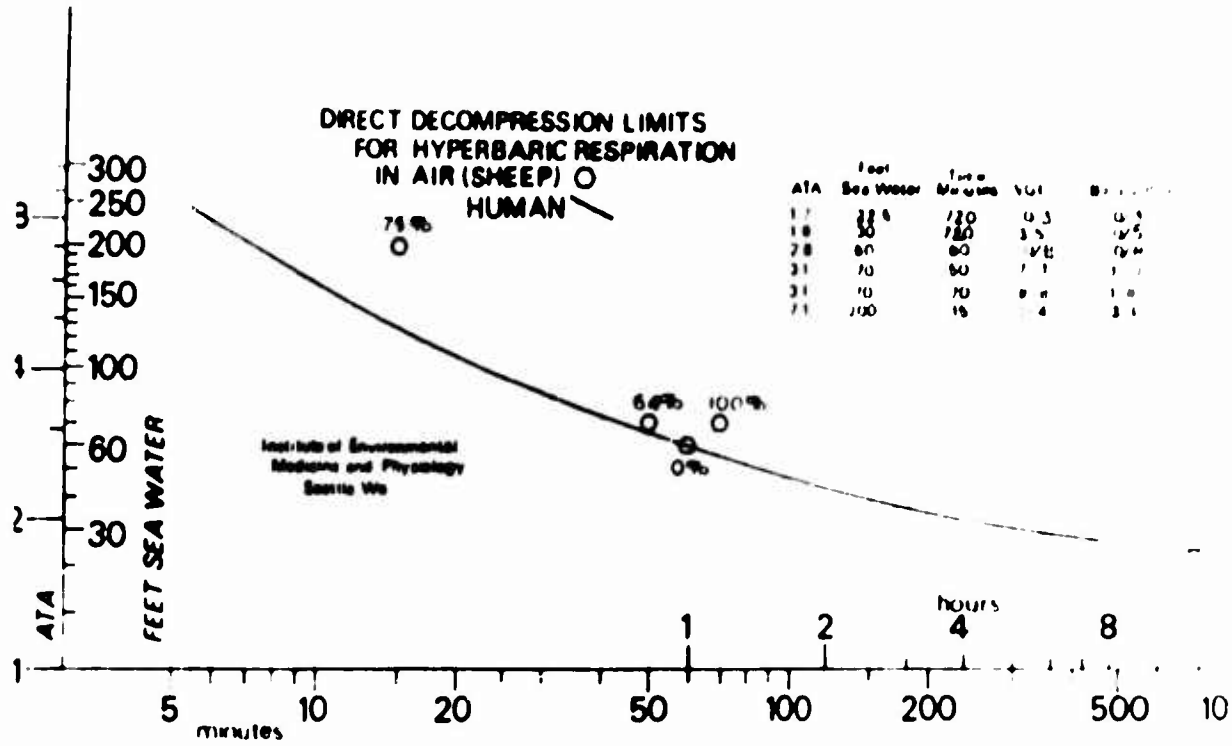

Fig. 43. Comparison of direct decompression limits for hyperbaric respiration on air for humans and sheep, suggesting that zero bends in humans is roughly equivalent to zero vge in sheep.

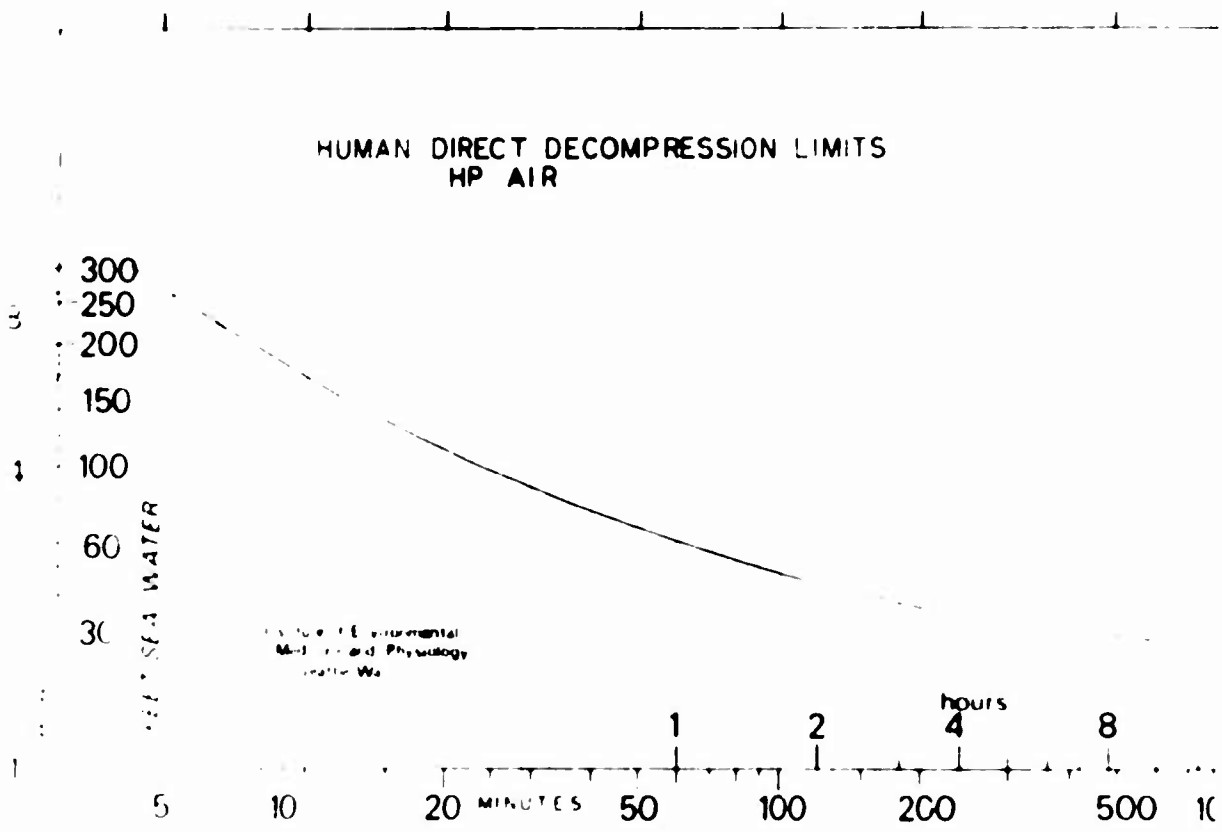

Fig. 44. Human direct decompression (Sc-D) limits after hyperbaric respiration on air, based on minimum bubbles, no bends data, (log-log plot).

C. DISCUSSION

The three most widely-used models for definition of the direct decompression limits following hyperbaric in air are the U.S. Navy No-D limits, the DeSanctis decompression meter, and the theoretical one-half times and M values. Two additional methods studied include the use of the theoretical predictions from nitrogen elimination data and that of experimental use of objective detection of venous gas emboli. Of these, only the DeSanctis meters individually represent a specific model. All the others represent more general ones.

The venous gas emboli method has been utilized in a time-intensity dosage black-box method, wherein we analyze the overall body response to the hyperbaric exposures. This method requires that the response to the given range of doses to an agent be objectively detected and plotted. The dosage limits are in terms of time and pressure, while the response is in the formation of vge. The method requires no knowledge of the detailed mechanisms of the body's handling of excess inert gas, and when examined over a wide range and plotted by smoothing curves, provides a practical nomogram for determining acceptable time pressure dosages. The vge time-intensity dosage model may, of course, be expressed as a series of exponentials which can be taken to represent a series of simultaneously acting tissue compartments and avoids the theoretical necessity of deciding whether the model is a perfusion limited or a diffusion limited one.

Any curve, out of a family of curves, which represents iso-embolic responses may be chosen as optimal limits, but we believe that a practical choice is that which represents a minimal vge formation without development of bends. The line is somewhat lower than the 2 to 1 N_2 predicted line from Behnke's data.

When compared with the U.S. Navy No-D limits, the vge (D-D) model proposed here is in excellent agreement around the point described by 60 feet for 60

minutes exposure, but indicates that the longer Navy exposures are not sufficiently conservative. In the short, deep exposures, the minimal vge no-bends curve is less conservative. Because, however, of the short absolute time differences at the short, deep end, we believe that the conservativeness of the present U.S. Navy limits is perferred because of the uncertainties in practical operations of knowing exactly the time and depth.

The DeSanctis (SOS) Decompression Meter definition of the Direct-Decompression limits which utilizes a single compartment, appears to be more in agreement with the experimental vge model in the short, deep ranges, though it is more conservative in the shallow, long term exposures. An improved pneumatic decompression meter should utilize more compartments, should provide greater reliability, and, of course, should be calibrated periodically.

The major differences between the vge experimental limits and the limits of Hawkins' chamber and Albano's open sea exposures may be explained by the greater sensitivity of the ultrasonic detection method over the use of bends as an end-point, as well as our earlier recognition of mild clinical bends. For example, we have recorded 25% bends on the 5.5 ata for 15 minutes exposure, an exposure which is indicated as safe by their results. All of our bends complaints (other than skin itching) were very mild joint pains and probably were below the level recognized by those investigators. In the middle points around 3 ata, there is good agreement between Albano, the U.S. Navy, and the vge models. The Albano model and the U.S. Navy model follow a linear plot on log-log coordinates while the N_2 elimination and our vge limits are curvilinear to the time abcissa. The difference implies two separate orders of exponentials. Hempleman's goat data tends to follow an iso-bends contour parallel to the nitrogen elimination predicted curve, (Fig. 37). The swine data of Gillis is not sufficient to determine the model's shape, but agrees that there is a gradient of iso-embolic lines over the range studied. It does bear out our findings of a gradient of iso-bends

lines over the range studied. The swine bends gradient appears to be very broad, ranging at 5.5 ata from 0% for 15 minutes to 80% for 50 minutes. The sheep vge data of Smith indicates 100% vge on all exposures except those at 7.5 ata where the gradient appears to be as broad as that for swine.

Figure 43 discloses our recent findings in sheep, and compares them to the human direct, decompression limits, (Fig. 44). These findings suggest that the zero incident lines for vge in sheep corresponds to the no-bends lines for humans. The difference between the sheep data and the human data may be explained on the basis of difference in body weight, and when compared to responses of small rodents, which are highly immune to bends, suggests that the heavier the species, the less immune the individual to the development of decompression sickness. The use of sheep as an experimental model, nevertheless, is a highly useful one, so long as this difference is quantitatively recognized. We believe that the use of sheep to simulate human responses is a valid one, and is certainly better than the use of lighter weight mammals.

Principles of Decompression Modeling

The unique principles utilized in our decompression model may be itemized as follows:

1. It is rooted in the theoretical prediction using nitrogen elimination data from human subjects—a separate but related phenomenon —taking place during the elimination of excess gas after hyperbaric exposure.

2. The decompression model is described by a time-intensity response curve on a broad scale basis, widely-separated points, including long, shallow exposures and short, deep exposures which, when the data is smoothed, provides greater accuracy within the more frequently used middle range.

3. The model is the first one to utilize a non-bends objective endpoint using precordially detected venous gas emboli with doppler ultrasound.

4. The model optimizes the problem of diving safety versus work exposures by allowing minimal bubbles, but no bends.

5. The model is determined by an engineering type input and output analysis using a square-wave exposure function and may be extended to both more complicated exposures and exposures requiring prolonged and staged decompression.

6. The model, albeit still not specific, may be graphically, mathematically, electrically or pneumatically simulated and used to test the validity of more specific models.

Peripheral Formation of Decompression VGE

The limitation of the doppler method of bubbles detection is that it does not detect static bubbles in the tissues or blood. The venous gas emboli, however, appear to be dislodged into the circulation very early after decompression, before symptoms develop and therefore, this limitation is not primarily important in research of static bubbles.

The question of whether or not tissue bubbles form in extravascular spaces at the time of or before their detection as venous gas emboli remains to be solved. Present evidence suggests that if static bubbles are formed at these early stages, they readily pass into the venous return through available channels. In open-chest anesthetized dogs, we have found that random injections of air by means of small hypodermic needles under the pericardium of the heart produces immediate gas emboli in the pulmonary artery. From this, it appears that the earliest decompression bubbles, in fact, form and grow in the capillaries and small veins where they are dislodged into the venous return. The formation of static bubbles in the tissues may require greater excess nitrogen states. We further believe that the precordial blood bubble detector will detect all physiological sized bubbles.

III.

DIVING TECHNIQUES AND OCCURRENCE OF VENOUS GAS EMBOLISM IN HAWAIIAN DIVERS

In an effort to correlate dry chamber results with openwater working experience, we studied the diving techniques and occurrence of venous gas emboli (vge) in eleven professional scuba divers working the coastal waters of Oahu and Maui. Both groups of divers were studied in November, 1973 and the Maui group again in February, 1974.

The time and depth of each dive was recorded by two methods. When available, a depth sounder developed by John Kanwisher was used. This equipment, shown in Figure 45, was strapped to the air tanks and produced a pulse interval every 15 seconds which was proportional to the divers' water depth. A hydrophone operated from the boat recorded on tape the depth. The device was calibrated by Ed Hayashi of S.K. Hong's University of Hawaii laboratory by suspending it to various known depths.

When the depth sounder was not available for the Maui divers, the divers' depth was determined by continuous sonar supplemented by the divers' report of depth gauge information. Dive time was recorded by noting the period between submergence and the appearance of the flotation bag which the diver rode to the surface. This time-depth estimate used in our 1st study with Maui divers (November, 1973) proved acceptably close to that of the depth sounder used in February, 1974.

The IEM6P precordial blood bubble detector was used to transcutaneously detect vge passing through the right ventricle and pulmonary artery. Monitoring of each dive began 5 minutes after surfacing and continued for 1-3 hours. Precordial vge quantities were graded 0-4.

A. Oahu Seafood Divers

Oahu seafood divers (Fig. 45) wore single 73 ft. tanks with regulators, pressure gauge, masks and flippers and carried a speargun. They also carried a line attached to a surface buoy so that the surface boat could maintain their exact position. They did not use reserve valves, but left the bottom when they felt increasing breathing resistance. W.V.'s last three dive series 205/11, 150/14, and 30/13+ demonstrated what we always found, that the last dive was always the most shallow dive and always longer than the other day's dives. Surface intervals were 78 and 109 minutes. This diver's 2nd series on another day is illustrated in Figure 47. Here the 2nd dive is the deepest and the 3rd and last dive of the day was shallowest. Surface intervals were 58 and 90 minutes. As shown here, the diver's ascending rates were always exponentially slowing near the surface. The 1/2 time of his ascending rates varied from 2.5 to 2.6 minutes averaging 24 to 33 ft/minute. Though these ascent rates were considerably more conservative than the U.S. Navy recommended 60 ft/minute, his total decompressions and surface intervals were considerably less than the U.S. Navy recommendations. Precordial monitoring for vge disclosed grade 2 bubbles 17 minutes after the 3rd dive which disappeared within one hour without the development of bends.

The second Oahu diver, R.K., performed 4 successive dives as illustrated in Figure 48. Dive #1 was 135/17, and dive #2 was 147/17. The 3rd and deepest dive was 200/7 and the last and shallowest was between 35 and 70 feet for 36 minutes. No staged decompression steps were taken. Ascent rates were at 24 to 38 ft/minute almost exactly the same as Oahu diver #1. Surface intervals were 72, 100, and 35 minutes--inadequate by USN standards. Grade 4 vge were produced after the 2nd dive, dissipated after the 3rd and reappearing in grade 2 quantities after the 4th dive. No bends was produced. Data on the precordial blood bubble detection is shown in Table III.

Fig. 45. Diving equipment worn by Oahu seafood divers showing depth sounding device strapped to side of tank. Unit produces pulse proportional to pressure every 15 seconds.

Fig. 46. Maui black coral diver prior to diving with 16 lb. hammer used to dislodge coral at depth.

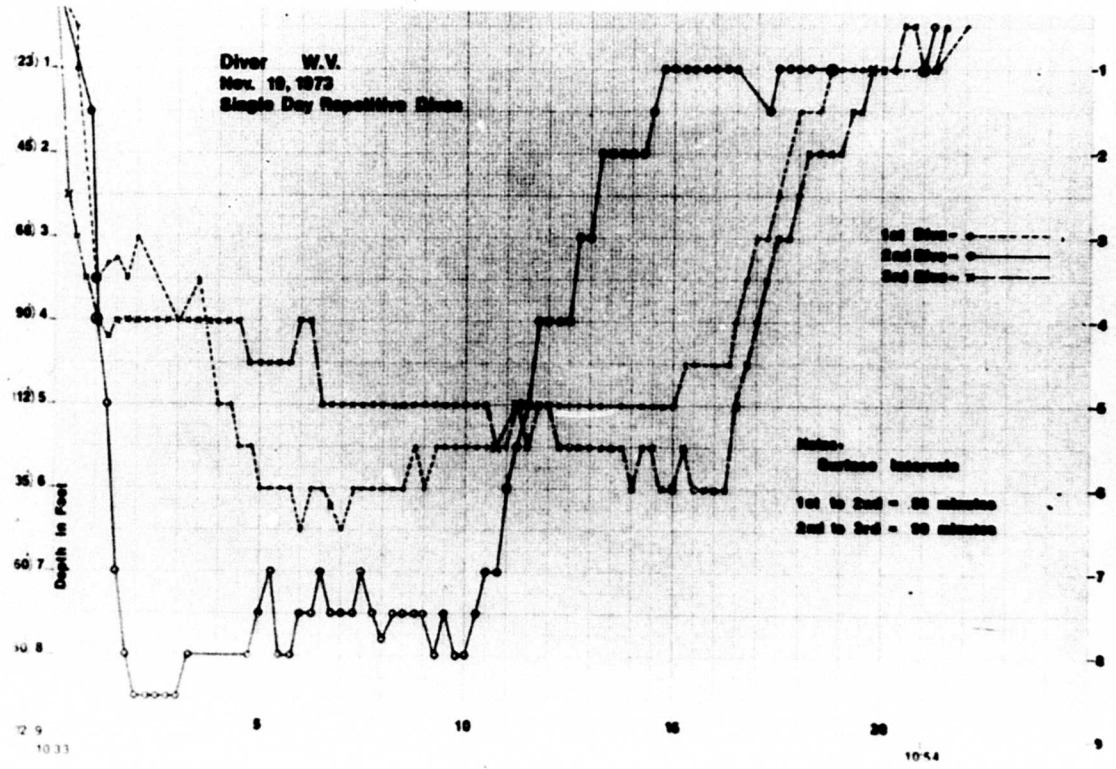

Fig. 47. Single day's dive schedule of Oahu sea-food diver (W.V.)

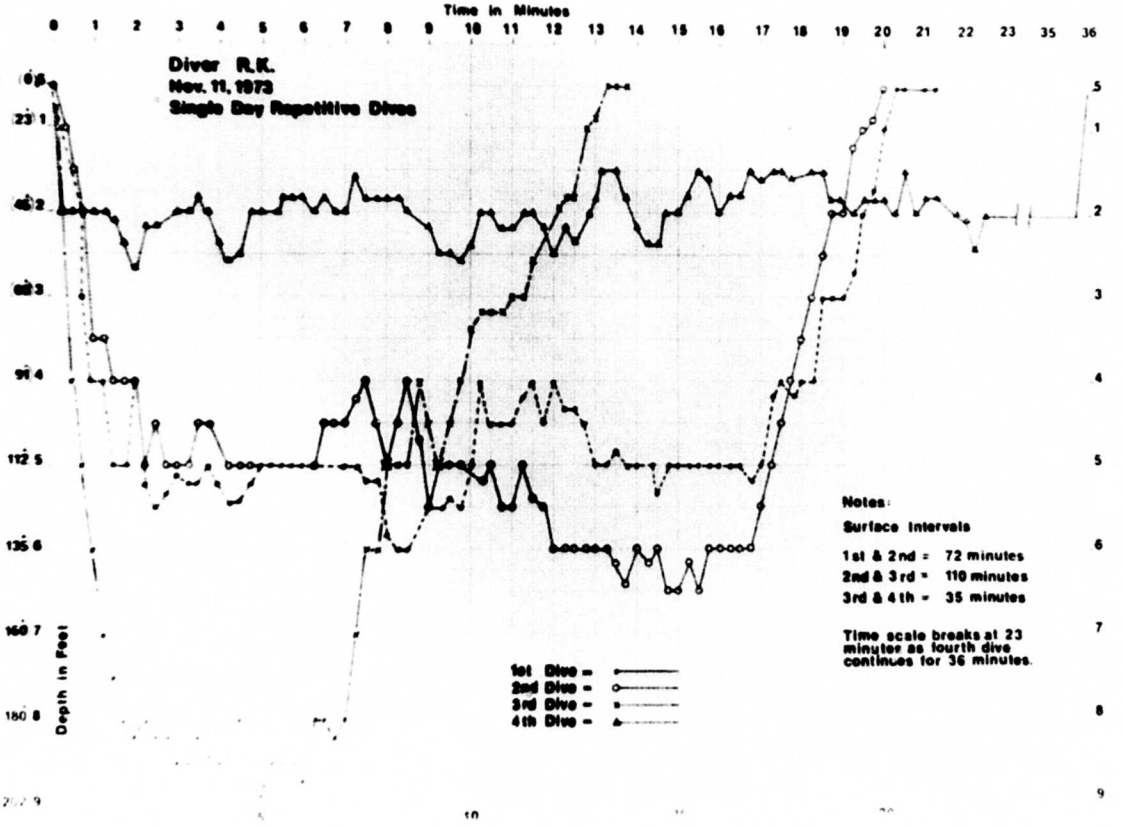

Fig. 48. Single day's dive schedule of Oahu sea-food diver (R.K.)
Last dive of day is generally the longest and shallowest.

TABLE III

OAHU DIVERS

Date	Max Depth Feet	Bottom Time Minutes	Total Time Minutes	Decompression Stops Ft/Min	U.S. Navy Recommended Stops Ft/Min	Post Dive Bubbles Grade 1–4 Grade/Min	Surf Inter Min	Time Surf Min
W.V. 11/19	137	16	22	30/1, 23/3	10/6	0/4, 0/20		10:54
	190	11(+15)	21	90/1,45/1,23/7	40/1,30/8,20/19, 10/32	0/3, 0/14	58	12:[illegible]
	135	16(+26)	21½	45/1, 23/2	30/6,20/24,10/44	2/17 0/69,0/142	90	14:04
R.K. 11/21	112	17	20	Linear Ascent	2/10	0/8		10:51
	145	17(+17)	20	3 min. Linear Ascent	30/5,20/19,10/33	2/5 3/16 4/83	1:12	12:22
	195	7(+16)	13	6 min. Exponent. Ascent	40/2,30/9,20/22, 10/37	0/2,0/9,0/15	1:50	14:20
	60	36(+?)	36	Linear Ascent		1/2 0/22 1/46	:35	15:36

Notes: W.V. dive profile was monitored continuously
R.K. dive profile monitored every 15 seconds

"□" represents presence of venous gas embolic signals (Bubbles)

We concluded from these studies that the Oahu divers' last dive of the day, always in shallower water, served as recompression R_x to prevent serious gas nucleation and bends. Also their use of slow and exponential ascent rates allows them to impose normal decompression procedures. In Figure 50 are plotted the dives of five of these divers as a comparison to our own D-D curve for human subjects.

B. Maui Black Coral Divers

Maui black coral divers working the channel off Lahaina wear twin 72's with reserve valves, single hose regulators, pressure gauges, decompression meters, and masks and flippers, (Fig. 46). In addition to a shark bang stick, they carry a 16 lb. hammer, an iron handled hatchet and 3 inflatable rubber bags with a 15 ft. line attached. They make one dive per day plummetting to the bottom reaching 180 feet in one minute, run over the bottom to find a coral, then work vigorously to dislodge the specimen which is attached to the line of a bag. The bag is inflated for ascent and the diver proceeds to the next coral. He returns to the surface on his last bag when his DeSanctis decompression meter indicates the 10 foot stop or until his air supply is depleted.

Blood bubble detection data is shown in Table IV. Bottom times in 20 dives ranged from 3 to 18 minutes, averaging 182 feet. Five No-D excursions were made 250/10, 210/19, 140/13, 140/19, and 200/19. All no decompression dives exceeded USN recommendations by 7 to 14 minutes or more. Nine out of 15 known divers have experienced paralytic consequences following exposures of this type. Figure 49 illustrates two representative decompression dives, showing the rapid descent and fairly constant bottom depth working gradually deeper and the rapid ascent rates. Decompression is taken on the coral bag at 20 feet but never as long as recommended by the USN exceptional exposure tables. This figure (49) shows the difference in actual and USN decompressions.

Results from monitoring 25 dives showed an 8/12 incidence of precordial vge

in the November, 1973 studies and 3/13 incidence in the February, 1974 series. The February series were more conservative with more decompression time taken. They were also less completely monitored due to unfortunate loss of tape data. From the November series, very completely monitored by M.P. Spencer, two principal factors appeared to influence the incidence of bubbles: (1) the time-depth factor and (2) individual differences.

By additional monitoring of the subclavian and jugular veins, we found that a starting propensity for bubbles to arise from the left arm though all divers used their right arm to swing the 16 lb. sledge while on the bottom. Table IV further documents this finding.

Ascent rates are shown in Figure 51 to exceed 120 ft/minute reaching as high as 5 ft/second near the surface. The depth is plotted in feet on an absolute scale and on semi-log paper to emphasize that ever a constant rate of ascent is relatively faster near the surface than at deeper pressures. Figure 52 illustrates ascents of 3 other divers who let go of the bag before reaching the surface.

C. Summary and Conclusions

Professional seafood and coral divers using scuba in the waters of the Hawaiian Islands routinely exceed limits of safe decompression recommended in the U.S. Navy diving manual.

——Oahu divers make repeat dives which utilize a final dive of the day in shallower water and for a longer period than the previous ones. This procedure apparently protects against bends and vge formation by providing preventative recompression R_x.

——Oahu divers also utilize slow and exponential ascent rates which avoid the sudden "pull" on the tissues which is especially important in the shallow depths.

——Their use of one tank of air per dive provides some limiting of tissue loading.

TABLE IV

[illegible]'I CORAL DIVERS

	Date	Dive[1] Ft/Min	Total Time	Decompression Stops Ft/Min	U. S. Navy Recommended Stops Ft/Min	Decompression Meter Reading on Surface	Precordial Bubble Signals Grade/Minutes[2]	Peripheral Source
R.S.	11/24	140/19		0	10/6	In Small Red	[illegible], 0/31	
	11/23	240/11		0	30/2,20/5,10/16	Top Middle Red	[illegible] 0/11, 0/22, 0/85	
	11/26	190/13		0	20/4,10/7	Lower 10' Red	[illegible] 2/26, 3/35	Lt IV Not Rt IV
B.O.	11/24	140/19		0	10/6	Small Red	3/27, 3/80, 1/88	Lt BV & Lt IV Not in Rt BV J Von Art
	11/23	215/8		25/9	20/2,10/5	Top Middle Red	3/13, 3/21, 2/83,	
	11/26	190/16		20/1½	20/2,10/7	Top Middle Red	0/23, 0/24, 4/114	Lt IV Not in Rt IV
H.B.	11/24	200/16		15/9	30/3,20/7,10/27	In Middle Red	0/13, 1/18	
	11/23	115/9		25/8	20/2,10/5	Top Middle Red	0/10, 0/17, 0/78	
	11/26	210/19		0	30/4,20/10,10/23	Middle 10' Red	0/13, 4/23	Lt IV & Arm
T.H.	11/24	150/10		15/5	10/1	Below Small Red	0/12, 0/23	
	11/23	200/10		15/1	20/1,10/4	Middle Small Red	4/13, 4/15, 4/32,	
J.T.	11/23	200/14		20/17	30/1,20/4,10/10	Middle 10' Red	0/19, 3/26, 4/54, 2/87	Lt BV Not Rt BV

1 Est max depth

2 Aster Surfacing or Beginning Decompression Precordial Bubbles

V = Vein
I = Innominate
B = Brachial

Lt = Left
Rt = Right

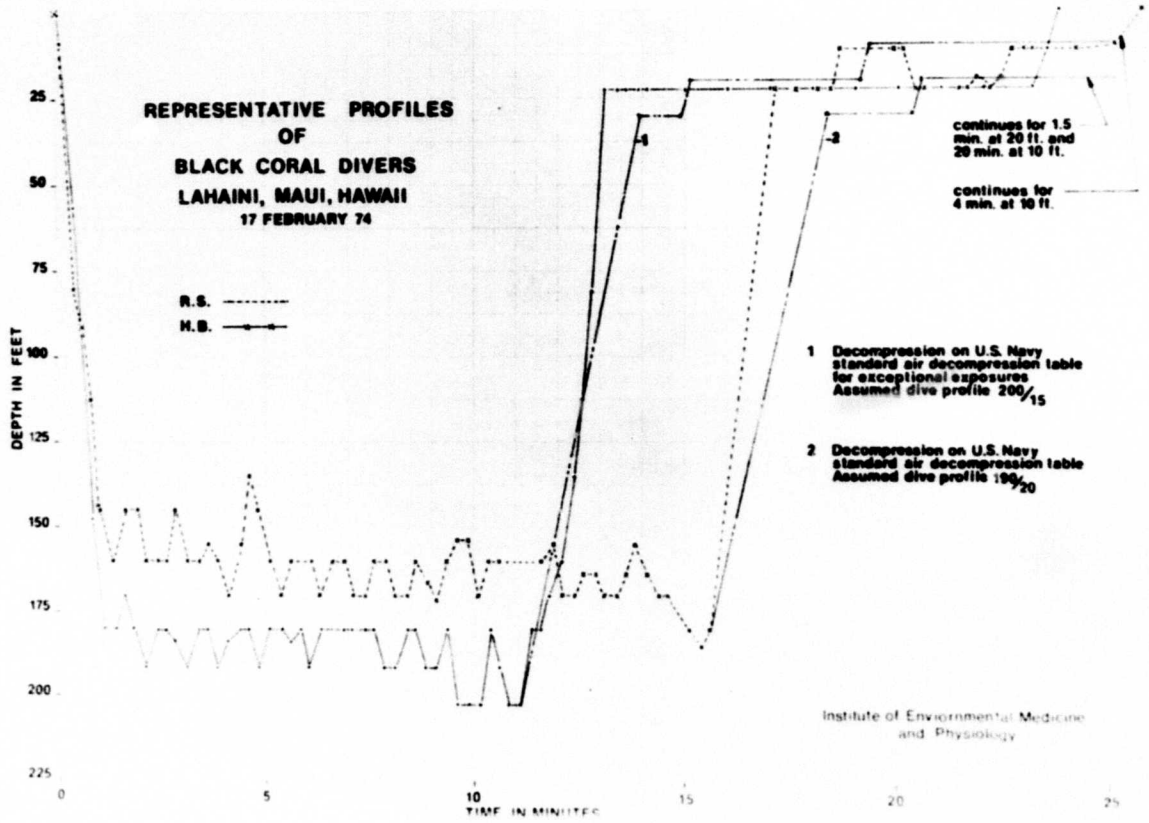

Fig. 49. Comparison of Maui black coral diver profiles with U.S. Navy exceptional exposure tables for similar profile.

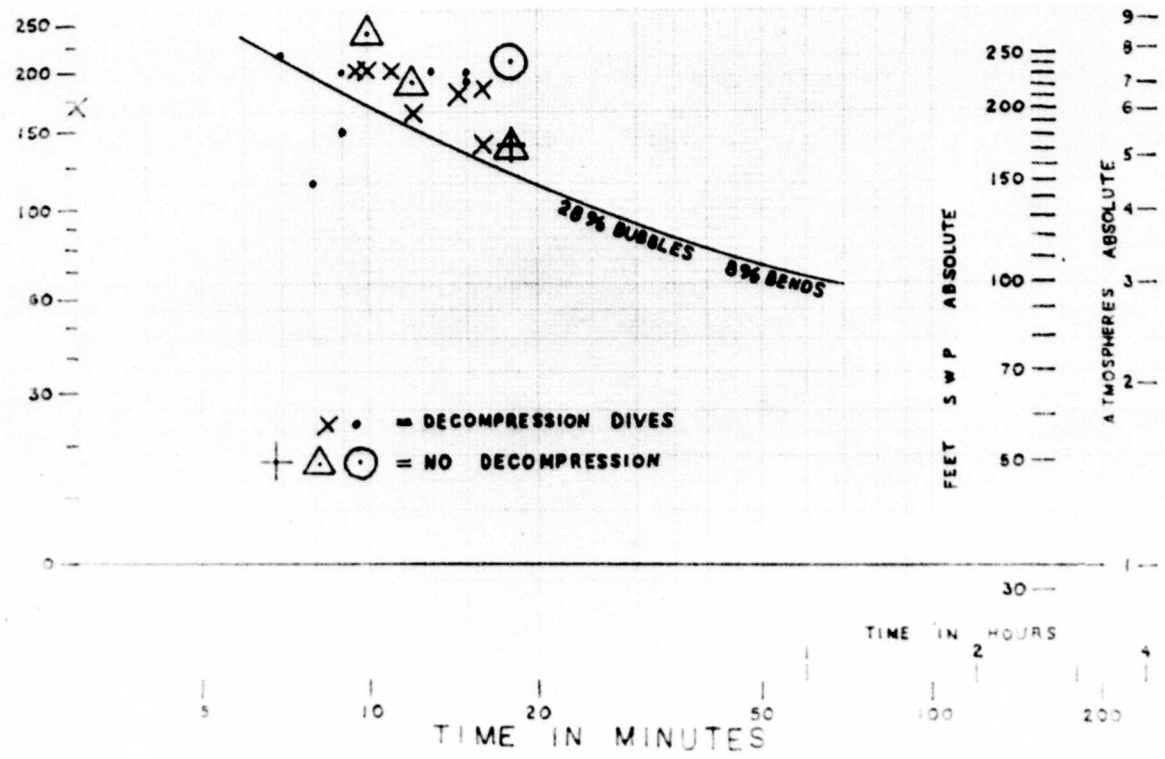

Fig. 50. Comparison of Maui black coral diver data with our laboratory results.

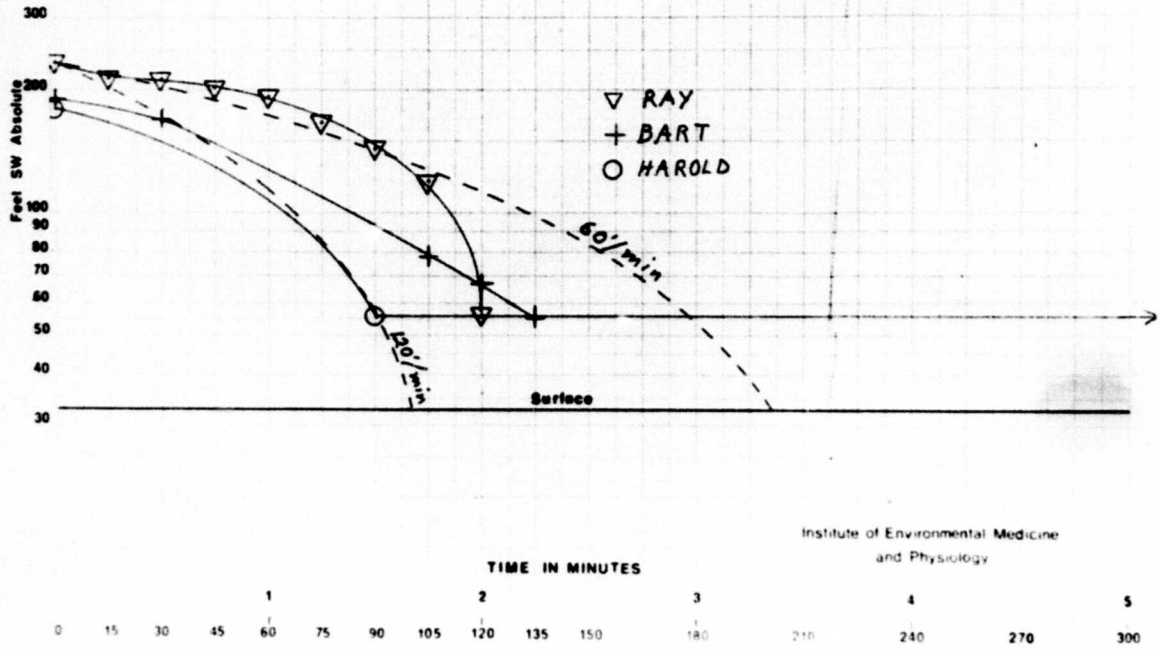

Fig. 51. Ascent rates of Maui coral divers. Collection bags inflated at depth are ridden to the surface.

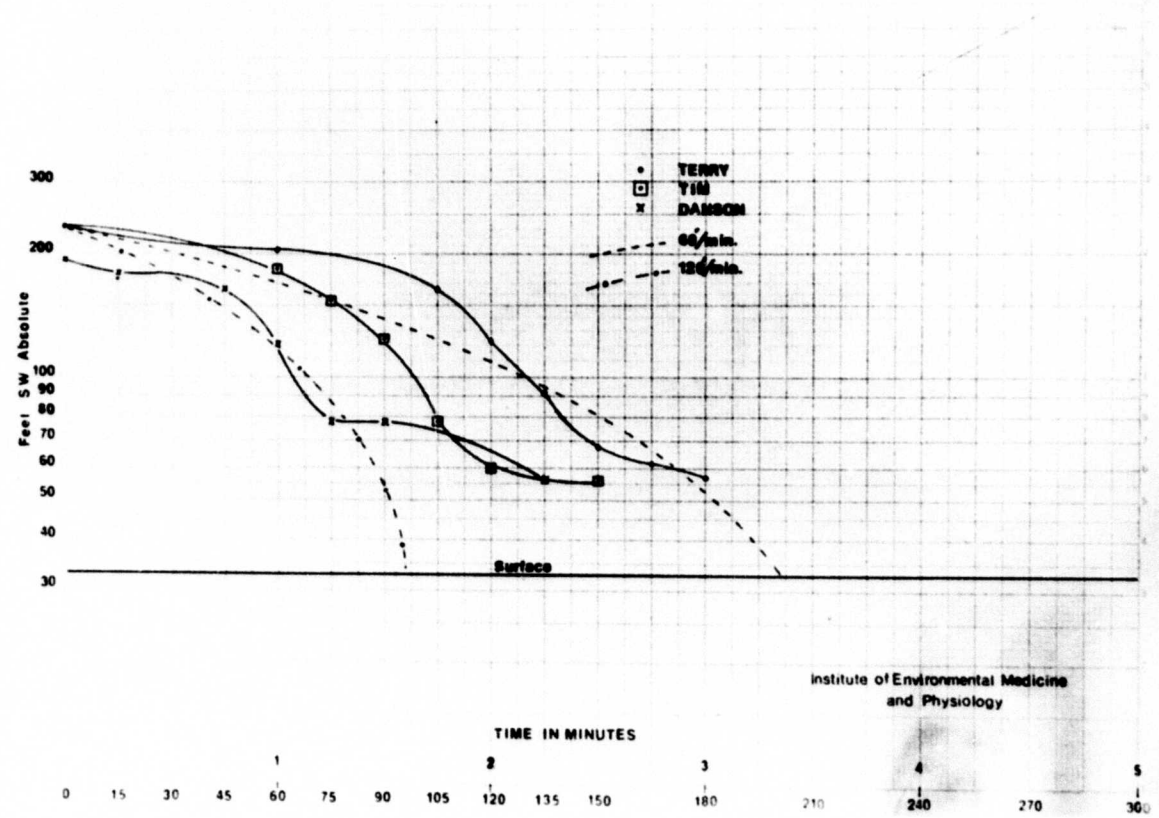

Fig. 52. Ascent rates of Maui coral divers who release collection bag before reaching the surface.

—Maui black coral divers make one 12 minute dive/day to 185 ft., normally ascend at exceedingly fast rates and decompress inadequately as judged by U.S. Navy standards. They produce frequent vge and sustain a high incidence of paralysis. Paralysis may be due to lung rupture consequent to rapid ascent rates.

—Vigorous exercise at depth until immediately before ascent may enhance N_2 elimination by means of post exercise hyperemia.

—The vge incidence of this open water no-stop decompression (66%) are in agreement with dry chamber tests which indicate a greater than 50% incidence will occur for corresponding exposures.

IV

CLINICAL USE OF BLOOD BUBBLE DETECTION IN OPEN WATER WORK

The physician caring for decompression problems with divers, caisson workers and others that work in hyperbaric environments now has available an "ultrasonic stethoscope" which detects venous gas emboli developing in advance of and during decompression sickness. Clinical experience with the precordial detector indicates that early gas bubbles which are dislodged from peripheral tissues into the venous return as emboli on the way to the lungs may be detected in the field where effective action can be taken to prevent decompression sickness. Interpretation of the bubble signal is similar but less complex than osculation for cardiac murmurs. Symptoms of decompression sickness, except for skin itching, may be prevented by early detection and use of surface oxygen respiration.

Open ocean diving applications of the detector have been made at Cobb Seamount, which lies 275 miles off the coast of Washington State. For several years, the diving operations have been approximately the same. Standard procedure would be for the diver to work at 100 to 130 feet salt water depth for 15 to 25 minutes with decompression at the 10 foot water stop for from 4 to 15 minutes. In 1972, 9 subjects performed a total of 38 dives. All subjects were monitored 5 to 15 minutes after surfacing by the diving physician (William Postles, Portland, Oregon). Eleven of these dives produced bubbles with a 29% incidence of vge. They were usually treated with surface oxygen or recompressed to 30 feet of sea water in the decompression chamber and were not allowed to make repeat dives for 24 hours. Water temperature was between 50 and 55 degrees F. No symptoms of decompression sickness developed during the 1973 operations. Dive profiles and results are shown in Table V.

T A B L E V

OPEN WATER DIVES

DIVER	DIVE DAY #	PROFILE DEPTH/TIME	LENGTH (TIME) OF DECO. STOP	ELAPSED SURFACE TIME	GRADE VGE.	RX
S.C.	6	150/20	NA	14	1	10 Min 100% O_2 @ 1 ATA
	7	130/24	10	30	1	10 Min 100% O_2 @ 1 ATA
	1	130/20	4	17.5	2	10 Min 100% O_2 @ 1 ATA
	3	120/18	4	24.0	1	15 Min 100% O_2 @ 1 ATA
	5	115/24	6	24.5	Ø	
M.R.	6	130/21	10	16	Ø	
	4	120/25	7	18	Ø	
	5	120/24	6	20	Ø	
	1	120/19	4	19.5	1	NONE
B.A.	6	130/20	10	25	Ø	
	1	130/19	6	13.5	Ø	
	4	120/24	6	12	Ø	
P.M.	6	130/21	10	12	Ø	
	1	130/20	4	20	Ø	
	4	130/25	7	37	1	10 Min 100% O_2 @ 1 ATA
J.E.	1	130/22	6	45	1	20 Min 100% O_2 @ 1 ATA
	6	130/20	NA	15.5	Ø	
	3	120/25	15	5	Ø	10 Min 100% O_2 S 30 FSW*
	5	120/24	6	24	Ø	
V.R.	6	130/20	10	32	Ø	
	1	130/15	4	15	Ø	
	3	120/25	15	42	2	10 Min 100% O_2 S 30 FSW*
	4	120/24	6	17	Ø	
R.W.	1	130/20	4	24	Ø	
	1	130/19	6	22	Ø	
	6	120/25	6	13	Ø	
	4	120/24	6	9.5	1	10 Min 100% O_2 @ 1 ATA
	4	120/18	6	23	1	10 Min 100% O_2 @ 1 ATA
	5	115/24	6	22	Ø	
M.S.	7	130/24	10	34	Ø	
	1	130/20	4	21.5	2	10 Min 100% O_2 @ 1 ATA
	6	130/20	NA	18.5	Ø	
	3	120/18	4	20	Ø	
	5	115/24	6	26	Ø	
P.M.	1	130/22	6	28	Ø	
	6	120/25	6	8.5	Ø	
	4	120/24	8	22	Ø	
	6	120/19	4	9.25	Ø	

LEGEND

Ø = No bubbles
1 = Minimal detectable bubbles
2 = Moderate bubbles
3 = Copious bubbles
4 = Extreme bubbles

NA = Information not available

* = Divers missed "D" stop. Surfaced, re-entered water for 15 minute stop.

All decompression stops at 10 ft. depth

All time in minutes, depth in feet.

All divers are experienced, healthy males.

Eight additional dives were performed on which no data is available.

In contrast, during 1971 the same diving operations produced 2 CNS "hits" which occurred after repeat dives and required recompression treatment.

Four of the 1972 divers were also members of the Experimental Diving Laboratory team who participated in the studies of defining unknown decompression limits. Diver S.C., who bubbled most frequently in the chamber dives, was also the same diver who bubbled most frequently during the open ocean dives. On the other hand, diver J.E., who never bubbled on the experimental No-D exposures, did produce bubbles from 2 water dives, one which followed prescribed decompression procedures and one which did not. Another experimental diver, who bubbled on one open water occasion, also bubbled on the 150 for 15 No-D experimental exposure. Even though there were differences in conditions between the working open-water decompression dives and the experimental No-D dry chamber resting dives, the differences in percentage occurrences of vge and absence of bends appears to be explainable on the differences of pressure profiles alone. It is therefore suggested that the dry chamber dives may effectively predict what can be expected in actual working open-water dives.

To test this idea, we exposed six divers to identical profiles in the chamber and open water. Efforts were made to keep the depth/time (profile) relationships as close to identical as possible. The chamber exposures were monitored by both mechanical and electrical pressure transducers. Individual depth gauges were exposed on these chamber profiles to select one or more which were in agreement with the chamber pressure monitors. One such depth gauge was in complete agreement from surface (1 ata) to depth (6 ata) and was therefore used to determine the depth of the open-water dive. Ascent and descent rates were maintained at 60 ft/minute in the chamber while ascent and descent in the water was performed by pulling one hand over the other, on a descending line, in one-foot increments while counting "one-thousand one, one-thousand two, etc.".

We did not expect to control other conditions such as temperature, workload,

psychological conditions, etc., and in fact, expected these variables to constitute the differences between the two exposures. The chamber exposures presented no workload other than respiration in a more dense medium, while the open water exposure presented, in addition to that above, restriction of the diving gear and its accompanying weight, efforts of swimming in 55 degree Fahrenheit water running at better than 1 knot and in moderately choppy seas.

Results of our findings are found in Table VI. Two of our divers bubbled on chamber exposure while five of them bubbled on the open water dive. Of obvious interest is the relationship between the chamber exposure induced bubbles and those resulting from the open water work. None of the divers (four), who exhibited low-grade vge following open water work, bubbled on the chamber exposures. The other (two) divers, both of whom exhibited moderate amounts (grade 2-3) of vge on the chamber exposure, produced grade 4 vge with rapid onset of bends pain on the open water exposure. Both of these divers were subsequently treated successfully with 100% O_2 respiration in the hyperbaric chamber.

Based on these results, we would suggest that the dry hyperbaric chamber can be utilized as a valuable tool in diver selection. By pre-exposing all divers to a simulated water dive, and monitoring post-dive for vge production, those divers tending to produce moderate (grade 2-3) or stronger embolic signals could be selected out and removed from the program. Such a program would not only reduce lost diving time to bends, but could substantially reduce the risk factor for the individual diver.

TABLE VI

CHAMBER EXPOSURE COMPARED TO OPEN OCEAN EXPOSURE

165 ft/10 min.

DIVER	PROFILE No-D	ELAPSED SURFACE TIME	GRADE VGE Chamber	GRADE VGE Open H_2O	R_X
S.C.	165/10	13 min.	3		None
	165/10	4 min.		4	Table V
T.L.	165/10	17 min.	2		None
	165/10	4 min.		4	45 min. O_2 @ 30 FSW
P.McK	165/10		0		
	165/10	20 min.		2	60 min. surface O_2
J.N.	165/10		0		
	165/1C	10 min.		1	
J.E.	165/10		0		
	165/10	12 min.		1	
G.A.	165/10		0		
	165/10			0	
			33%	83%	

V.

SAFETY CONSIDERATIONS

The question of safety in using the precordial detector and other ultrasonic transducers on humans has been under consideration since their first use. Most ultrasonic applications to humans have been made before proof that they would not produce adverse effects. Adverse effects may be expected either by direct thermal damage from the sonic irradiation or by the growth of bubbles in the tissues and blood. Of special concern in divers is the possibility of promoting bubble production or growth in tissues that contain excess nitrogen ("super saturation"). We have examined several lines of evidence, both theoretical and experimental, that bear on the safety question.

A. THEORETICAL CONSIDERATIONS

Power Levels Used

The peak-to-peak voltage applied to the precordial transmitter's ultrasonic crystals from the power oscillator of our design does not exceed 5 volts. The precordial ultrasonic detector as designed and used in this laboratory, has an energy level not exceeding 10 mW/cm^2 deliverable to the transmitter crystal. The crystal efficiency in producing ultrasonic energy in the sonically conducting medium probably ranges 10 to 20 percent. We found, by measuring by radiation force studies, that the ultrasonic energy delivered to the skin surface does not exceed 3 mW/cm^2.

Attenuation in the Tissues

Any transducer radiating into an absorbing medium which is uniformly homogenous will have its intensity reduced by the inverse exponential of the medium depth or distance from the crystal. This may be formalized in the fol-

lowing equation: $I_d = I_{max} e^{-kd}$ where I = intensity, I_{max} = intensity at the medium entrance, d = depth in the medium, and k = a proportionality constant. While the body is far from a homogenous absorbing medium, the inhomogeneities will produce an additional attenuation by means of reflection from the acoustical interfaces. Each tissue tends to absorb ultrasonic power to a greater or lesser degree. From Wells, (1969), we estimate tissue losses at 5 MHz, varying from 0.9 db/cm for blood, 16 db/cm crossing muscle fibers, 100 db/cm for bone, 205 db/cm for lung tissue, and in fat a rate of 3 db/cm. Additional attenuation at points of ultrasonic reflection may be expected at many interfaces such as between the crystal surface and the skin, and between concentration of fatty, muscle, aqueous, bony and lung tissue.

A conservative estimate of the power delivered to the surface of the heart with the precordial transducer indicates that this cannot exceed 30 $\mu W/cm^2$. The subambient pressure generated by 30 $\mu W/cm^2$ of 5 MHz ultrasound is equivalent to approximately 3 inches of water. Even assuming a possible "pumping" effect due to the rapidity of sonic oscillations, three inches of water pressure imposed by the first steps of decompression has been used safely for years in diving decompression practices.

Biological Effects

While no one has yet defined a specific end point for acceptable, safe tissue ultrasonic levels, Wells (1969) states that biological effects have not been observed at intensity levels below 100 mW/cm^2. Intensity levels varying from 0.05 mW/cm^2 to 0.001 mW/cm^2 for durations varying from 15 to 1,440 minutes at frequencies from 5 to 15 MHz have failed to demonstrate tissue damage in animals, including fish, amphibia and mammals. A study in human physiotherapy utilizing 10 minutes duration of 1 to 3 MHz ultrasound at varying intensity levels of <1 to 5 W/cm^2 provided similar results. Though this evidence does not conclu-

sively prove that the presently utilized levels of ultrasonic energy are safe, no experiments utilizing the levels of energy which we provide have shown any tissue damage to date. Ulrich (1971) concluded from a literature search study that exposures of 100 $\mu W/cm^2$ of CW ultrasound were harmless for periods in excess of three hours.

Cavitation Bubbles

Cavitation in aerated water at 5 MHz requires a power of 5×10^5 Watts/cm^2, Heuter and Bolt (1955). The sound pressure necessary for vaporous-type cativation increases rapidly above 0.1 MHz and becomes as great as 100 ata at 5 MHz. Heuter and Bolt have shown the need for a power level in excess of 50,000 [illegible] produce cavitation bubbles with a 5 MHz ultrasound while only 2 to [illegible] required in the 20 kilohertz range. Cavitation is not, therefore, a phenomenon of concern at the frequencies and power used in medical doppler ultrasonic devices.

Bubble Growth

Experimental evidence indicates that the smallest stable bubbles have radii of the order of 5×10^{-7} (0.5 microns), Heuter and Bolt (1955). Concerning the possibility that ultrasonic energy may produce bubble growth by resonant oscillation of microbubbles already present, the following are pertinent. Even bubbles as large as 7 micra in diameter possess such high damping factors in solutions that they do not strongly resonate at their expected resonant frequency. 5 MHz is the expected resonance frequency of a bubble of air in water of 8×10^{-7} diameter. It would appear, therefore, that a resonance phenomenon is unlikely to be in effect to promote growth of bubbles. There remains, however, the possibility of growth from non-resonant oscillations of the bubble.

B. EXPERIMENTAL AND PRACTICAL EXPERIENCES

Ideal experimentation calls for the production of bubbles in the tissues by ultrasound and determining the levels at which it is insured that the level of operation is well below this level. Because cavitation and supersaturation bubbles have never been produced by 5 MHz ultrasound, this ideal approach to experimentation has not been necessary.

In-Vitro Experiments

Our laboratory investigations have never generated bubbles or indicated promotion of bubble growth. These investigations, to be sure, have been preliminary. We have energized with both 5 and 10 MHz doppler crystals, positioned in columns of supersaturated soda water, and have consistently failed to produce clouding with the laboratory-produced energies well above those used in our experimental and clinical doppler flowmeters and bubble detectors. Five megahertz doppler transducers, focused on a moving column of blood, passing through dialysis tubing, have also failed to produce detectable downstream bubble signals.

Animal Experimentation

We have positioned, in tandem, large crystal 5 and 10 megahertz doppler flowmeter cuffs on the inferior vena cava of sheep. Following recovery from the surgical procedure, the animal was compressed and decompressed to produce a supersaturated condition, which produced decompression bubbles heard while monitoring with the 10 megahertz doppler. The five megahertz doppler was then energized in an on-and-off cycle during a 30 minute period when the 10 megahertz bubble signals were produced at a relatively constant rate. We were unable to produce any change in the downstream bubble signals by this means. Powers into the five megahertz crystal exceeded by a factor of 10 those normally used for energizing them.

Human Experience

Experience with clinical monitoring of more than 500 subjects, studied by means of precordial bubbles using the precordial and peripheral detectors, whom may be presumed to be in an excess nitrogen state, has failed to produce any observable symptom or sign of tissue damage or bubble formation.

In most chamber exposures "skin bends" is produced, which amount to an itching and reddening of the skin, presumed to be due to formation of nitrogen bubbles in the skin itself. In spite of the fact that the phenomena occurred frequently over the arms and back, we have never observed and have never had a complaint of symptoms or signs developing in the skin beneath the transducers. There has never been any skin reddening and there has never been any subject observed to be scratching the precordial area. Even on direct questioning of subjects, local effects have been consistently denied. Since the maximum amount of energy available might be expected to occur near the crystal itself, in the skin, this practical experience argues strongly against the possiblity that bubbles are formed at any level in the tissues by means of our transcutaneous transducers and the energies used. No cardiac abnormalities have been associated with the use of the transducer, although premature contractions are occassionally heard, as are noted in many normal subjects by other monitoring means.

C. CONCLUSIONS

While our studies and considerations have not been exhaustive, and no project funds have been available to directly investigate in detail the basic factors, we feel that practical experience and theoretical considerations strongly indicate that the 5 megahertz doppler units used at no more than 10 mW/cm^2 of ultrasonic energy into the crystal, produce no dangerous effects. It is further concluded that the importance of the information available to the diver and the diving supervisor from the use of this detector far exceeds any probable deleterious effects which might be expected.

VI.

NEW ENGINEERING

Bubble Counting

After detecting the presence of blood gas emboli, it is desirable to correlate the rate of gas emboli ratio with the appearance and sensitivity of decompression sickness. When the number of bubbles has risen to the point where decompression sickness is incipient, it is impossible to count them manually. Attaching an electronic pulse counter straight to the precordial detector does not serve well since the bubble signals are often present, but masked by artifacts from the heart motion and blood flow. Something is needed having a little of the autocorrelation capability of the human ear.

In-Vitro Signal Generation

In the present precordial signal, the signals of heart motion are often larger than the bubble signals. Users learn to listen through, or past, the rhythmic heart sounds for the occassional non-rhythmic "chirp" or whistle indicating the passage of a bubble. These artifacts will, of course, complicate the effort required to recognize and count the bubble sounds by automatic means. Our first efforts were directed to developing a means which would recognize and count bubbles in the presence of a flow signal without the heart artifacts. We began by trying to produce machine equipment which would discriminate a bubble signal from the noise-like background of blood flow signals. A mixture of flow and bubble signals is produced by passing the blood with bubbles through a section of dialysis tubing, which is suspended in a bath of water, (Fig. 53 & 54). If the transducer of the precordial detector is also placed in the water bath, and arranged to look at an angle at the center of the length of dialysis

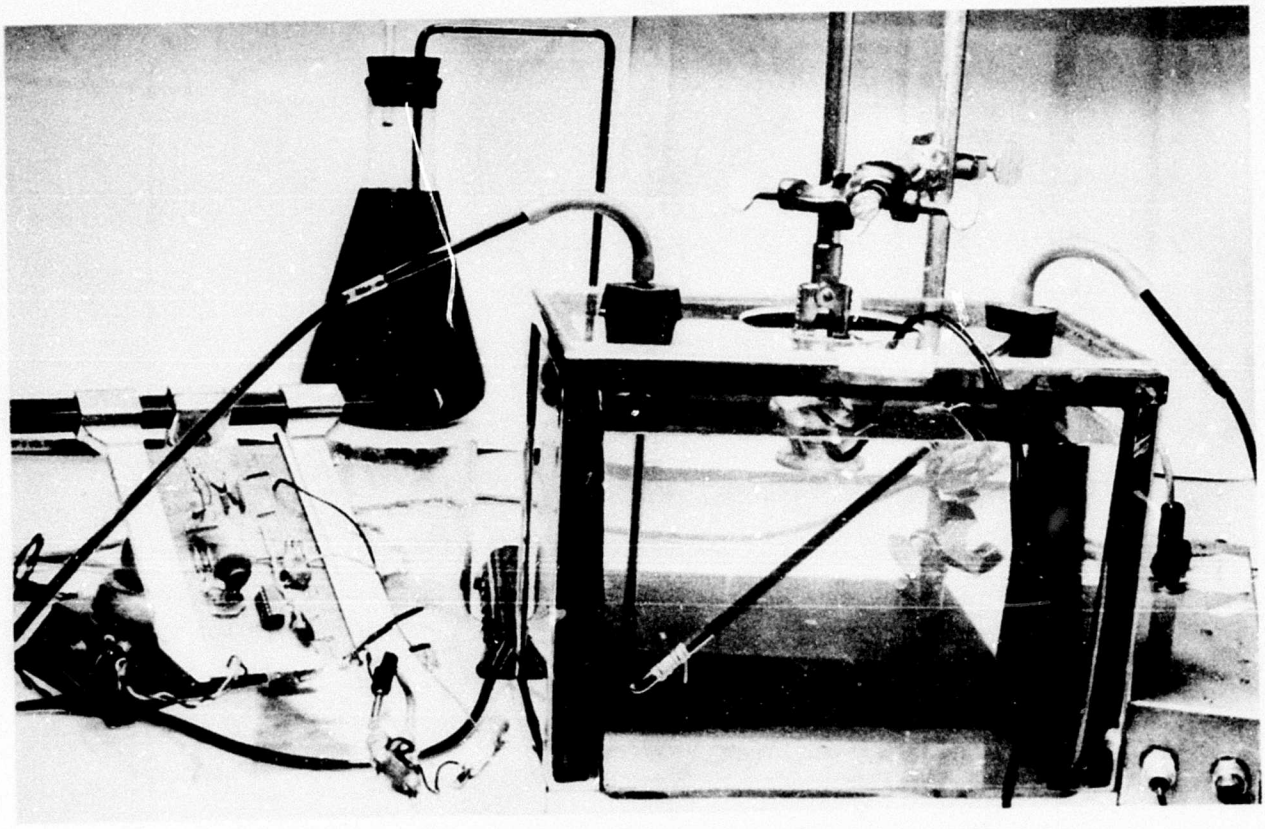

Fig. 53. Set-up for in-vitro bubble counting work. Phase lock loop circuitry accounts for the majority of the electronics shown.

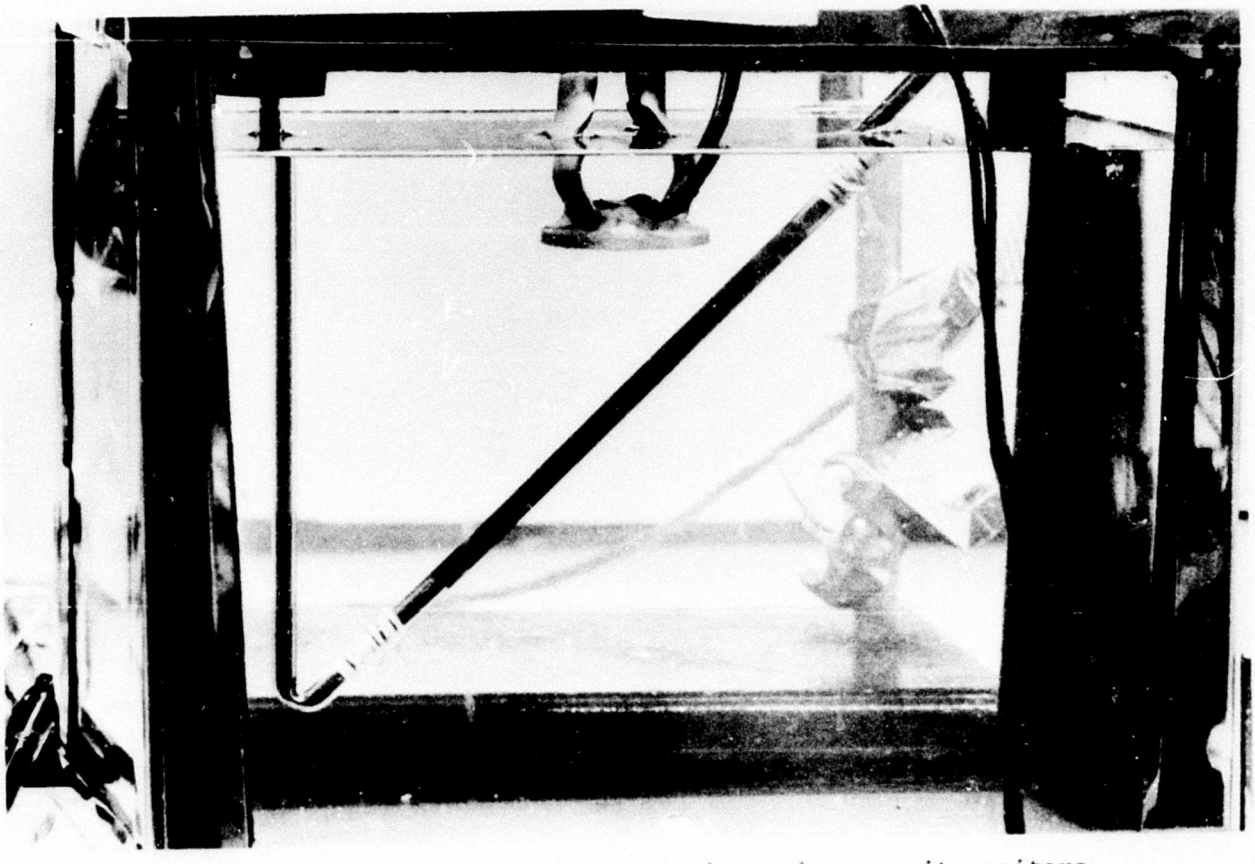

Fig. 54. Close-up of the transducer shown above as it monitors the flow stream inside the dialysis tubing beneath it.

tubing, flow and bubble signals are readily produced, Recording these on magnetic tape conveniently stores the signals from such an arrangement, and allows the counting electronics to be tested, without the necessity of the bubble and flow signal generator, at later dates.

Electronic Counting

Straight amplitude discrimination after selective filtering has been employed in the past, Smith (1970). The burst of sound from the bubbles was rectified, filtered, and the envelope fed to a counter. However, since the present purpose is to develop equipment which will ultimately be able to overlook heart artifacts of larger amplitude, this does not seem promising.

We sought a method which would perform like the ear discriminating between the chirp and the flow sounds even when the two are of equal amplitude. Since the chirp sounds as a clear tone (coherent sound) against the windy noise of the flow sounds, something is needed that takes into account the coherence as well as the amplitude. If the amplitude of the chirp is larger than that of the flow sounds, this will add assurance of making the count.

The locking onto and tracking of a coherent signal in the presence of a non-coherent signal is accomplished when a tracking filter is used to bring a frequency modulated radio signal out of enveloping noise. Since it seemed reasonable to examine the tracking filter for use with the bubble signals, we chose a commercial form of the tracking filter (the phase-locked loop) through which were fed signals from the bubble tapes. The signal from the filter output was examined with an oscilloscope. Using eye and ear correlation techniques, the excursions of the filter were found to correlate with the audible sounds of bubbles. A further study of the correlation was made by simultaneously recording the bubble sounds and the frequency excursions of the filter output voltage. They were again found to agree within reasonable limits. Further efforts in

bubble counting using this technique should be made.

The IEM&P-Reid CW doppler ultrasonic flowmeter (Reid, Davis, Ricketts & Spencer, 1973) has been tested with regard to its bubble counting ability and compared on-line with a band passed zero crossing method. The Reid analogue readout circuit is a directional one which senses the direction of flow in an RF mixer with two phase-modulated signals--one for frequencies representing velocities toward the transducer and the other for velocities away from the transducer. In a special analogue converter the frequency shifted doppler signal is processed to a net directional velocity signal.

The flowmeter readout is remarkably immune to large broadband artifacts, but is greatly disturbed by large sinusoidal transients which often characterize the chirping blood bubble signals. The output responds therefore with a large pulse whenever a bubble chirp appears above the level of the doppler audio signal. These pulses can be counted as a minimal bubble count. The well-known zero-crossing meter when operating on the simple audio doppler signal from the same transducer failed to respond to the same bubble chirps clearly recognized by the IEM&P-Reid directional instrument.

VII.

OTHER APPLICATIONS

Gas embolization occurs not only in diving but also accidently in many surgical and catheterization procedures, as well as in traumatic accidents. Doppler ultrasonic blood flowmeters provide many possibilities for sensing intravascular gas emboli in hospital medicine. The safety of deliberate injection of micro bubbles of CO_2 as well as O_2 in denitrogenated subjects provides a potential for enhancement of ultrasonic vascular visualization techniques and for new methods of determining cardiac output and blood flow distribution.

Surgical Procedures

All disc and bubble type extracorporeal oxygenators we have examined contain and pass micro gas emboli, (Fig. 55) to the patient's arterial system during cardiopulmonary bypass, Spencer, Lawrence, et al, (1969). Oxygenators examined to date include the Bently bubble oxygenators, as well as three different disc oxygenators. Ventriculotomy also always produces arterial gas embolization (Fig. 56) regardless of the preventative techniques employed.

No method of debubbling examined to date completely eliminates bubbles which are produced or introduced by extracorporeal oxygenation. The use of ultrasound pressure has been proposed, Macedo (1973). Large bubbles rise quickly and break on the surface or in a defoaming device. Micro bubbles, however, do not rise readily under gravitational force and are swept along in the blood stream passing all meshes and bubble traps until they enter the patient's arterial system and are lodged in the peripheral capillaries. The venous return from the patient, during bypass, is clear of detectable bubbles. Venous gas emboli are capable of overloading the pulmonary filtering and elimination capacity,

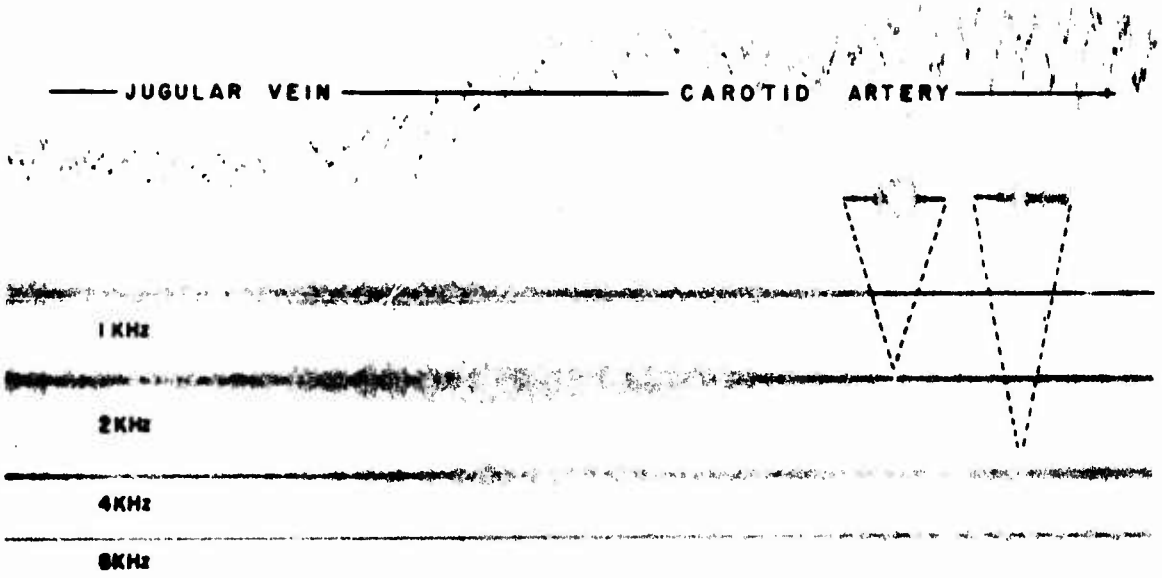

Fig. 55. Carotid artery bubble signals detected during cardiopulmonary bypass for open-heart surgery.

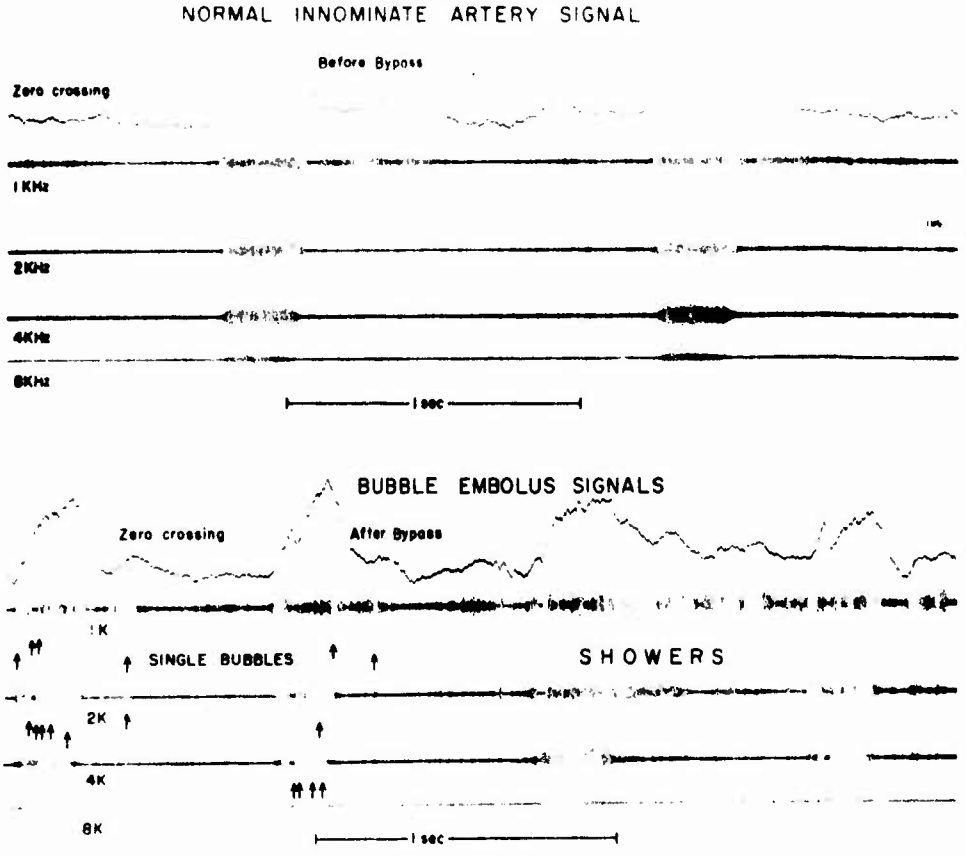

Fig. 56. Flow signals in the innominate artery before and after cardiopulmonary bypass bubble showers.

(Fig. 57).

In all oxygenators, a major source of microbubbles is the suctioned blood from the operative wound even though passed through a defoaming mesh. Another cause is that of injection into the sump of drugs or blood which when passing through the surface of the blood entrains bubbles in great numbers. Overt clinical signs are usually not caused in the patient presumably because they are denitrogenated and the brain and other tissues have a great tolerance to microemboli.

Surgical applications of ultrasonic blood bubble detection include monitoring crainiotomies, especially in the head-up position, angiography and other high-pressure injection procedures, open-heart surgery, and extracorporeal circulations.

Deliberate Injection of Gas Emboli

Carbon dioxide gas has been shown to be innoxious when injected in large quantities into the venous circulation. Disc and bubble oxygenators also deliver, as stated, hundreds of O_2 bubbles into denitrogenated patients with little apparent harm.

Because of the excellent reflection coefficient between gas-blood interfaces, we propose that the use of calibrated numbers of microbubbles be used for measurement of the distribution of cardiac output and in regional blood flow measurements. In addition, the future may bring improved vascular visualization techniques with the enhancement of gas emboli deliberately injected.

Additional Ultrasonic Techniques

Other ultrasonic techniques for the detection of stationary bubbles in tissues and blood have been attempted, Rubissow and MacKay (1971). These ultrasonic techniques for detection of stationary bubbles in tissue are based on through-transmission of reflected ultrasound using either continuous wave or pulse ultrasonic energy. The transducer is localized over an area of expected bubble

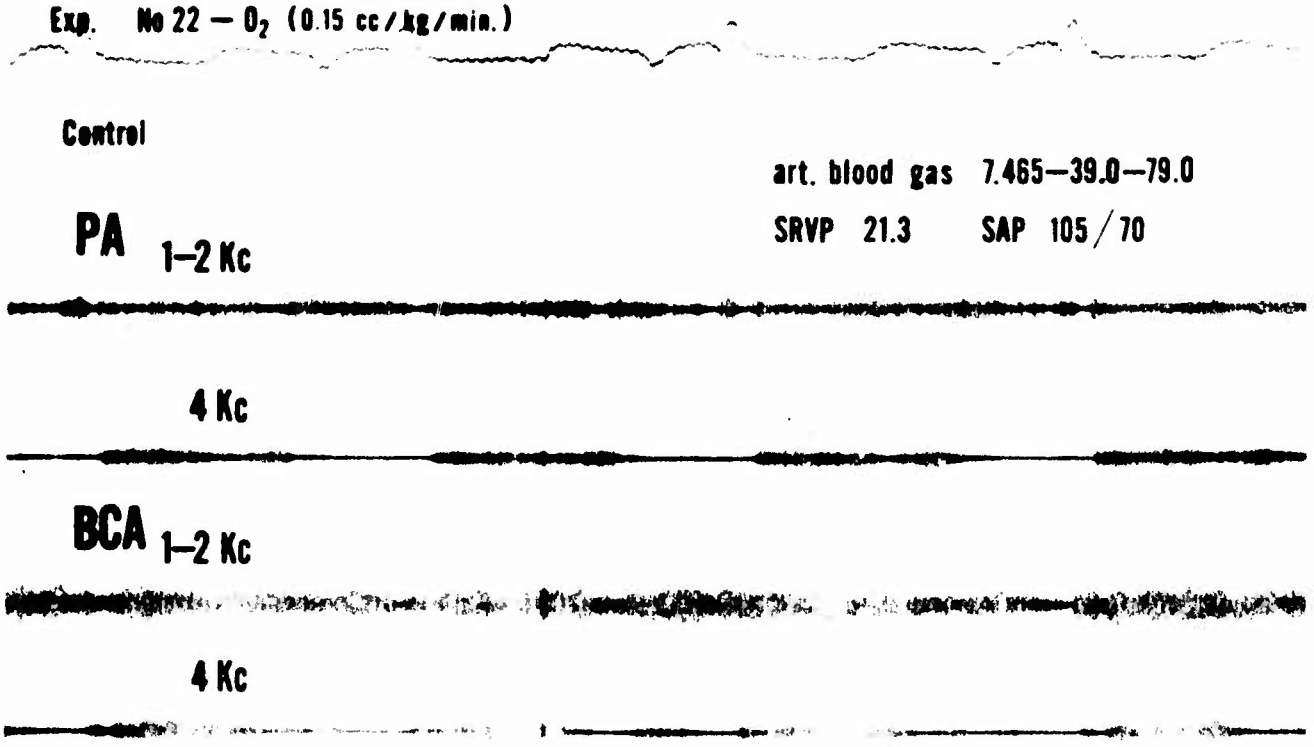

Fig. 57. Upper panel: control doppler pulmonary artery (PA) blood flow signals.

Lower panel: superimposed pulmonary bubble signals following N_2 injection. Dosage of 0.15 cc/kg/min. did not embolize to the brachiocephalic artery (BCA).

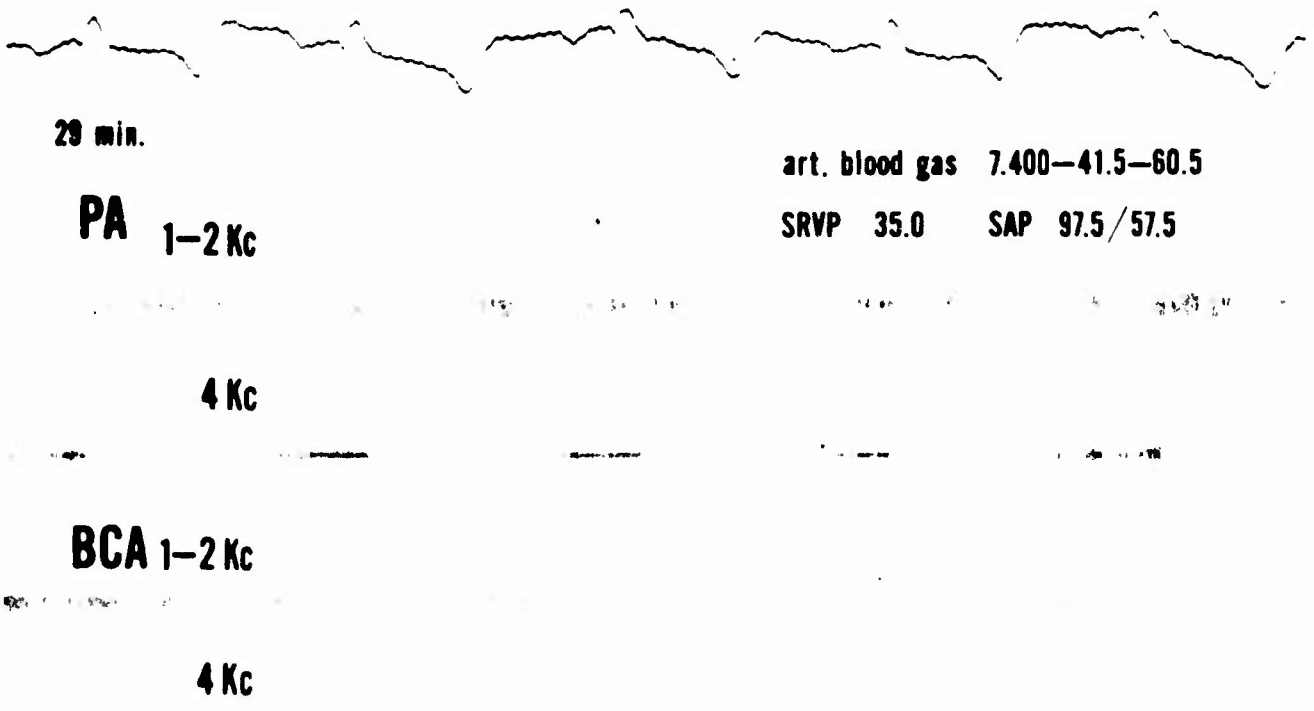

formation and the subject decompressed until a change in transmission or reflectance is obtained. A serious limitation of these techniques presently is similar to that initially found with the doppler peripheral searching, namely that early bubble formation is unlikely to occur under the selected local tissue. The randomness of early development of decompression bubbles, symptoms, and signs means that a local detector has a very poor chance of giving an early warning, because it necessarily limits the observer to one particular localized tissue site (usually on the accessible extremities or in the superficial tissues of the body). To detect the earliest developing static bubbles, such transmission techniques will be required to scan all points simultaneously on the entire body, or as a possible compromise, be so flexible and reliable that they can find use by moving rapidly from one suspect area to another.

VIII.

CONCLUSIONS

1. We have continued to find the technique of doppler ultrasonic detection of decompression venous gas emboli useful in preventing, diagnosing, treating and investigating the pathophysiology of decompression sickness.

2. Investigating hyperbaric air exposures ranging from 7 to 720 minutes and at pressures from 25 to 233 feet sea water, we have always found that decompression venous gas emboli (vge) are detected before bends pain occurs.

3. Musculoskeletal pain has never been found prior to detectable vge.

4. Certain divers are prone towards development of vge and bends while others, on identical insults, remain relatively resistant to both.

5. Bubbles-prone subjects tend to produce vge in the same body area regardless of the insult.

6. Arterial bubble signals have not been detected in mild decompression sickness.

7. For earliest detection, precordial monitoring is preferred to peripheral monitoring.

8. After exceeding some critical tissue and blood supersaturation state, the venous gas emboli (vge) collect in the small peripheral blood vessels and are extruded by blood flow or muscular contraction into the systemic veins where they embolize to the lungs.

9. Peripherally sequestered venous gas emboli may be dislodged by manipulation, promoting early detection and confirmation.

10. Decompression vge without attendant bends may be cleared by 30-60 minutes surface (1 ata) respiration on 100% oxygen.

11. Recompression treatment to 30 fsw with 100% O_2 respiration clears vge and bends formed by much deeper initial exposures.

12. Precordial vge signals serve as a practical clinical guide in preventing bends by indicating the need for preventative and/or treatment measures to include the deferring of repetitive dives.

13. The lack of vge can be used as an indication of the success of, or the desirability of, proceeding with decompression.

14. Surgically implantable doppler flowmeter cuffs can be used to measure blood flow simultaneously with their use as bubble detectors.

15. Currently utilized U.S. Navy No-D tables tend to be too conservative on the deep end and not conservative enough on the shallow end.

16. Open water dives have tended to produce greater quantities of vge than similar dives simulated in the dry hyperbaric chamber.

IX.

SCIENTIFIC COMMUNICATIONS AND COLLABORATIONS

Since the first introduction of doppler ultrasonics to detect vascular gas emboli, the authors have provided equipment and advice to many colleagues.

Training

During the past contract year several sessions were held to further increase the number of people qualified to operate the precordial blood bubble monitor. These sessions included a two day symposium conducted at Providence Hospital, Seattle, Washington, attended by 50 persons representing physicians, technicians, and divers. The entire second day was used to demonstrate the use of the bubble monitor; a tape demonstration of bubbles presented at the Undersea Medical Society meeting in Las Vegas during the May, 73 Annual meeting; a presentation of the 5th International Congress on Hyperbaric Oxygen and other on-site demonstrations to purchasers of the bubble detector.

Training has also been given our experimental divers such that at this time each one of the divers is fully capable of operating the doppler on himself without the need for assistance. This is in itself a significant endeavor in that the majority of these divers are either assistant or certified diving instructors. Several of the instructors have requested that we develop for them a cheaper model doppler that they could use in their diving instruction programs. This interest is leading to the exposure of a greater number of people to the concept of decompression problems being related to the presence of detectable venous gas emboli.

On the 18th and 19th of August, 1973, the Institute of Environmental Medicine and Physiology co-hosted a symposium on Decompression Gas Bubbles, as mentioned

above. This 2-day affair was divided between one day of scientific exchange and one day of demonstrations. During the first day, 17 papers were presented dealing with the various aspects of and problems associated with decompression gas emboli. In conjunction with this, the founding meeting of the North Pacific Chapter, Undersea Medical Society, was also conducted. On the second day, laboratory sessions were held demonstrating:

1. The use of the bubble detector in an actual dive sequence,
2. Use of a bubble counting device resulting from a feasibility investigation, and
3. A taped bubble identification session.

During the chamber dive, gas bubbles were detected both during two of the decompression stops and while on the surface. Surface bubbles of varying intensity were demonstrated for an excess of three hours following return to (surface) atmospheric pressure. These were dissipated in a demonstration of surface-applied 100% O_2 administered via an oral-nasal mask.

A taped demonstration was also set up illustrating the use of a device to count bubbles when not masked by the presence of cardiac motion signals. The counter was far from being fully developed at this time, but never-the-less, did demonstrate the feasibility of bubble quantification.

A tape lab was conducted which consisted of several tape recordings made throughout the last three years. Several tapes were presented to demonstrate the various signals that represent the gas emboli, as well as a tape representing the time course development of venous gas emboli. Additional tapes, brought by the participants, were also presented, and observations and comments were offered concerning them. A final lab was held during which time all those participants possessing an ONR-purchased doppler were encouraged to discuss any questions relevant to the more expiditious use of the doppler.

In May, 1973, a tape recording of bubbles was presented at the Annual Meeting of the Undersea Medical Society held in Las Vegas, Nevada. Following the presentation of this tape, a discussion ensued relative to the identification of which sounds were or were not bubbles. General consensus, following the presentation, seemed to be one of having cleared up an area of confusion.

In addition to this, several tours have been conducted through the facility, during which complete demonstrations on the use of the doppler have been given, with a period following during which questions concerning the doppler and its use have been entertained.

Consulting

Consultation of various kinds has been rendered throughout the contract year. This has ranged from general advice on particular problems to ultrasonic engineering to specific suggestions in regard to the application of the doppler ultrasonic emboli detector. Consultant areas have ranged from the surgical operative area to the applied research laboratory.

Presentations

During the course of the contract, several papers were presented to help disseminate the information as gathered on the project. The first of these, Ultrasonic Detection of Intravascular Gas Emboli, was presented in May, 1973, in Beerse, Belgium at the "Symposium of Cardiovascular Applications of Ultra-Sound". This was followed in June, 1973, with a six months Progress Report on the present contract. Two papers were presented in August, 1974; the first at the Institute sponsored symposium entitled Precordial Blood Bubble Detection and Bubble Signal Analysis, and the second, Clinical Use of Blood Bubble Detection in Diagnosis, Prevention, and Treatment of Decompression Sickness at the 5th International Congress of Hyperbaric Medicine. Included in the publication

materials presented at the 5th O_2 Congress, was an abstract of another paper entitled Objective Development of Decompression Tables using Ultrasonic Blood Bubble Detection. Another paper, Diving Techniques and Occurrence of Venous Gas Embolism in Hawaiian Divers, was presented in May, 1974 at the Washington, D.C. meeting of the Undersea Medical Society. Two additional papers are anticipated for presentation at the September, 1974 meeting of the of the North Pacific Chapter of the Undersea Medical Society.

Publications

Following the presentations of the above-mentioned papers, several were published. Two of these, Clinical Use of Blood Bubble Detection in Diagnosis, Prevention, and Treatment of Decompression Sickness, and Objective Development of Decompression Tables Using Ultrasonic Blood Bubble Detection, were incorporated in the Proceedings of the 5th International Congress on Hyperbaric Oxygen. Another paper, Ultrasonic Detection of Intravascular Gas Emboli, was incorporated in the Proceedings of the Symposium of Cardiovascular Applications of Ultrasound. An abstract entitled Venous Gas Embolism (vge) in Hawaiian Divers was published in Undersea Biomedical Research, Volume 1, Number 1. These publications are listed in the Bibliography as numbers 50, 51, 49 and 56.

X.

BIBLIOGRAPHY AND SELECTED REFERENCES

1. Albano, C. (1960). Etudes sur la decompression chez l'homme, 2. Les Valeurs critiques du gradient de pression a la remontie sans paliers. In 1st chpt., "Conf. Subscquatic Med." Cannes, June 15-19.

2. Albano, C. (1970). "Principles and Observations on the Physiology of the Scuba Diver," ONR Report DR-150.

3. Behnke, A.R. (1937). The Application of Measurements of Nitrogen Elimation to the Problem of Decompressing Divers. U.S. Navy Med. Bull. 35:219-240.

4. Bernstine, R.L., and Dickson, L.C. (1972). "Study of Effects of Ultrasound as Determined by Electron Microscopy. Interaction of Ultrasound and Biological Tissues," DHEW Publication (FDA) 73-8008 p.77.

5. Buckles, R.C. (1960). The Physics of Bubble Formation and Growth. Aerospace Med. 39:1062-1069.

6. Buckles, R.C. (1971). Discussion Remarks in Proceedings of the Fourth Symposium on Underwater Physiology, pp. 161 & 162. Academic Press.

7. Buckles, R.C., (1969). In Vivo Bubble Detection by Acoustic Optical Imaging Techniques. Nature 222:771-772.

8. Campbell, S.D., and Spencer, M.P. (1968). Prevention of Experimental Decompression Sickness with Theophylline and Water. Federation Proceedings Vol. 27, No. 2

9. Campbell, S.D., and Spencer, M.P. (1969). Pharmacologic Agents in the Prevention of Decompression Sickness. J. Occup Med. 11:252-256

10. Carstensen, E.L., and Foldy, L.L. (1947). Propagation of Sound Through a Liquid Containing Bubbles. J. Accous. Soc. Am. 19:481-501.

11. Dyson, M., Pond, J., and Woodward, B. (1972). "The Induction of Red Cell Stasis in Embryos by Ultrasound. Interaction of Ultrasound and Biological Tissues," DHEW Publications (FDA) 73-8008 p.139-40.

12. Franklin, D.L., Schlegal, W.A., and Rushmer, R.F. (1961). Blood Flow Measured by Doppler Frequency Shift of Backscattered Ultrasound. Science 134:654-565.

13. Fry. F.J. and Dunn, F. (1972). "Interaction of Ultrasound and Tissue. Interaction of Ultrasound and Biological Tissues," DHEW Publications (FDA) 73-8008 p.111.

14. Gillis, M.R., Karagianes, M.T., and Peterson, P.L. (1968). Bends: Detection of Circulating Gas Emboli with External Sensor. Science 161:579-580.

15. Gillis, M.F., Peterson, P.L., and Karigianes, M.T. (1968). In Vivo Detection of Circulating Gas Emboli Associated with Decompression Sickness Using the Doppler Flowmeter. Nature 217:965-967.

16. Gillis, M.F. (1971). "Research on Deep Submergence Diving Physiology and Decompression Technology Utilizing Swine: Evaluation of Swine as a Hyperbaric Analog to Man and Detection of Emboli by Use of the Ultrasonic Doppler Flowmeter," Final Report to ONR, Contract No. N00014-69-C-0350.

17. Hawkins, J.A., Schilling, C.W., and Hansen, R.A. (1935). A Suggested Change in Circulating Decompression Tables for Diving. U.S. Navy Med. Bull. 33:372-338.

18. Hempleman, H.V. (1963). Tissue Inert Gas Exchange and Decompression Sickness in "Proceedings of the Second Symposium of Underwater Physiology" (C.J. Lambertson & L.J. Greenbaum, Jr., ed.), p.6-13. Publ. No. 1181 Nat. Acad. Sci. Nat. Res. Council, Washington D.C.

19. Hempleman, H.V. (1971). Discussion Remark in "Proceedings of the Fourth Symposium on Underwater Physiology." p.162. Academic Press.

20. Hueter, T.F., and Bolt, R.F. (1955). Sonics. p. 230. John Wiley and Sons, New York.

21. Hill, C.R. (1972). "Interaction of Ultrasound with Cells. Interaction of Ultrasound with Biological Tissues," DHEW Publications (FDA) 73-8008 p.57.

22. Kanwisher, J., Lawson, K. and Strauss, R. (1974). Acoustic Telemetry from Human Divers. Undersea Biomed. Res. 1:99-107.

23. Lele, P.P., and Pierce, A.D. (1972). "The Thermal Hypothesis of the Mechanism of Ultrasonic Focal Destruction in Organized Tissues," DHEW Publications (FDA) 73-8008 p. 123-128.

24. Macedo, I.C., and Yang, Wan-Jei. (1973). Acoustic Effects on Gas Bubbles in the Flows of Viscous Fluids and Whole Blood. J. Acoust. Soc. Am., 53:1327.

25. Mackay, R.S. (1963). Discussion Remark in "Proceedings of the Second Symposium on Underwater Physiology." p.41. Publ. No. 1181 Nat. Acad. Sci. Nat. Res. Council, Washington, D.C.

26. Mackay, R.S. (1971) Discussion Remark in "Proceedings of the Fourth Symposium on Underwater Physiology." p.161.

27. Mackay, R.S. and Rubbissow, G. (1971). Detection of Bubbles in Tissues and Blood, in Proceedings of the Fourth Symposium on Underwater Physiology. p.151-160.

28. Manley, D.M. (1969). Ultrasonic Detection of Gas Bubbles in Blood. Ultrasonics 102, April.

29. Maroon, J.C., Edmonds-Seal, J., and Campbell A. (1969). An Ultrasonic Method for Detecting Air Embolism. J. of Neurosurg. 31:191-201.

30. Nyborg, W.L. (1972). "Summary: Effects of Ultrasound on Cells. Interaction of Ultrasound and Biological Tissues." DHEW Publication (FDA) 73-8008. p.53.

31. Oyama, Y., and Spencer, M.P. (1971). Cardiopulmonary Effects of Intravenous Gas Embolism with Special References to the Fate of Intravascular Gas Bubbles. Japanese Circulation Journal. 35(12):1547-1549.

32. Powell, Michael, R. (1972). Leg Pain and Gas Bubbles in the Rat Following Decompression from Pressure: Monitoring by Ultrasound. Aerospace Med. (43)2.

33. Reid, J.M., Davis, D.L., Ricketts, H.J. and Spencer, M.P. (1973). A New Doppler Flowmeter System and its Operation with Catheter Mounted Transducers, in "Cardiovascular Applications of Ultrasound" p.32. North-Holland Publ. & Am. Elsevier Publ. Co.

34. Rubissow, C.J., and Mackay, R.S. (1971). Ultrasonic Imaging of In Vivo Bubbles in Decompression Sickness. Ultrasonics p.225.

35. Rubissow, C.J., and Mackay R.S. (1974). Decompression Study and Control Using Ultrasonics. Aerospace Med. 45(5):476-478.

36. Satomura, S. (1957). Ultrasonic Doppler Method for the Inspection of Cardiac Functions. J. Acous. Soc. Am. 29:1181-1185.

37. Satomura, S. (1959). Study of the Flow Patterns in Peripheral Arteries by Ultrasonics. Nahom Onkyo-gakkai Shi J. of the Acous. Soc. of Japan 15:151-158.

38. Schnitzler, R.M. (1972). "Ultrasonic Effects on Mitosis--A Review. Interaction of Ultrasound and Biological Tissues." DHEW Publications (FDA) 73-8008. p.69.

39. Shea, Richard F. (1957). Transistor Circuit Engineering. John Wiley and Sons, New York, p.161.

40. Smith, K.H., and Johanson D.C. (1970). "Hyperbaric Decompression by Means of Bubble Detection." Technical Report to ONR, Contract No. N00014-69-C-0402.

41. Smith, K.H., and Spencer, M.P. (1970). Doppler Indices of Decompression Sickness: Their Evaluation and Use. Aerospace Med. 42(12):1396.

42. Spencer, M.P. (1971). Discussion Remark in "Proceedings of the Fourth Symposium on Underwater Physiology," p. 161-162.

43. Spencer, M. P. and Campbell, S.D. (1968). Development of Bubbles in Venous and Arterial Blood During Hyperbaric Decompression. Bull. of the Mason Clinic, 22(1):26-32.

44. Spencer, M.P., and Campbell, S.D. (1968). Bubbles in the Blood During Hyperbaric Decompression. Proc. of Int'l Union of Phys. Sci. V11:412.

45. Spencer, M.P., Campbell, S.D., and Eurick, C.V. (1969). Diving to Cobb Seamount. J. Occup. Med. 11:285-291.

46. Spencer, M.P., Campbell, S.D., Sealey, J.L., Henry, F.C., and Lindberg, J. (1969). Experiments on Decompression Bubbles in the Circulation Using Ultrasonic and Electromagnetic Flowmeters. J. Occup. Med. 11(5):238.

47. Spencer, M.P., Clarke, H.F. and Simmons, H. (1971). Precordial Monitoring of Pulmonary Gas Embolism and Decompression Bubbles. J. of Aerospace Med. 43:762-767.

48. Spencer, M.P., Johanson, D.C., and Campbell, S.D. (in press). Safe Decompression with the Doppler Ultrasonic Blood Bubble Detector, in "Proceedings of the Fifth Symposium on Underwater Physiology." 1972.

49. Spencer, M.P., Johanson, D.C., and Clarke, H.F. (1973). Ultrasonic Detection of Intravascular Gas Emboli. Cardiovascular Applications of Ultrasound. North-Holland Publ. & Am. Elsevier Publ. Chapt. 30 p.380-388.

50. Spencer, M.P., Johanson, D.C., Campbell, S.D., and Postles, W.F. (1974). Clinical Use of Blood Bubble Detection in Diagnosis, Prevention and Treatment of Decompression Sickness, in "Proceedings of the Fifth International Congress on Hyperbaric Oxygen." 2:589.

51. Spencer, M.P., Johanson, D.C., Campbell, S.D. (1974). Objective Development of Decompression Tables Using Ultrasonic Blood Bubble Detection, in Proceedings of the Fifth International Congress on Hyperbaric Oxygen. 2:946.

52. Spencer, M.P., Lawrence, G.H., Thomas, C.I., and Sauvage, L.R. (1969). The Use of Ultrasonics in the Determination of Arterial Aeroembolism During Open Heart Surgery. Annals of Thoracic Surgery. 8(6):489-497.

53. Spencer, M.P., and Okino, H. (1972). Venous Gas Emboli Following Repeated Breathold Dives. Fed. Proc. p.718.

54. Spencer, M.P., Oyama, Y.T. (1971). Pulmonary Capacity for Dissipation of Venous Gas Emboli. J. of Aerospace Med. 42(8):822-827.

55. Spencer, M.P., Simmons, N., and Clarke, H.F. (1971). A Precordial Transcutaneous Cardiac Output and Aeroembolism Monitor. Fed. Proc. 30(2):705 Abs.

56. Spencer, M.P., Hong, S.K., and Strauss, R.H. (1974). Venous Gas Embolism (vge) in Hawaiian Divers. Undersea Biomed. Res. 1:A18.

57. Sutphen, J.F. (1958). "The Feasibility of Using Pulsed Ultrasound to Detect the Presence of In Vivo Tissue Gas Bubbles." Bureau of Med. and Surg., Navy Dept. Research Work Unit MFB11. 99-9003.01. U.S. Naval Submarine Med. Center, Submarine Base, Groton, Conn. Report No. 508.

58. Tucker, D.G., and Welsby, V.G. (1968). Ultrasonic Monitoring of Decompression. Lancet 1:1253.

59. Ulrich, W.D. (1971). "Ultrasound Dosage for Experimental Use on Human Beings". NMRI Research Dept. #2.

60. U.S. Navy Diving Manual (1970) NAVSHIPS 9004-001-9010. Wash. D.C. Navy Dept.

61. Van Liew, H.D. (1971). Discussion Remark in "Proceedings of the Fourth Symposium on Underwater Physiology," Academic Press, pg. 162-163.

62. Walder, D.N., Evans, A., and Hempleman, H.V. (1968). Ultrasonic Monitoring of Decompression. Lancet 1:897-898.

63. Wells, Peter N.T. (1969). Physical Principles of Ultrasonic Diagnosis. Academic Press, London, pg.25,55, & 226.

XI.

APPENDIX

HYPERBARIC FACILITIES OF THE IEM&P

Laboratory Space

The Institute of Environmental Medicine and Physiology hyperbaric facility is located on the premises of Providence Hospital immediately across the street from the Institute's principal office and engineering laboratory facilities. Primary access to the hyperbaric laboratory is on street level via a large set of doors which allows easy entrance and exit of the personnel and experimental animals as well as the equipment, including the largest chamber. Additional access to Providence Hospital clinical resources is by means of an additional doorway opening directly into the hospital proper. The main entrance opens onto the courtyard which serves the facility as well as the emergency room of the hospital. The floor space is sufficient for training programs accomodating groups of 20 to 30 individuals.

Hyperbaric Chambers

Three chambers are housed in the laboratory facility whose volumes are 0.5, 70, and 205 cubic feet. The smallest chamber is an instrument testing unit. The two larger ones (Fig. 58) are ASME and USCG certified. The largest chamber, 205 $ft.^3$, is double locked, triple hatched and mounted on skids for ease of relocation. Padeyes and jacking pads are provided for ease of handling and leveling. This chamber is capable of simulating dives to 292 feet (130 psig working pressure) and is provided with 75 two-inch through-hull penetrators for gas, communication, and instrumentation leads. Hatches are 30 inches in diameter and four six-inch plexiglass ports are provided for visibility and lighting,

three in the main lock and one in the transfer lock. The main chamber is equipped to administer 100% oxygen via oral-nasal masks to a maximum of four subjects simultaneously. Lighting is by means of surgical type spot lamps mounted exterior to the chamber. 110 volt sources are highly restricted within the chamber and normally physiological detectors with their accompanying D.C. packages are the only electronics allowed within the chamber. The communications system is an exception at the present time, having 0.1 volts p-p on the speakers. It is intended that this be the only exception.

Primary air supply support for the 205 ft.^{3} chamber is from a 34 ACFM 175 psi air-cooled compressor rated for continuous duty (duty cycle 50% unloaded). Primary air supply for the smaller chamber is a four bottle (220 ft.^{3}) high pressure (2,000 psi) bottle bank. Either of the two chambers may be used as an air storage vessel while operating the other chamber. A high-pressure (2,200 psi) 15 bottle backup, capable of pressurizing the largest chamber to a 200 ft. depth, twice in succession, is available should the primary source fail. At least an additional 15 bottles are maintained at all times to back up the high pressure bank.

The 70 ft.^{3} chamber (Fig. 58), likewise double locked with two 24 inch circular hatches, is rated at 550 ft. salt water working pressure. It is provided with three plexiglass ports and is mounted on skids for portability. It is capable of administering 100% O_2 to two subjects at a time and has it's own integral communications system. It is capable of being supported by a portable air compressor should the need arise. It frequently sees service on the Cobb Sea-Mount operations of Project Sea-Use as well as in the diving training programs of both Bellevue and Shoreline Community Colleges.

The 0.5 ft.^{3} chamber (Fig. 59), rated to 1,000 feet salt water pressure, has a single circular bolt-down hatch, four instrumentation through-hulls, and provided with one glass flange on the end opposite the door allowing observation

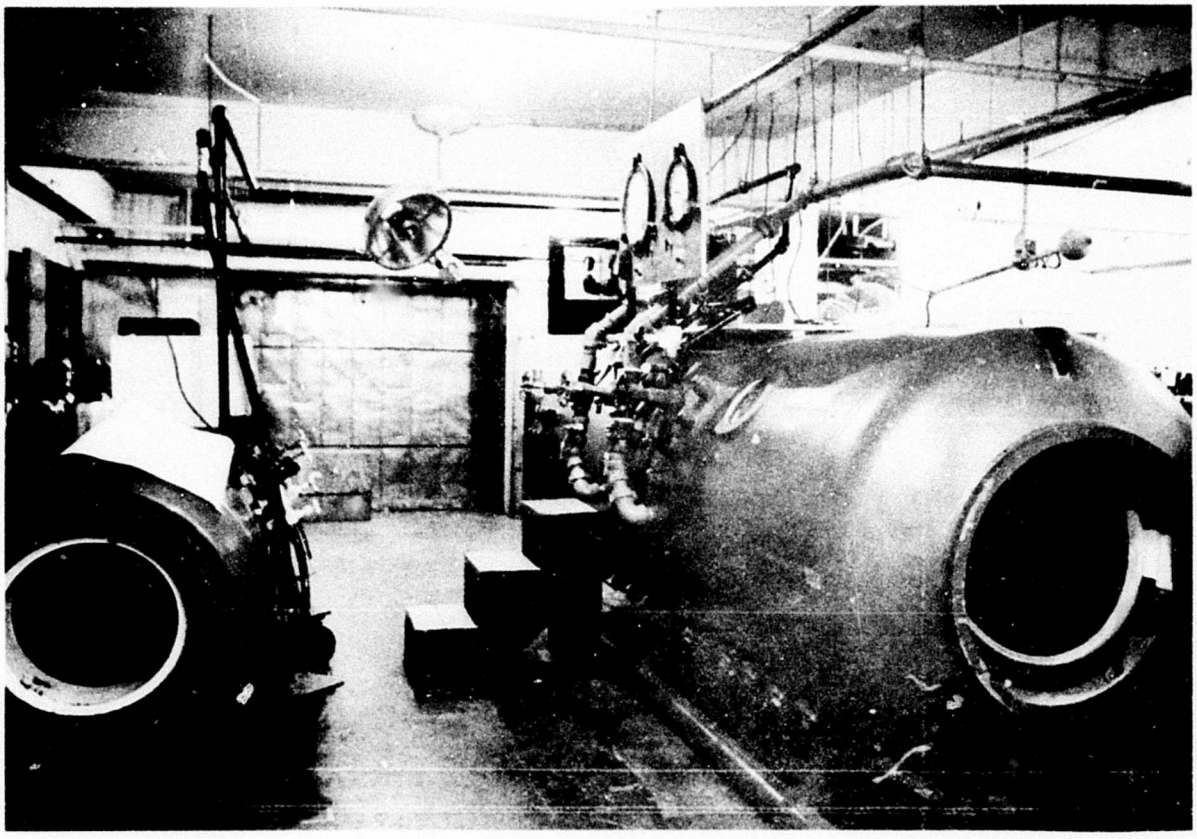

Fig. 58. The 200 ft^3 (right) and the 70 ft^3 (left) deep diving double lock chambers.

Fig. 59. The 0.5 ft^3 high pressure test chamber.

of the behavior of test items within the chamber. Replacement of this glass flange with a metal flange allows the chamber to be used at depths to 2,000 feet salt water.

Recording Systems

All data are recorded on multi-channel strip charts and tape recorders for future replay and analysis. The recorders include a four-channel audio recorder, several two-channel cassette recorders, an eight-channel instrumentation recorder, and a two-channel instrumentation recorder. A time code generator/translator produces a digital time code for both recordings and playback, as well as continuous electronic monitoring off a chamber-mounted strain gauge which is recorded on a wide channel strip chart recorder displaying both instantaneous pressure and rate of change of pressure (dp/dt). The dp/dt indication provides the chamber operator input in addition to that of the direct dial pressure gauge reading to better enable him to maintain a more constant rate of change of pressure, thereby eliminating one more variable in the effort to maintain reputable conditions in the experimental protocol. (The differentiator operates by passing the output voltage of the pressure transducer through a capacitor, followed by a current-to-voltage transducer comprised of two chips, Fairchild A72713 and A741, to make a single operational amplifier.)

The data acquisition/retrieval system also includes zero-crossing meters, oscilloscopes, and variable band-pass filters. Doppler instrumentation (institute designed and built) incorporates the audio signal of bubbles along with an analog readout of blood flow and velocity.

Through-Hull Signal Transfer

The transfer of information through-hull has long been a problem in the hyperbaric facility. In a pervious report, we discussed an IEM&P designed and

built through-hull connector which allowed for low-loss transmission of signal material. This device, which had the center lead of its individual connectors floating from the chamber, is now being replaced with an improved version of the same connector. By so doing, it is now possible to pass (float) both the center and common leads of the connector through the chamber without making any contact with the chamber itself. This new through-hull (Figs. 60-61) enables us to utilize 7 wire pairs insulated from the chamber instead of the 3 pairs available previously. Also, due to the need for fewer wires and associated connectors, there is less opportunity for RFI and 60 cycle disturbances to interfere with acquisition of data.

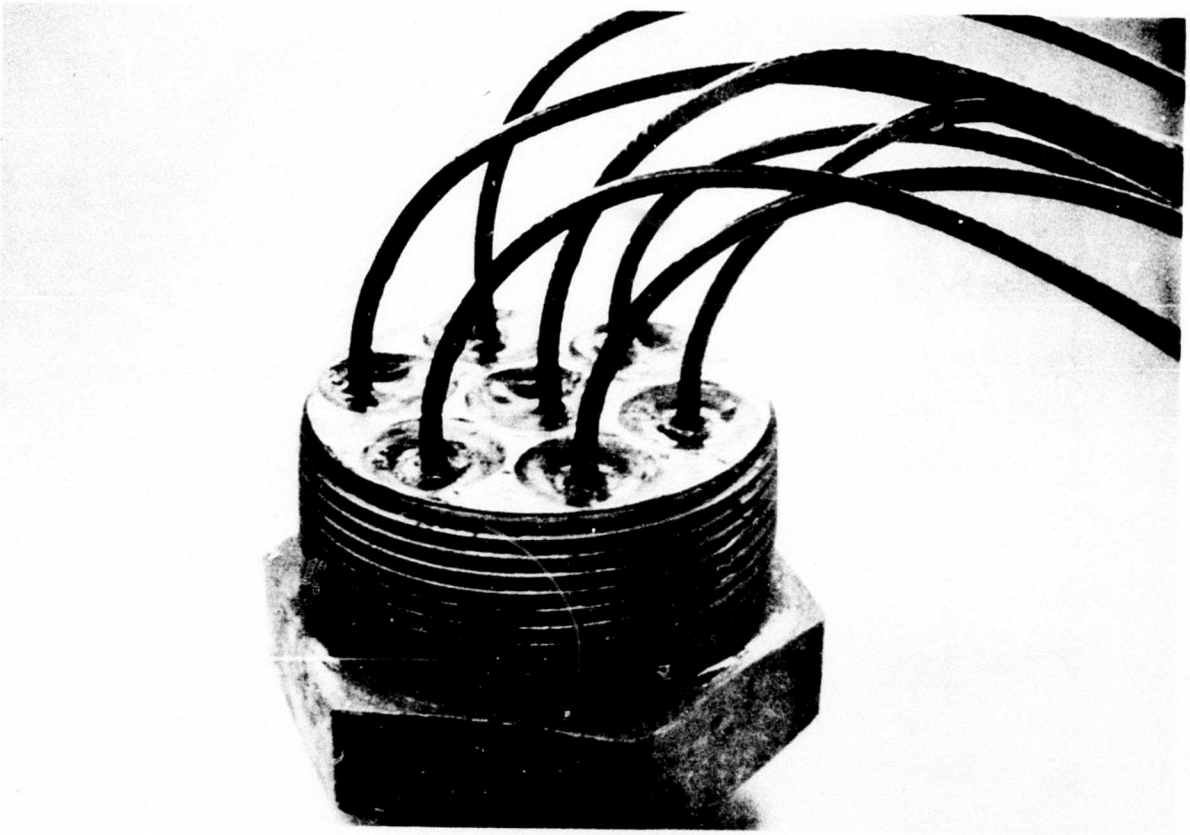

Fig. 60. Through-hull coaxial leads with outer plastic insulation removed are potted in epoxy to insure against gas leakage and isolation from the plug itself.

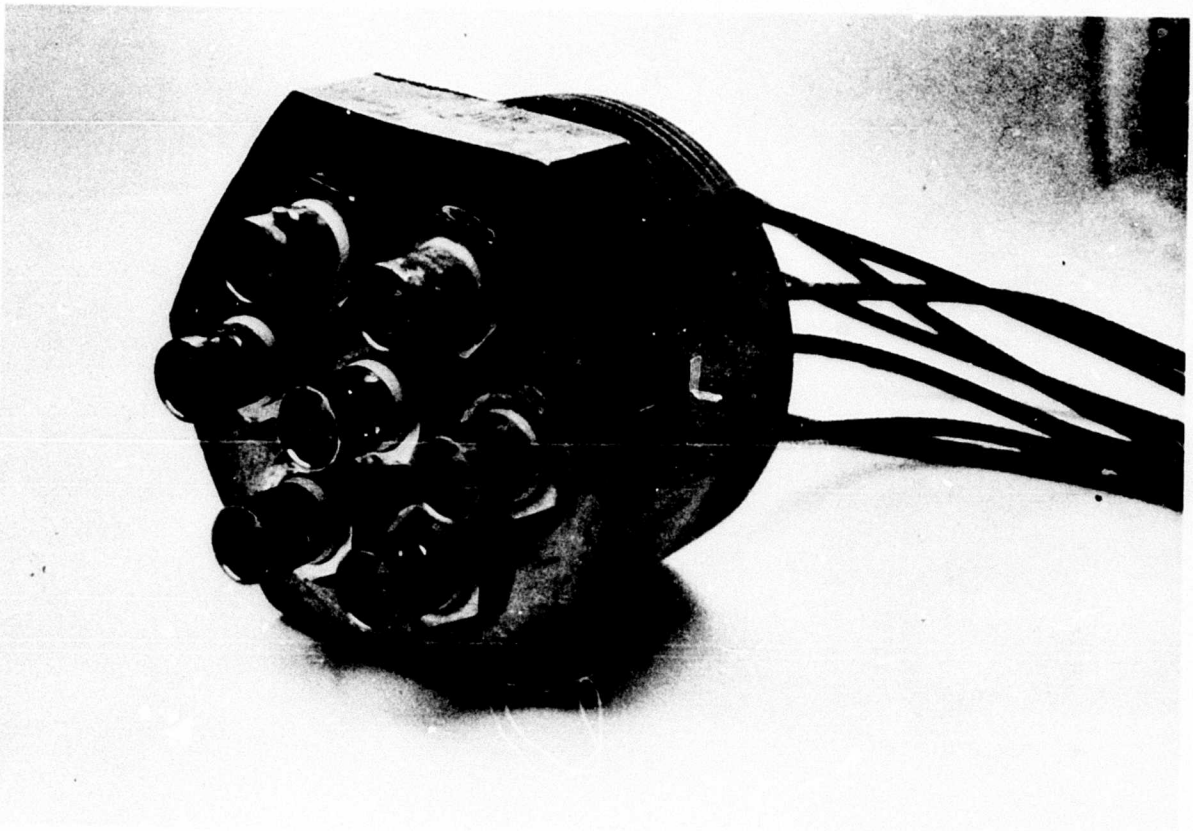

Fig. 61. The finished IEM&P BNC multiple channel through-hull connector. Both the common lead and the high lead are isolated from the chamber wall.